# The evolution and explosion of massive stars

S. E. Woosley* and A. Heger†

*Department of Astronomy and Astrophysics, University of California, Santa Cruz, California 95064*

T. A. Weaver

*Lawrence Livermore National Laboratory, Livermore, California 94551*

(Published 7 November 2002)

Like all true stars, massive stars are gravitationally confined thermonuclear reactors whose composition evolves as energy is lost to radiation and neutrinos. Unlike lower-mass stars ($M \lesssim 8M_{\odot}$), however, no point is ever reached at which a massive star can be fully supported by electron degeneracy. Instead, the center evolves to ever higher temperatures, fusing ever heavier elements until a core of iron is produced. The collapse of this iron core to a neutron star releases an enormous amount of energy, a tiny fraction of which is sufficient to explode the star as a supernova. The authors examine our current understanding of the lives and deaths of massive stars, with special attention to the relevant nuclear and stellar physics. Emphasis is placed upon their post-helium-burning evolution. Current views regarding the supernova explosion mechanism are reviewed, and the hydrodynamics of supernova shock propagation and "fallback" is discussed. The calculated neutron star masses, supernova light curves, and spectra from these model stars are shown to be consistent with observations. During all phases, particular attention is paid to the nucleosynthesis of heavy elements. Such stars are capable of producing, with few exceptions, the isotopes between mass 16 and 88 as well as a large fraction of still heavier elements made by the *r* and *p* processes.

## CONTENTS



*Electronic address: woosley@ucolick.org

†Also at Enrico Fermi Institute, University of Chicago, 5640 S. Ellis, Chicago, IL 60637. Electronic address: alex@ucolick.org

 

## I. INTRODUCTION

Massive stars, by which we shall mean those massive enough to explode as supernovae, are fundamental to the evolution of the universe. They light up regions of stellar birth and create the elements necessary to life. In their explosions, they produce spectacular fireworks and leave as remnants exotic objects—neutron stars and black holes. Their winds and radiation stir the interstellar medium and may even affect the evolution of galaxies. Their interiors are physical laboratories with conditions not seen elsewhere in the universe. The neutrino burst that announces their death is one of the most powerful events in the universe.

We review here the community's current understanding of these stars—their evolution, their explosion as supernovae, and especially their nucleosynthesis. Such a comprehensive review is a daunting task, given the scope of the subject and its rapid rate of development, and some topics will necessarily receive short shrift. Among the subjects we are compelled to leave to others are the evolution of massive stars in the Hertzsprung-Russell diagram as well as the historical aspects of the subject. The latter have been recently reviewed by Wallerstein *et al.* (1997). There are also many excellent related reviews of the subject[1] as well as two outstanding monographs by Clayton (1968) and Arnett (1996).

Our review was begun approximately ten years ago and was intended as a 40-year celebration of the seminal works of Burbidge, Burbidge, Fowler, and Hoyle (1957, also known as $B^2FH$) and Cameron (1957). Although we missed our mark by about five years, we would still like to devote this review to these founding fathers of the field. A lot has changed in 55 years, but the general conclusion that the heavy elements are a by-product of stellar evolution, especially of massive stars (see also Fowler and Hoyle, 1964), has stood the test of time. In 1957, this was but one of four theories being considered, the remainder involving synthesis in the early universe.

Nowadays no serious scientist would question the stellar origin of heavy elements. Moreover, the delineation of isotopes according to a physical synthesis process—*p* process, *r* process, *s* process, *e* process—still persists. In some cases, such as the *r* and *s* processes, the conditions required—density, temperature, and neutron abundance—have not changed greatly since 1957. In the case of the *s* process, we know much more about the sites; for the *r* process, the sites are still debated. The *p* process has been greatly modified and proton capture no longer plays a dominant role. The $\alpha$ process of Burbidge *et al.* (1957) has given way to carbon, neon, and oxygen burning, and the nature of explosive synthesis has been greatly clarified. New processes have appeared—the $\nu$ process, the $\gamma$ process, the *rp* process, neutron-rich nuclear statistical equilibrium. Early ideas of iron-group synthesis in which iron was made chiefly as stable $^{56}$Fe have been replaced by a more violent, dynamical view in which many species are made as radioactive progenitors—$^{56}$Fe as $^{56}$Ni by explosive silicon burning.

Still, it was Burbidge *et al.* and Cameron who gave us the alphabet from which the field of nuclear astrophysics was written. We celebrate their work and hope to live up to it in some small way.

## II. PRESUPERNOVA EVOLUTION—GENERAL FEATURES

### A. Physical overview

The preexplosive life of a massive star is governed by simple principles. Pressure—a combination of radiation, ideal gas, and, later on, partially degenerate electrons—holds the star up against the force of gravity, but because it radiates, the star evolves. When the interior is sufficiently hot, nuclear reactions provide the energy lost as radiation and neutrinos, but only by altering the composition so that the structure of the star changes with time. Nondegenerate stars have a negative heat capacity. Taking energy away causes the internal temperature to rise. Thus the exhaustion of one fuel, e.g., hydrogen, leads to the ignition of the next, e.g., helium, until finally an inert core of iron is formed, from which no further energy can be gained by nuclear burning.

Hydrostatic equilibrium requires that the pressure $P$ obey

$$\frac{dP}{dr} = -\frac{GM(r)\rho(r)}{r^2}, \tag{1}$$

where $M(r)$ is the mass interior to radius $r$ and $\rho(r)$ is the density there. For a given polytropic index $n$ such that $P \propto \rho^{(n+1)/n}$, the integration of Eq. (1) implies a relation between the central pressure $P_c$ and the central density $\rho_c$,

$$\frac{P_c^3}{\rho_c^4} = 4\pi G^3 \left(\frac{M}{\phi}\right)^2, \tag{2}$$

where $\phi(n)$ is 4.899, 10.73, and 16.15 for $n=0$, 1.5, and 3, respectively. It is convenient to define an abundance variable, $Y_i$, which is like a dimensionless number density,

$$Y_i = \frac{X_i}{A_i} = \frac{n_i}{\rho N_A}, \tag{3}$$

where $n_i$ is the number of species $i$ per cm$^3$, $X_i$ is its

[1]See, for example, Trimble (1975, 1991, 1996), Wheeler, Sneden, and Truran (1989), Bethe (1990), Maeder and Conti (1994), Meyer (1994), Thielemann, Nomoto, and Hashimoto (1996), and Vanbeveren, De Loore, and Van Rensbergen (1998).

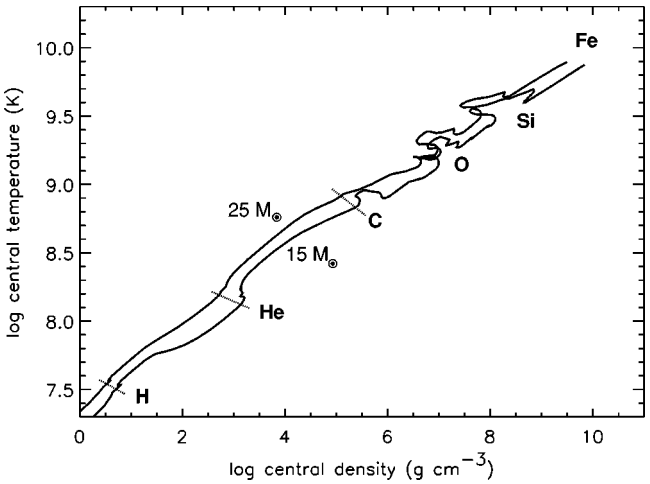


FIG. 1. Evolution of the central temperature and density in stars of $15M_\odot$ and $25M_\odot$ from birth as hydrogen-burning stars until iron-core collapse (Table I). In general, the trajectories follow a line of $\rho \propto T^3$, but with some deviation downwards (towards higher $\rho$ at a given $T$) due to the decreasing entropy of the core. Nonmonotonic behavior is observed when nuclear fuels are ignited and this is exacerbated in the $15M_\odot$ model by partial degeneracy of the gas.

mass fraction, and $N_A$ is Avogadro's number. A similar definition exists for the electron mole number,

$$Y_e = \frac{n_e}{\rho N_A}, \tag{4}$$

where $n_e$ is the electron number density. Thus the ideal-gas pressure is

$$P_{\text{ideal}} = \frac{\rho}{\mu} N_A k T, \tag{5}$$

with $\mu = (\Sigma Y_i + Y_e)^{-1}$, and, from Eq. (2) for a given polytropic index, it follows that

$$\frac{T_c^3}{\rho_c} \propto M^2 \mu^3, \tag{6}$$

with $T_c$ the central temperature. This relation holds so long as the polytropic index remains constant and the pressure is either dominantly due to ideal gas or has ideal gas as a constant fraction.

Consequently a contracting core of constant composition, in which energy generation and neutrino losses are negligible, supported by pressure that has as a constant ideal-gas fraction, will follow a path $\rho_c \propto T_c^3$. This trend continues until one of the assumptions is violated, e.g., by nuclear ignition or the onset of degeneracy.

Figure 1 shows the evolution of the central temperature and density for two stars of solar metallicity having mass $15M_\odot$ and $25M_\odot$. The tendency of $T_c$ to scale with $\rho_c^{1/3}$ is apparent throughout the entire evolution. The curves fall below a strict extrapolation of the initial values owing to a decrease in the entropy of the core as it evolves (see Fig. 11 below). They are also punctuated with "wiggles" showing the effects of nuclear ignition, both in the center and in shells. Nuclear burning changes the entropy in the core and, moreover, the cores become partially degenerate during their late evolution and prone to mildly degenerate flashes (more violent below $12M_\odot$). These are particularly apparent in the $15M_\odot$ model in Fig. 1.

Since radiation entropy is proportional to $T^3/\rho$ and ideal-gas entropy depends on $T^{3/2}/\rho$, Eq. (6) also implies that more massive stars will have higher central entropy. This too is a characteristic that persists throughout the evolution despite the fact that the pressure at late times is not ideal. Consequently lighter stars tend to converge more in their late stages on the Chandrasekhar mass and, in the simplest case, end up with smaller iron cores. Since the nuclear burning rates are proportional to high powers of the temperature, lighter stars will also burn a given fuel at higher densities. The competition between reactions with different density dependencies—for example, $^{12}\text{C}(\alpha,\gamma)^{16}\text{O}$ vs helium burning by the $3\alpha$ reaction—will thus yield different compositions in stars of different mass.

### B. Equation of state and initial composition

Except during iron-core collapse and explosion when the density exceeds $10^{11}$ g cm$^{-3}$, the equation of state relating energy and pressure in massive stars to temperature, density, and composition is straightforward, if not simple. The electrons and, at high temperatures, the electron-positron pairs can be described as a perfect, thermal gas of arbitrary relativity and degeneracy. Efficient subroutines have been given by Blinnikov, Dunina-Barkovskaya, and Nadyozhin (1996) and Timmes and Swesty (2000). The ions can be treated, to first order, as an ideal gas and radiation pressure is given well by blackbody equations.

An important complication is the electric interaction between ions and among ions and electrons, sometimes referred to as "Coulomb corrections" (Abrikosov, 1960; Salpeter, 1961; Fontaine, Graboske, and van Horn, 1977). These cannot be neglected during the post-helium-burning stages (Nomoto, 1982, 1984; Nomoto and Hashimoto, 1988; Woosley and Weaver, 1988) and generally act to decrease the mass of the iron core in the presupernova model by approximately $0.1M_\odot$.

Stars of many different compositions are studied, but most of the standard ones use initial compositions like that of the sun (Anders and Grevesse, 1989; Grevesse and Noels, 1993; Grevesse, Noels, and Sauval, 1996).

### C. Opacities

The opacities necessary for understanding the evolution of massive stars can be segregated into those needed to understand the interior and those necessary for the cooler, low-density envelope. Throughout most of the stellar interior on the main sequence, the plasma is fully ionized and the opacity is predominantly due to electron scattering, $\kappa_e \approx 0.2(Y_e/0.5)$ (Fig. 2). At higher temperatures this opacity must be modified (decreased) because of Klein-Nishina corrections to Compton scat-

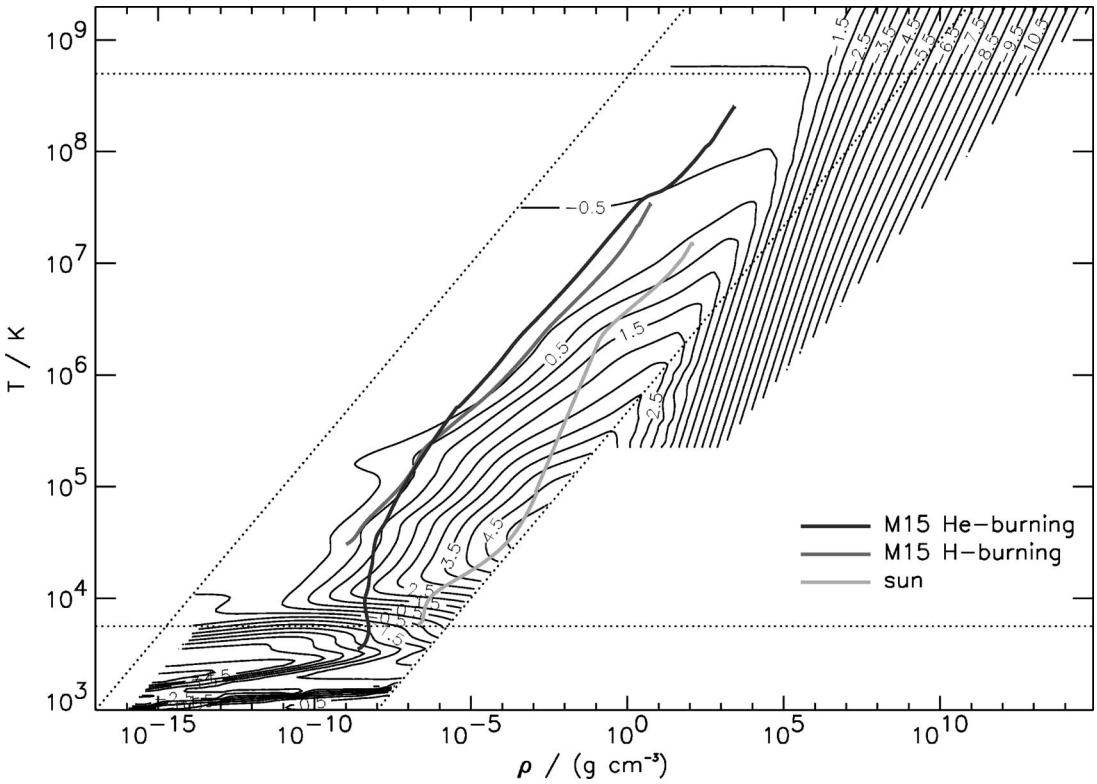


FIG. 2. Opacity from the studies of Rogers and Iglesias (1992) and Iglesias and Rogers (1996) compared with conditions in a $15M_{\odot}$ star on the main sequence and during helium burning. The interior of the sun is given for comparison. Curves are labeled by the log base 10 of the opacity in $\mathrm{cm}^2\ \mathrm{g}^{-1}$.

tering (see, for example, Weaver, Zimmerman, and Woosley, 1978). At still higher temperatures, electron-positron pairs also contribute. At high density the opacity is also modified by electron conduction (Itoh *et al.*, 1983; Mitake, Ichimaru, and Itoh, 1984; Itoh, Nakagawa, and Kohyama, 1985) and can become small owing to filling of the electron phase space when the gas becomes degenerate.

In the atmospheres of main-sequence stars and the convective envelopes of helium-burning stars, the opacity differs appreciably from electron scattering. Most researchers employ the tables of Rogers and Iglesias (1992) and Iglesias and Rogers (1996; see also Fig. 2).

### D. Neutrino losses

Neutrino losses are a critical aspect of the evolution of massive stars once they finish helium burning (Sec. IV). Until silicon burning, when neutrino losses from electron capture become important (Secs. IV.C and V.B), these neutrinos are chiefly due to thermal processes, especially pair annihilation (see Fig. 12 of Itoh *et al.*, 1996 and Table I). This gives a loss term that is very roughly proportional to $T^9$ in the range of interest for advanced burning stages (Clayton, 1968). It is the temperature sensitivity of these neutrino losses, combined with the need to go to higher temperatures in order to burn fuels with larger charge barriers, that leads to a rapid acceleration of the stellar evolution during carbon, neon, oxygen, and silicon burning, the latter typically taking only a day or so (Table I). Most modern calculations use fitting formulas to represent these thermal losses (Beaudet, Petrosian, and Salpeter, 1967; Munakata, Kohyama, and Itoh, 1985; Itoh *et al.*, 1996).

### E. Convection

The greatest source of diversity and uncertainty in attempts to model the evolution of stars of all masses is the way in which compositional mixing is handled, especially at the boundaries of convective regions. An additional problem peculiar to massive stars is that, during the latest stages of evolution, convective and nuclear time scales become comparable. Almost all models use some variation of "mixing-length theory" (see, for example, Clayton, 1968) wherein the convective velocity is

$$V_{\mathrm{conv}}=\frac{1}{2}\left(\frac{GM}{\rho r^2}\Delta\nabla\rho\right)^{1/2} l, \tag{7}$$

with $\Delta\nabla\rho/\rho$, the excess of the density gradient over and above that given by the adiabatic condition (see below) and the *mixing length* $l$, typically some fraction of the pressure scale height. The diffusion coefficient for both compositional mixing and energy transport, $D_{\mathrm{conv}}$, is then

$$D_{\mathrm{conv}}=\frac{1}{3}V_{\mathrm{conv}}l. \tag{8}$$

TABLE I. Burning stages of stars.

Hydrogen burning

| $M_{\rm initial}$ $M_\odot$ | $T$ $10^7$ K | $\rho$ g cm$^{-3}$ | $M$ $M_\odot$ | $L$ $10^3$ $L_\odot$ | $R$ $R_\odot$ | $\tau$ Myr |
|---|---|---|---|---|---|---|
| 1[a,b] | 1.57 | 153 | 1.00 | 0.001 | 1.00 | ~1100 |
| 13 | 3.44 | 6.66 | 12.9 | 18.3 | 6.24 | 13.5 |
| 15 | 3.53 | 5.81 | 14.9 | 28.0 | 6.75 | 11.1 |
| 20 | 3.69 | 4.53 | 19.7 | 62.6 | 8.03 | 8.13 |
| 25 | 3.81 | 3.81 | 24.5 | 110 | 9.17 | 6.70 |
| 75 | 4.26 | 1.99 | 67.3 | 916 | 21.3 | 3.16 |
| 75[c] | 7.60 | 10.6 | 75.0 | 1050 | 9.36 | 3.44 |

Helium burning

| $M_{\rm initial}$ $M_\odot$ | $T$ $10^8$ K | $\rho$ $10^3$ g cm$^{-3}$ | $M$ $M_\odot$ | $L$ $10^3$ $L_\odot$ | $R$ $R_\odot$ | $\tau$ Myr |
|---|---|---|---|---|---|---|
| 1[b] | 1.25 | 20 | 0.71 | 0.044 | ~10 | 110 |
| 13 | 1.72 | 1.73 | 12.4 | 26.0 | 359 | 2.67 |
| 15 | 1.78 | 1.39 | 14.3 | 41.3 | 461 | 1.97 |
| 20 | 1.88 | 0.968 | 18.6 | 102 | 649 | 1.17 |
| 25 | 1.96 | 0.762 | 19.6 | 182 | 1030 | 0.839 |
| 75 | 2.10 | 0.490 | 16.1 | 384 | 1.17 | 0.478 |
| 75[c] | 2.25 | 0.319 | 74.4 | 1540 | 702 | 0.332 |

Carbon burning

| $M_{\rm initial}$ $M_\odot$ | $T$ $10^8$ K | $\rho$ $10^5$ g cm$^{-3}$ | $M$ $M_\odot$ | $L$ $10^3$ $L_\odot$ | $R$ $R_\odot$ | $\tau$ kyr |
|---|---|---|---|---|---|---|
| 13 | 8.15 | 3.13 | 11.4 | 60.6 | 665 | 2.82 |
| 15 | 8.34 | 2.39 | 12.6 | 83.3 | 803 | 2.03 |
| 20 | 8.70 | 1.70 | 14.7 | 143 | 1070 | 0.976 |
| 25 | 8.41 | 1.29 | 12.5 | 245 | 1390 | 0.522 |
| 75 | 8.68 | 1.39 | 6.37 | 164 | 0.644 | 1.07 |
| 75[c] | 10.4 | 0.745 | 74.0 | 1550 | 714 | 0.027 |

Neon burning

| $M_{\rm initial}$ $M_\odot$ | $T$ $10^9$ K | $\rho$ $10^6$ g cm$^{-3}$ | $M$ $M_\odot$ | $L$ $10^3$ $L_\odot$ | $R$ $R_\odot$ | $\tau$ yr |
|---|---|---|---|---|---|---|
| 13 | 1.69 | 10.8 | 11.4 | 64.4 | 690 | 0.341 |
| 15 | 1.63 | 7.24 | 12.6 | 86.5 | 821 | 0.732 |
| 20 | 1.57 | 3.10 | 14.7 | 147 | 1090 | 0.599 |
| 25 | 1.57 | 3.95 | 12.5 | 246 | 1400 | 0.891 |
| 75 | 1.62 | 5.21 | 6.36 | 167 | 0.715 | 0.569 |
| 75[c] | 1.57 | 0.434 | 74.0 | 1560 | 716 | 0.026 |

Oxygen burning

| $M_{\rm initial}$ $M_\odot$ | $T$ $10^9$ K | $\rho$ $10^6$ g cm$^{-3}$ | $M$ $M_\odot$ | $L$ $10^3$ $L_\odot$ | $R$ $R_\odot$ | $\tau$ yr |
|---|---|---|---|---|---|---|
| 13 | 1.89 | 8.19 | 11.4 | 64.5 | 691 | 4.77 |
| 15 | 1.94 | 6.66 | 12.6 | 86.6 | 821 | 2.58 |
| 20 | 1.98 | 5.55 | 14.7 | 147 | 1090 | 1.25 |
| 25 | 2.09 | 3.60 | 12.5 | 246 | 1400 | 0.402 |
| 75 | 2.04 | 4.70 | 6.36 | 172 | 0.756 | 0.908 |
| 75[c] | 2.39 | 1.07 | 74.0 | 1550 | 716 | 0.010 |

TABLE I. (*Continued*).

| | | | Silicon burning | | | |
|---|---|---|---|---|---|---|
| $M_{\text{initial}}$ $M_\odot$ | $T$ $10^9$ K | $\rho$ $10^7$ g cm$^{-3}$ | $M$ $M_\odot$ | $L$ $10^3$ $L_\odot$ | $R$ $R_\odot$ | $\tau$ d |
| 13 | 3.28 | 4.83 | 11.4 | 64.5 | 692 | 17.8 |
| 15 | 3.34 | 4.26 | 12.6 | 86.5 | 821 | 18.3 |
| 20 | 3.34 | 4.26 | 14.7 | 147 | 1090 | 11.5 |
| 25 | 3.65 | 3.01 | 12.5 | 246 | 1400 | 0.733 |
| 75 | 3.55 | 3.73 | 6.36 | 173 | 0.755 | 2.09 |
| 75[c] | 3.82 | 1.18 | 74.0 | 1540 | 716 | 0.209 |

[a]Central hydrogen-burning values for the current sun. From Bahcall, Pinsonneault, and Basu (2001).
[b]Central burning lifetimes and all helium-burning values (horizontal branch only). From Sackmann, Boothroyd, and Kraemer (1992).
[c]Stellar model with 0.0001 solar metallicity.

Once the diffusion coefficient is known, convective mixing is calculated from the diffusion equation,

$$\left(\frac{\partial Y_i}{\partial t}\right)_{\text{conv}} = \frac{\partial}{\partial M(r)}\left[(4\pi r^2\rho)^2 D \frac{\partial Y_i}{\partial M(r)}\right], \tag{9}$$

and is added to the purely nuclear terms for $(dY_i/dt)$. So far it has not proven numerically feasible to couple convection in the advanced burning stages with nuclear burning directly in a single matrix (though see Herwig *et al.*, 1999 for a calculation relevant to lower-mass stars). Thus the nuclear burning is usually carried out first and the stellar zones are then mixed as a separate operation afterwards in the converged model.

This convective transport is far more efficient at both carrying energy and mixing the composition than radiation, for which

$$D_{\text{rad}} = \frac{1}{3}\frac{acT^3}{\kappa\rho^2}\left(\frac{\partial\epsilon}{\partial T}\right)_\rho^{-1}, \tag{10}$$

where $\kappa$ is the opacity and $\epsilon$ is the internal energy.

### 1. Semiconvection

A historical split in the way convection is treated in a stellar model comes about because the adiabatic condition can be written in two ways:

$$\frac{dP}{P} - \Gamma_1\frac{d\rho}{\rho} = 0,$$

$$\frac{dP}{P} + \frac{\Gamma_2}{1-\Gamma_2}\frac{dT}{T} = 0. \tag{11}$$

For convective instability, $A>0$ or $B>0$, where

$$A = \frac{1}{\rho}\frac{d\rho}{dr} - \frac{1}{\Gamma_1 P}\frac{dP}{dr},$$

$$B = \frac{\Gamma_2 - 1}{\Gamma_2}\frac{1}{P}\frac{dP}{dr} - \frac{1}{T}\frac{dT}{dr}. \tag{12}$$

Here $A$ is known as the *Ledoux condition* for instability and $B$ is the *Schwarzschild condition*. These two conditions are equivalent except when there are gradients in composition or when radiation pressure is important. Then the Ledoux criterion is more restrictive since, for the simple case of an ideal gas plus radiation,

$$A = \frac{4-3\beta}{\beta}B + \frac{1}{\mu}\frac{d\mu}{dr}, \tag{13}$$

where $\beta$ is the ratio of gas pressure to total pressure. Expressions for the $\Gamma$'s are given by Woosley and Weaver (1988). Those regions of the star that are unstable by the Schwarzschild criterion but stable by the Ledoux criterion are called *semiconvective*.

It is unknown exactly what to use for the diffusion coefficient for ionic mixing in semiconvective regions. Kato (1966) treats semiconvection as an overstable oscillation between two layers having different temperatures and compositions. The leakage of heat out of a perturbation of the boundary causes its amplitude to grow, eventually leading, after very many oscillations, to mixing. Such a picture can be developed into an approximate numerical model (Langer *et al.*, 1983) and suggests an important role for the radiative diffusion coefficient, but it is not parameter free. More recently, Spruit (1992) modeled semiconvection as a "double diffusive" phenomenon, with the unstable region breaking down into cells. Inside each cell there is no composition gradient and convection proceeds as normal. In the cell boundaries, however, the composition gradients are expressed and energy and mass only cross these by diffusion. Spruit obtains for the semiconvective diffusion coefficient

$$D_S = (D_{\text{rad}}D_{ion})^{1/2}\left(\frac{4}{\beta} - 3\right)\frac{\nabla_r - \nabla_a}{\nabla_\mu}, \tag{14}$$

where $D_{\text{rad}}$ was given in Eq. (10) and $D_{ion}$ is the ionic diffusion coefficient, $\beta$ is the ratio of gas pressure to total pressure, $\nabla_r$ is the logarithmic derivative of the radiation temperature with respect to radius, $\nabla_\mu$ is a similar derivative of the composition, and $\nabla_a$ is the adiabatic gradient (Clayton, 1968). In typical circumstances, the

ionic diffusion coefficient is about $10^6$ times smaller than the radiative diffusion coefficient, and the logarithmic derivative terms give a number less than unity. Unmodified, Spruit's formalism thus suggests a very small diffusion coefficient ($D_s \ll D_r$) and an evolution that resembles Ledoux convection more than Schwarzschild. However, Spruit's cellular structure is probably unstable after many convective cycle times within a cell and may not be as persistent in three dimensions as in two. Instabilities, as well as rotationally induced mixing, will go in the direction of increasing the diffusion. Numerical calculations (in two dimensions) by Merryfield (1995) suggest that the efficiency of semiconvection—and the stability of Spruit's cells—depend on the magnitude of the driving force for the instability, i.e., the efficiency of semiconvection may depend on the specific circumstances. More recent (two-dimensional) calculations by Biello (2001) show a sensitive dependence on the ratio of kinematic viscosity to heat diffusion (Prandtl number). For low Prandtl numbers, as are appropriate to stars, the cellular structure is unstable, suggesting relatively efficient semiconvection. Further numerical work, especially in three dimensions and at low Prandtl number, is definitely needed here.

Various empirical prescriptions exist for the semiconvective diffusion coefficient among those groups that study massive stars (Langer, El Eid, and Fricke, 1985; Woosley and Weaver, 1988; Langer, El Eid, and Baraffe, 1989). Other groups (e.g., Nomoto and Hashimoto, 1988; Maeder and Meynet, 1989; Bressen *et al.*, 1993) do not include semiconvection, but employ the Schwarzschild criterion, some with overshoot mixing (Sec. II.E.2; Maeder and Meynet, 1989), some without (Nomoto and Hashimoto, 1988). Still other groups prefer the strict Ledoux criterion (Stothers and Chin, 1992; Brocato and Castellani, 1993). Probably the strongest observational diagnostic of semiconvection is the statistics of red vs blue supergiants (Sec. III.B.1), but no single choice of convection parameter explains all the data (Langer and Maeder, 1995). The situation is further complicated because rotation can induce mixing in some of the same regions (Sec. II.F), and its effects might masquerade as a large semiconvection diffusion coefficient.

Practically speaking, semiconvection matters most (i) in the region outside of the helium core just following central hydrogen depletion; (ii) during convective helium-core burning; and (iii) during silicon burning. In the first case, the gradient of hydrogen to helium left behind as the convective hydrogen core receded either mixes or does not mix depending on the prescription adopted. This mixing affects the gravitational potential where the hydrogen shell ignites, which in turn affects whether the star is a red or blue supergiant (Lauterborn, Refsdal, and Roth, 1971; Lauterborn, Refsdal, and Weigert, 1971; Kippenhahn and Weigert, 1990). A deeper potential, which happens with less mixing (Ledoux), means a redder star. Figure 3 shows "fingers" of semiconvective mixing outside the hydrogen convective core as it shrinks (more apparent in higher masses) and at the boundary of the helium convective core. This calculation and others to follow in this review used a relatively large semiconvective diffusion coefficient amounting to approximately 10% $D_r$ (Woosley and Weaver, 1988). Equation (14) gives a much smaller value, and the use of $D_{semi}=0.1D_r$ implies that rotation plus instabilities have been effective at breaking down the cellular structure assumed in Eq. (14).

During helium burning, stellar evolution models with a very small amount of semiconvection sometimes develop a numerical instability in which an atomic weight barrier develops and grows about halfway out in the helium core. This has the effect of bifurcating a region that, according to Schwarzschild, would have mixed. If it does not mix, the outer part of the convective core burns little helium and the inner part evolves as a smaller carbon-oxygen core, thus producing fewer heavy elements and a smaller iron core. It seems unlikely that this bifurcation would persist in a multidimensional model, but such calculations are thus far absent. The larger value of diffusion coefficient used by Woosley and Weaver (1988) and in the models presented in this review suppresses that instability. The resulting helium cores and carbon-oxygen cores are shown in Fig. 4.

In silicon burning, electron capture leads to a discontinuity in $Y_e$ [Eq. (4)] at the outer edge of the convective zone. This inhibits the growth of the convective shell if the Ledoux criterion (or Ledoux plus semiconvection) is used, but does not if the Schwarzschild criterion is used. This may be one of several reasons for different iron-core sizes among the groups who study silicon burning (Sec. V.A).

#### 2. Overshoot mixing

The transport of energy by convection implies inertial motion and the mixing requires a turbulent cascade, both of which are usually neglected in the stellar models. Physically, one expects that the tops and bottoms of convective regions will not be precisely defined, but spread over some distance that might depend on the convective velocities and entropy barriers. A physical theory is presently lacking. What is usually employed instead is diffusive mixing over a characteristic length scale, e.g., a fraction of a pressure scale height. Maeder and Meynet (1989), Chin and Stothers (1991), and Stothers and Chin (1991) have shown that the degree of overshoot mixing during hydrogen and helium burning cannot be too large or conflicts with observations result. In particular, the blue loops tend to disappear.

Less well studied, but of special significance in massive stars after helium burning, is the merger of multiple burning shells of heavy elements (carbon, neon, and oxygen) that can affect the nucleosynthesis and presupernova structure dramatically (Sec. VIII.B.2; Fig. 10, below).

### F. Rotation

It is well known that massive stars on the main sequence rotate rapidly. Typical equatorial rotation veloci-

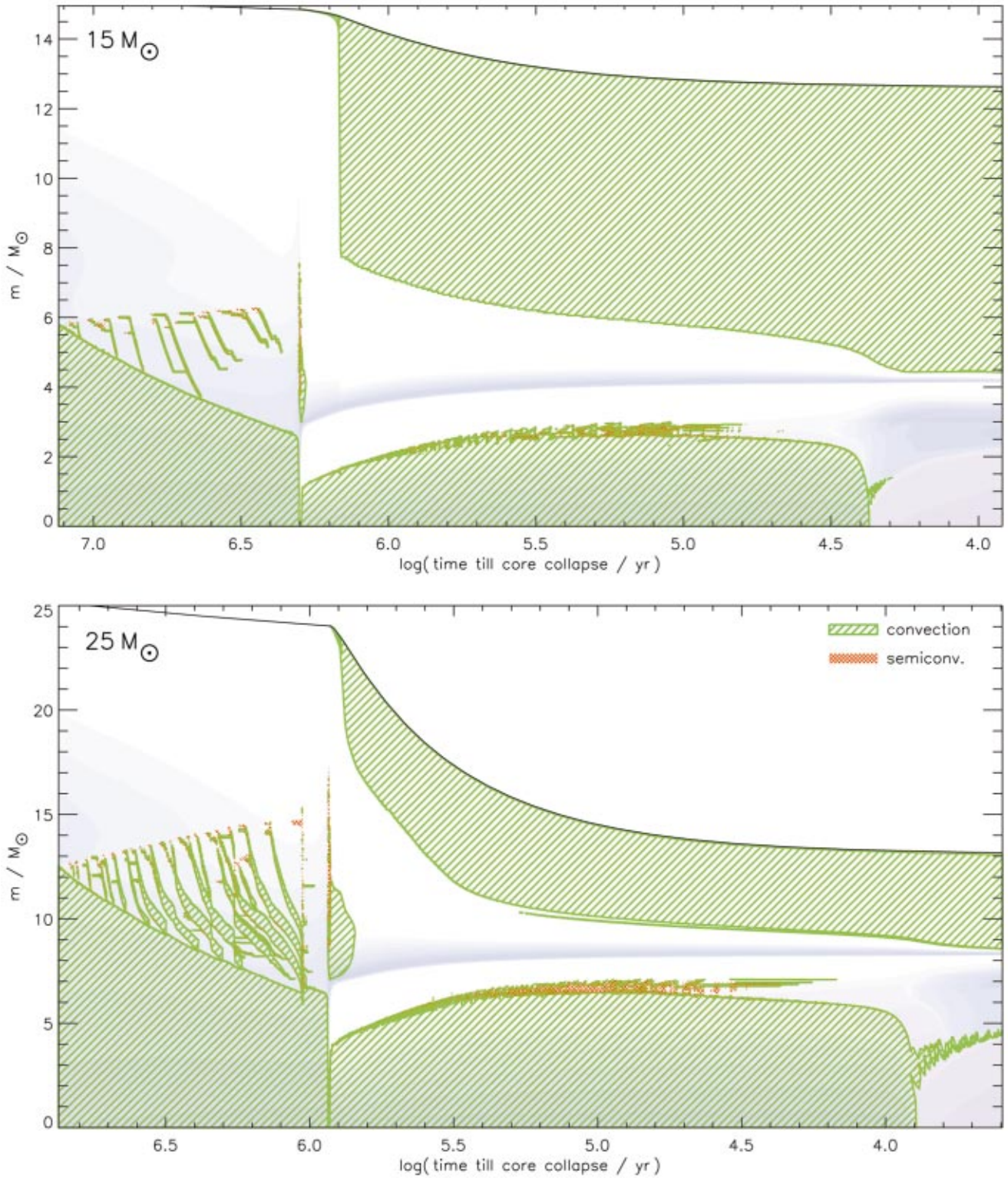


FIG. 3. Convective history as a function of interior mass for $15M_\odot$ and $25M_\odot$ stars of solar metallicity during hydrogen and helium burning. Evolution is measured by the logarithm of the time remaining until the death of the star as a supernova, plotted so as to exaggerate the later burning stages. Green hatched regions are fully convective and red cross-hatched regions are semiconvective (see Sec. II.E.1). Levels of blue and pink shading indicate orders of magnitude of net energy generation (nuclear energy generation minus neutrino losses), with blue reflecting positive values and pink indicating negative ones. Note the development of an extended convective envelope characteristic of a red supergiant late during helium burning. The hydrogen core shrinks towards the end of hydrogen burning; the helium core grows as helium is depleted. The entire star shrinks in mass owing to mass loss [Color].

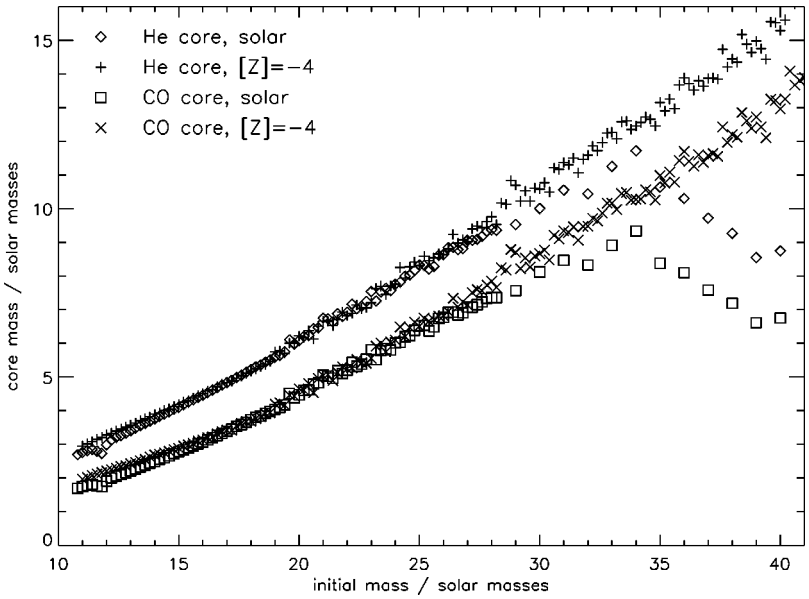


FIG. 4. Final helium and carbon-oxygen core masses for a grid of single stars of solar metallicity and $10^{-4}$ solar metallicity. All stars were evolved including mass loss as described in Sec. II.G. For stars heavier than about $35M_{\odot}$, mass loss in solar metallicity stars appreciably reduces the final helium-core mass.

ties are on the order of 200 km $s^{-1}$ (Fukuda, 1982), i.e., a significant fraction of their breakup rotation velocity. Even if such stars rotate rigidly, specific angular momenta this large implies that centrifugal effects could play an important, even dominant, role in the advanced stages of evolution (Endal and Sofia, 1976, 1978). The situation is complicated, however, because the star can transport angular momentum in convective regions and in radiative layers due to circulation and other instabilities (see, for example, Endal and Sophia, 1978; Knoblock and Spruit, 1983; Zahn, 1992; Talon *et al.*, 1997; Maeder and Zahn, 1998; Maeder and Meynet, 2000a) and lose mass. When the outer layers of a star expand, their angular velocity decreases. If this slower rotation rate is communicated to layers deeper in, angular momentum can be extracted from the core by a wind (Langer, 1998). The actual distribution of angular momentum in advanced stages is sensitive to the efficiency for coupling differentially rotating regions by instabilities and magnetic torques (Maheswaran and Cassinelli, 1994) and the magnitude and geometry of mass loss (bipolar outflow?); see Maeder and Meynet (2000b). Fortunately the results are not too sensitive to the initial distribution of angular momentum, since convection and Eddington-Sweet circulation tend to enforce rigid rotation early on the main sequence.

Heger, Langer, and Woosley (2000) and Maeder and Meynet (2000a, 2000c) describe the various instabilities and processes that lead to mixing and angular momentum transport in massive stars. Chief among these are Eddington-Sweet circulation and shear instabilities, the latter being particularly effective at convection boundaries (and therefore mimicking convective overshoot and semiconvection in some ways). For the simplest assumptions—rigid rotation on the main sequence, radial mass loss, no magnetic fields—they and Meynet and Maeder (2000) find that large angular momenta persist inside the carbon-oxygen core, sufficiently large to affect the explosion mechanism (Fryer and Heger, 2000) and produce submillisecond pulsars (Heger, Langer, and Woosley, 2000). However, magnetic fields may play an important role and are just starting to be considered (Sec. IV. E). The situation could be different in Wolf-Rayet stars since they experience more mass loss. (Wolf-Rayet stars are massive stars with strong winds and thus broad emission lines and altered surface compositions reflecting the presence of ashes from nuclear burning. Hydrogen is either deficient, as in WNL stars, or completely absent, as in WC and WO stars. Because of the lack of hydrogen, supernovae coming from such stars are of type I. The N, C, and O subtypes of Wolf-Rayet stars indicate the presence of strong lines of nitrogen, carbon, or oxygen in their spectra. Supernovae originating in such stars are classified as type I, though they are not related to the typical type-Ia supernovae.)

Most Wolf-Rayet stars are probably slow rotators when they die as type-I supernovae (Maheswaran and Cassinelli, 1994). For stars that lose only a little mass, the angular momentum in the core will be larger. It is not certain, however, that convection will naturally lead to rigid corotation within the convective region (Kumar, Narayan, and Loeb, 1995), and the details of the angular momentum transport are uncertain, especially at boundary layers.

While angular momentum is an important consideration for the late stages, the effects of rotation on the observed properties of hydrogen- and helium-burning stars are much better documented and studied. Deeper mixing than occurs without rotation seems necessary to explain the observed surface enhancements of helium, nitrogen, and sodium and the surface depletion of boron (Fliegner, Langer, and Venn, 1996; Heger and Langer, 2000; Maeder and Meynet, 2000c). Rotation also leads to larger helium cores for a given main-sequence mass and to larger carbon oxygen cores for a given helium-core mass. By altering the ratio of core mass to envelope, the late evolution of stars of a given main-sequence mass is appreciably affected. By inducing

additional mixing, rotation reduces the disparity between results obtained using the Ledoux and Schwarzschild convective criteria. Entropy barriers that would have inhibited convection in the Ledoux case are traversed by rotational mixing. Because of the larger helium core, rotating stars also have higher luminosities as supergiants and thus, for a given main-sequence mass, experience more mass loss

### G. Mass loss

#### 1. Single stars

O and B stars have radiatively accelerated winds that are relatively well understood (Lamers and Cassinelli, 1999; Kudritzki and Puls, 2000) and do not represent a major source of uncertainty for stellar evolution models. Commonly employed prescriptions are given by Chiosi and Maeder (1986), DeJager, Nieuwenhuijzen, and van der Hucht (1988), Maeder (1990), and Nieuwenhuijzen and DeJager (1990). However, massive stars may lose much of their mass during post-main-sequence evolution, i.e., as red supergiants for $M \lesssim 35 M_\odot$ and as luminous blue variables or Wolf-Rayet stars for higher masses. For all these late stages, we have neither reliable empirical mass-loss rates nor quantitative mass-loss theories.

Significant constraints on the post-main-sequence mass loss come from the distribution of luminous stars in the Hertzsprung-Russell (HR) diagram. First, the absence of luminous red supergiants with $\log L/L_\odot > 5.7$ (Humphreys and Davidson, 1979) can be reconciled with stellar models by assuming that correspondingly massive stars ($M \gtrsim 50 M_\odot$) lose most of their hydrogen envelope before helium ignition. The idea that they do so as luminous blue variables at the Humphreys-Davidson (1979) limit—the location of the observed, highly unstable luminous blue variables, which apparently all have ejected circumstellar nebulae (Nota *et al.*, 1995)—results, for a given stellar model, directly in a mass-loss rate (Langer, 1989a). Second, the large number of relatively faint ($\log L/L_\odot \approx 4.5$–$5.0$) Wolf-Rayet stars (Hamann, Koesterke, and Wessolowski, 1995), which, due to a very narrow mass-luminosity relation for those objects (Maeder, 1983; Langer, 1989b), indicates a mass in the range $\sim 5$–$8 M_\odot$ for them, as well as the large number of WC-type stars (which show core-helium-burning products at their surfaces), implies a very large amount of mass loss in the Wolf-Rayet stage.

In fact, for current empirical mass-loss rates, all solar metallicity stars initially more massive than $\sim 35 M_\odot$ are thought to end their lives as hydrogen-free objects of roughly $5 M_\odot$ (Schaller *et al.*, 1992; Meynet *et al.*, 1994). This not only prevents the very massive stars ($M \gtrsim 100 M_\odot$) from exploding through the pair-formation mechanism, but also limits the mass of the iron core produced at the end of their thermonuclear evolution to values below $\sim 2 M_\odot$ (Fig. 17 below) and drastically increases the probability for a successful hydrodynamic supernova explosion compared with the situation without mass loss. Due to the lack of hydrogen, those supernovae would be classified as type Ib or Ic (Sec. IX.E).

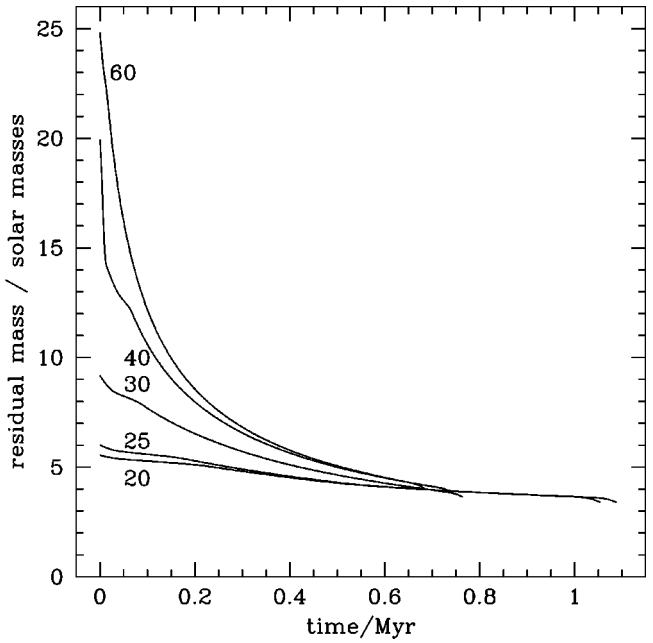


FIG. 5. The mass of helium cores for a grid of helium cores evolved through helium burning using mass-dependent mass loss. These stars lost their hydrogen-rich envelopes early in helium burning to a binary companion and originally had masses on the main sequence of $60 M_\odot$, $40 M_\odot$, $30 M_\odot$, $25 M_\odot$, and $20 M_\odot$. The cores converge on a narrow range of final masses between $4.07 M_\odot$ and $3.39 M_\odot$, which may be appropriate for type-Ib and type-Ic supernovae (Woosley, Langer, and Weaver, 1995). From Wellstein and Langer (1999) and N. Langer (2001).

Once the helium core is uncovered, the nature and rate of mass loss changes appreciably. Langer (1989a) has argued for a strongly mass-dependent mass-loss rate. The masses derived for Wolf-Rayet stars on the basis of their mass-luminosity relation (Maeder, 1983; Langer, 1989b; Schaerer and Maeder, 1992) can be as small as $\sim 4 M_\odot$ (van der Hucht, 1992; Hamann, Koesterke, and Wessolowski, 1993) without showing any major deviation from the general mass-loss relation. A recent linear analysis of pulsational instability (Glatzel, Kiriakidis, and Fricke, 1993) showed helium stars above $\sim 4 M_\odot$ to be unstable with respect to radial pulsations, with a growth time of order only a few dynamical time scales. Such instabilities are a possible physical explanation of the strong Wolf-Rayet wind observed for helium stars with $M \gtrsim 4 M_\odot$ and might imply a pileup of final masses near this value (Langer *et al.*, 1994; Fig. 5).

One current prescription (Wellstein and Langer, 1999) for mass loss in massive stars would be to use (a) the mass-loss rate of Niewenhuijzen and DeJager (1990) for stars cooler than 15 000 K; (b) theoretical radiation-driven wind models by Kudritzki *et al.* (1989) and Pauldrach *et al.* (1994) for OB stars with temperatures over15 000 K; and (c) empirical mass-loss rates for Wolf-Rayet stars from Hamann, Schoenberner, and Heber (1982) reduced by a factor of 3 (Hamann and Koesterke, 1998; Langer, 2001),

$$\log\left(\frac{\dot{M}}{M_\odot\ \mathrm{yr}^{-1}}\right)=\begin{cases}-12.43+1.5\log(L/L_\odot)-2.85X_s & \text{if } \log(L/L_\odot)\geqslant 4.45\\ -36.28+6.8\log(L/L_\odot) & \text{if } \log(L/L_\odot)<4.45,\end{cases} \tag{15}$$

with $X_s$ the surface mass fraction of hydrogen. An important consideration, aside from the accuracy and generality of the equations themselves, is their scaling with metallicity. The above values are for stars of solar metallicity. There is some suggestion that radiative winds may scale with $(Z/Z_\odot)^{1/2}$ (Kudritzki, 2000; Vanbeveren, 2001) or perhaps $Z^{2/3}$ (Vink, de Koter, and Lamers, 2001). The dependence of Wolf-Rayet mass-loss rates on the initial metallicity of the star is unknown, but there are indications that the mass-loss rate of WC stars also scales as $Z^{1/2}$, where $Z$ is approximately the surface carbon abundance made by the star (Nugis and Lamers, 2000).

### 2. Mass loss in binaries

If a star is located in a binary system with separation small enough that one star or the other crosses its Roche lobe before dying, the evolution of both stars is obviously altered (Podsiadlowski, Joss, and Hsu, 1992; Vanbeveren, DeLoore, and Van Rensbergen, 1998; Wellstein and Langer, 1999). This may occur for approximately one-third of all massive stars. Possibilities range from complete loss of the hydrogen envelope—ultimately leading to death as a type-Ib/c supernova—to the complete merger of the two stars by way of a common envelope phase (the designation Ib or Ic has to do with the strength of a helium line feature in the spectrum, but both are thought to be produced by the deaths of Wolf-Rayet stars). The possibilities and literature are beyond a short summary here, but we mention just a few key points.

Mass transfer can be segregated into three categories, depending on the evolutionary state of the primary: (a) In case A, transfer occurs while the primary is still on the main sequence; (b) case B occurs after H depletion but before helium depletion; and (c) case C occurs after helium depletion (Kippenhahn and Weigert, 1967). Most interacting massive stars are believed to follow case B/case C without the formation of a common envelope (Fig. 16 of Podsiadlowski *et al.*, 1992) and end up as either type-Ib supernovae or type-II with very-low-mass hydrogen envelopes. Table II (Wellstein and Langer, 1999) lists some possible outcomes for stars of different masses. It is interesting that membership in a close binary can raise the threshold mass for making a supernova from $8M_\odot$ or so to $13M_\odot$. This is because removing the envelope early in helium burning puts a halt to the growth of the helium core by hydrogen-shell burning and also removes some of the helium core itself. Type-Ib and type-Ic supernovae are made when the hydrogen envelope is lost (Sec. IX.E); it is assumed that if the helium layer is also mostly shed, leaving only part of the carbon-oxygen core, the supernova will be of type Ic. The critical masses for black-hole formation depend on uncertain aspects of the explosion mechanism (Secs. V and VI.A).

In addition to the parameters of the binary (masses, separation, etc.), the outcome of binary evolution is sensitive to the theory of convection employed (Sec. II.E). Use of the Ledoux criterion causes the star to become a red giant and to commence mass transfer when the helium mass fraction is higher than that obtained using the Schwarzschild criterion.

One well-studied example of binary evolution affecting a supernova progenitor is SN 1993J. Aldering, Humphreys, and Richmond (1994) estimated the bolometric magnitude of the progenitor star, corrected for the presence of a binary companion, to be $-7.8$, or $L=4.0\times10^{38}\ \mathrm{erg\,s^{-1}}$, appropriate for a star of approximately $16M_\odot$, and yet the evolution of the light curve suggests that the star had an envelope mass of about $0.2M_\odot$ (Woosley, Eastman, *et al.*, 1994). Since stars of this mass

TABLE II. Supernovae and remnants of massive stars of solar metallicity. Note: Based on Wellstein and Langer (1999), slightly altered.

| Initial mass ($M_\odot$) | Binary mass transfer | | | |
|---|---|---|---|---|
| | Case A | Case B | Case C | Single star |
| 8···13 | | | SN Ib | SN IIp |
| | WD | WD | NS | NS |
| 13···16 | | SN Ib/Ic | SN Ib | SN IIp |
| | WD | NS | NS | NS |
| 16···25 | SN Ib | SN Ib | SN Ib | SN IIp |
| | NS | NS | NS | NS |
| 25···35 | SN Ic | SN Ic | SN Ib | SN IIL |
| | NS | NS | BH | BH |
| >35 | SN Ic | SN Ic | SN Ib | SN Ic |
| | NS/BH | NS/BH | NS/BH | NS/BH |

are not expected to lose a significant fraction of their hydrogen envelope to a wind, the implication is that a binary companion was instrumental in stripping the star (Nomoto *et al.*, 1993; Podsiadlowski *et al.*, 1993; Bartunov *et al.*, 1994; Filippenko, Matheson, and Barth, 1994; Utrobin, 1994). Since it also turns out that $0.2M_\odot$ is the minimum envelope mass required to maintain a red supergiant structure for a helium core of $5M_\odot$ (implied by the presupernova luminosity), the implication is that rapid mass transfer occurred until all the envelope was lost except that part necessary to maintain the Roche radius. Had such mass loss occurred by a wind early during helium burning instead of by Roche lobe overflow late during carbon burning, one would have expected all the remaining hydrogen to be lost to a radiative wind and the supernova to be type Ib rather than type II as was observed. Thus SN 1993J is apparently an example of case C or at least late case B mass transfer.

## III. MAIN-SEQUENCE AND HELIUM-BURNING EVOLUTION

A massive star spends about 90% of its life burning hydrogen and most of the rest burning helium (Table I). Typically these are the only phases of the star that can be studied by astronomers (the progenitors of SN 1987A and SN 1993J were exceptions). These relatively quiescent phases, when convection and radiation transport dominate over neutrino emission, also determine what follows during the advanced burning stages and explosion. A good recent review of all aspects of massive stellar evolution during hydrogen and helium burning has been given by Maeder and Conti (1994). Chiosi, Bertelli, and Bressen (1992) have discussed massive stellar evolution as a part of a larger review of the Hertzsprung-Russell diagram. Maeder and Meynet (2000a) have reviewed rotation and the upper main sequence. Grids of stellar models, including massive stars, have been evolved through hydrogen and helium burning by Schaerer, Meynet, *et al.* (1993), Schaerer, Charbonnel, *et al.* (1993), Schaller *et al.* (1992), Meynet *et al.* (1994), and Charbonnel *et al.* (1993, 1996). Because we wish to give emphasis to supernovae and the advanced stages of evolution, our discussion of main-sequence evolution and helium burning is relatively brief and concentrates on nuclear physics issues.

### A. Nuclear physics

#### 1. Hydrogen burning

The relevant nuclear reactions for hydrogen burning in massive stars are the carbon-nitrogen-oxygen-cycle, especially $^{12}\mathrm{C}(p,\gamma)^{13}\mathrm{N}(e^+\nu)^{13}\mathrm{C}(p,\gamma)^{14}\mathrm{N}(p,\gamma)^{15}\mathrm{O}(e^+\nu)^{15}\mathrm{N}(p,\alpha)^{12}\mathrm{C}$ and various side channels thereof (i.e., the "CNO tricycle"; see, for example, Rolfs and Rodney, 1988). The energy released by hydrogen burning depends upon the initial composition, but for a composition of 70% hydrogen by mass it is $4.51\times10^{18}$ erg g$^{-1}$ (26.731 MeV per helium produced). Subtracting the energy carried away by neutrinos (1.71 MeV per helium) gives the net energy deposition, $\sim4.22\times10^{18}$ erg g$^{-1}$ ($\sim$24.97 MeV per helium). This is somewhat less than that deposited by hydrogen burning in low-mass stars like the sun because the neutrinos emitted in the CNO cycle are more energetic. Reaction rates that govern energy generation and stellar structure (in contrast to nucleosynthesis) are relatively well determined for the CNO cycle (Caughlan and Fowler, 1988; Rolfs and Rodney, 1988; Adelberger *et al.*, 1998; Angulo *et al.*, 1999; and references therein), though recent studies (Adelberger *et al.*, 1998; Angulo and Descouvemont, 2001) suggest some uncertainty in $^{14}\mathrm{N}(p,\gamma)^{15}\mathrm{O}$.

#### 2. Helium burning

The two principal nuclear reactions by which helium burns are $3\alpha\rightarrow{}^{12}\mathrm{C}$ and $^{12}\mathrm{C}(\alpha,\gamma)^{16}\mathrm{O}$. The nuclear energy release is 7.275 MeV for the first reaction and 7.162 MeV for the second. Assuming a starting composition of pure helium, this gives $5.85+2.86X(^{16}\mathrm{O})\times10^{17}$ erg g$^{-1}$, where $X(^{16}\mathrm{O})$ is the final mass fraction of oxygen. Stars of solar metallicity additionally contain about 2% of $^{14}\mathrm{N}$ in the helium core after completion of hydrogen burning. Before the energy release by the $3\alpha$ reaction becomes appreciable, this nitrogen burns away completely by $^{14}\mathrm{N}(\alpha,\gamma)^{18}\mathrm{F}(\beta^+\nu)^{18}\mathrm{O}$, releasing approximately $10^{16}$ erg g$^{-1}$ for solar metallicity. This powers a brief episode of convective nitrogen burning that precedes helium burning. Later, towards the end of helium burning, this $^{18}\mathrm{O}$ is converted to $^{22}\mathrm{Ne}$ and still later provides neutrons for the *s* process (Sec. III.E)

Rates for the $3\alpha$ reaction and $^{14}\mathrm{N}(\alpha,\gamma)^{18}\mathrm{F}$ are relatively well determined (Caughlan and Fowler, 1988; Rolfs and Rodney, 1988; Angulo *et al.*, 1999; and references therein). However, the reaction $^{12}\mathrm{C}(\alpha,\gamma)^{16}\mathrm{O}$ warrants special discussion as it affects not only the ratio of carbon and oxygen to come out of helium burning, but indirectly the nucleosynthesis of many other species and the very structure of the presupernova star (Sec. V.A). Determination of an accurate rate for this reaction is experimentally challenging because it proceeds predominantly through two subthreshold resonances whose critical alpha widths must be determined indirectly [the excited states are at 7.117 MeV($1^-$) and 6.917 MeV($2^+$); the $Q$ value is 7.162 MeV]. Though the temperature sensitivity of the rate is of some importance (Buchmann, 1996), the rate is often expressed in terms of the $S$ factor at 300 keV, a representative energy for the Gamow peak during helium burning. The rate is divided into three parts: (a) the electric dipole part that proceeds through the $1^-$ resonance; (b) the electric quadrupole part that goes through the $2^+$ state; and (c) everything else. Recent studies by Azuma *et al.* (1994) and summarized by Barnes (1995) suggest an $S$ factor for the $E1$ part of $79\pm21$ keV b (one-sigma error bar). The $E2$ part is less certain but is thought to lie in the range $44^{+12}_{-18}$ keV b (Tischhauser, 2000). Including a contribution from other states and from direct capture adds $16\pm16$ keV b for a total of $137\pm33$ keV b. Buchmann *et al.* (1996) have suggested a value with a broader

range, $165 \pm 75$ keV b, and Buchmann (1996) recommends a value of 146 keV b with lower and upper limits of 62 and 270 keV b, respectively. More recently, Kunz *et al.* (2001, 2002) using an $R$-matrix fit to new data, obtained an $S$ factor of $165 \pm 50$ keV b and a temperature dependence—at helium-burning conditions—very much like that found by Buchmann. In summary, the preferred values of the day for $S(300\,\text{keV})$ lie in the range 100–200 keV b, but with a preference for 150–170 keV b. This uncertainty is far too large for a rate of this importance. Based upon nucleosynthesis arguments, Weaver and Woosley (1993) estimated a total $S$ factor of $170 \pm 20$ keV b, which is quite consistent with current experiments. An implication of their work is that the acceptable experimental error bar on the total rate must be $\lesssim 10\%$.

### B. Observational diagnostics of hydrogen and helium burning

We shall be brief in discussing this diverse and well-studied topic. See the references given at the beginning of this section for such topics as the evolution of massive stars in the HR diagram as a function of mass and metallicity. Here we briefly consider one issue, the nature of the star whose explosion we observed as SN 1987A, and the related topic of red and blue supergiants. These are important in understanding the kinds of supernovae that massive stars will produce.

#### 1. Red-to-blue supergiant ratios

Models for supergiant stars, those with extended envelopes supported by helium burning either central or in a shell, are often found near a boundary separating a red and a blue solution, the red solution being a convective envelope with lower temperatures, higher opacities, and a much larger radius than the blue radiative one (Woosley, Pinto, and Ensman, 1988; Tuchman and Wheeler, 1989, 1990). Intermediate solutions are thermally unstable. The ratio of blue to red supergiants is thus a sensitive test of stellar structure calculations, especially of semiconvection. Langer and Maeder (1995) and Maeder and Meynet (2000a, 2001) recently surveyed the observations and models. Observations show that the blue-to-red ratio is an increasing function of metallicity. All present-day models have difficulty producing this trend. Models that use the Ledoux criterion and a moderate amount of semiconvection agree with observations at low metallicity, but produce too many red supergiants at high metallicity. On the other hand, models that use the Schwarzschild criterion with some convective overshoot mixing agree with observations at high metallicity, but predict too many blue supergiants at low metallicity. Some solution incorporating aspects of both is indicated, with effects of molecular weight gradients important in low-metallicity stars but an increasing amount of semiconvection and convective overshoot in higher-metallicity stars. Rotationally induced mixing may also be important and is just starting to be explored in this context (Maeder and Meynet, 2001).

#### 2. SN 1987A

Related to the issue of red and blue supergiants is the progenitor star of Supernova 1987A (see reviews by Arnett, Bahcall, *et al.*, 1989; Arnett, Fryxell, and Müller, 1989; Hillebrandt and Höflich, 1989). Sk 202-69 was known to be a blue supergiant at the time it exploded. However, observations of low-velocity, nitrogen-rich circumstellar material (Fransson *et al.*, 1989) show that the star was a red supergiant until roughly 30 000 years before the explosion. Explanations for this behavior (blue on the main sequence; red, at least at the end of helium burning; blue supernova progenitor), in a star known to be about $20M_\odot$ (Walborn *et al.*, 1987; Woosley, 1988; Woosley, Pinto, and Ensman, 1988), separate into two classes: single-star models and binaries.

In the single-star models, the evolution inferred from observations is best replicated by a combination of reduced metallicity and reduced semiconvection (see, for example, Woosley, 1988; Langer, El Eid, and Baraffe, 1989; Weiss, 1989; Langer, 1991a). The reduced metallicity, appropriate to the Large Magellanic Cloud, decreases the energy generation at the hydrogen shell and the opacity of the envelope, both of which favor a radiative solution. Hints that low metallicity might be involved in making a blue supernova progenitor were found in earlier calculations by Brunish and Truran (1982), Arnett (1987), and Hillebrandt *et al.* (1987), but none of these gave an evolution in the HR diagram like SN 1987A, which, as noted, was a red supergiant until shortly before it exploded. Restricted semiconvection is also required. Reducing semiconvection changes the gravitational potential at the helium-burning shell in the presupernova star in such a way as to favor blue loops. In particular, the helium-burning shell (edge of the carbon core) is located much deeper in the star in the low-semiconvection case. If this is the correct explanation, one would expect many other stars of Large and Small Magellanic Cloud composition to produce SN 1987A-like events, but not stars of all masses. Using the same prescription, stars of less than about $15M_\odot$ or more than about $22M_\odot$ would still die as red supergiants (Langer, 1991b). Rotation may also be important in explaining the history of Sk 202-69 (Saio, Kato, and Nomoto, 1988; Weiss, Hillebrandt, and Truran, 1988; Langer, 1991c, 1992). Extra mixing may make an envelope that is rich in helium, hence heavier and more prone to a blue solution. Rotation may also be necessary to explain the large nitrogen enrichment in the red supergiant wind and the asymmetric mass outflow implied by the observed circumstellar ring structure (Chevalier and Soker, 1989). However, rotational mixing might negate the effects of reduced semiconvection in the helium core, leading to a helium-burning shell further out and a red progenitor.

Binary solutions to the Sk-202-69 problem also exist and have been given added impetus by the observations of the double-lobed shell structure recently observed by the Space Telescope (Braun and Langer, 1995). Explanations for this require a strong asymmetry in the red

giant mass outflow that might be more easily understood in a binary system. The binary solutions further subdivide into accretion models (Podsiadlowski and Joss, 1989; Tuchman and Wheeler, 1990; De Loore and Vanbeveren, 1992) and merger models (Hillebrandt and Meyer, 1989; Podsiadlowski, Joss, and Rappaport, 1990; Podsiadlowski, 1992, 1994). The accretion models invoke the addition of mass, which may be helium and nitrogen rich, after the main-sequence evolution of the supernova progenitor is complete. This requires some tuning of time scales and the disappearance of the mass donor in an earlier supernova explosion, but creates a blue solution by increasing the envelope mass and helium content of the SN 1987A progenitor. The merger scenarios, which may be more natural, invoke a common envelope phase that triggers the transition from red to blue. A red supergiant of about $16–18M_{\odot}$ becomes a red supergiant late during helium burning (true if there is ample semiconvection) and expands to encompass a companion of $\sim 3M_{\odot}$, which is probably a main-sequence star. Part of the ensuing common envelope is ejected in the merger, but the main-sequence star is eventually tidally disrupted. Much of the material lost in the common envelope phase comes out in the orbital plane. Some helium may be dredged up or donated in the merger. The larger mass of the envelope plus its helium content cause the star to move to the blue on a thermal time scale. The additional dredging up of core material might explain the large nitrogen enhancement observed in the circumstellar medium and, in extreme cases, even *s*-process elements (Williams, 1987; Danziger *et al.*, 1988). A possible difficulty with the merger model is that it requires fine tuning to get the merger to happen just 30 000 years before the supernova and makes SN 1987A an uncommon event.

Podsiadlowski, Joss, and Hsu (1992) estimate that 5% of all massive stars may end their lives as blue supergiants because of merger with a companion. If this is the explanation for the progenitor of SN 1987A one would expect most (other) supernovae in the Large Magellanic Cloud to occur in red supergiants and further that a few percent of all supernovae, even those occurring in regions of solar metallicity, would be like SN 1987A. So far observations do not test this prediction.

### C. Nucleosynthesis during hydrogen burning

In massive stars, hydrogen burning is not particularly productive nucleosynthetically, at least compared with hydrogen burning in lower-mass stars (which make most of $^{13}$C, $^{14}$N, and some $^{23}$Na) and with other hotter burning stages in massive stars. It is estimated (Timmes, Woosley, and Weaver, 1995) that massive stars produce about one-fifth of the $^{14}$N in the sun and even less $^{13}$C and $^{15}$N (Sec. VIII.E.1).

Another hydrogen-burning product of interest is the long-lived radioactivity $^{26}$Al made in hydrogen burning and ejected in the winds of those massive stars that end up as Wolf-Rayet stars ($M>35M_{\odot}$). The $^{26}$Al is made by proton capture on $^{25}$Mg and is ejected before it has time to decay. Meynet *et al.* (1997) estimate that from 20% to 70% of the two $M_{\odot}$ of $^{26}$Al inferred to exist in the interstellar medium could be produced by such winds. However, Timmes *et al.* (1995) find that neon and carbon burning alone, without any contribution from stellar winds, can produce the abundance of $^{26}$Al inferred from measurements of gamma-ray lines (Sec. VIII.E.2).

The production of $^{17}$O in massive stars calculated by Woosley and Weaver (1995), though in good agreement with the solar value, is an overestimate when recent revisions to key reaction rates are included. Aubert, Prantzos, and Baraffe (1996) and Hoffman, Woosley, and Weaver (2001) find a substantially smaller yield using much larger reaction rates for $^{17}\mathrm{O}(p,\gamma)^{18}\mathrm{F}$ and $^{17}\mathrm{O}(p,\alpha)^{14}\mathrm{N}$ (Landré *et al.*, 1990; Blackmon *et al.*, 1995). Should these larger cross sections be confirmed [see the critical discussion of $^{17}\mathrm{O}(p,\alpha)^{14}\mathrm{N}$ in Adelberger *et al.*, 1998], $^{17}$O may have to be attributed to lower-mass stars or to novae (Jose and Hernanz, 1998).

### D. Nucleosynthesis during helium burning

#### 1. Carbon and oxygen

The principal products of helium burning are $^{12}$C and $^{16}$O. The ratio of these products affects not only their own nucleosynthesis but the future evolution of the star during carbon, neon, and oxygen burning. This ratio is determined by competition between the $3\alpha$ reaction and $^{12}\mathrm{C}(\alpha,\gamma)^{16}\mathrm{O}$, as shown in the rate equation

$$\frac{dY(^{12}\mathrm{C})}{dt} = Y_{\alpha}^{3}\rho^{2}\lambda_{3\alpha} - Y(^{12}\mathrm{C})Y_{\alpha}\rho\lambda_{\alpha\gamma}(^{12}\mathrm{C}). \tag{16}$$

It is an interesting coincidence of nature, characteristic only of helium burning, that two reactions should compete so nearly equally in the consumption of a major fuel. Carbon production occurs early on when the abundance of carbon is low and helium high; oxygen is made later. Equation (16) also shows that carbon production will be favored by high density, i.e., will be larger in stars of lower mass (lower entropy). A larger rate for $^{12}\mathrm{C}(\alpha,\gamma)^{16}\mathrm{O}$ also obviously favors a larger oxygen-to-carbon ratio at the end of helium burning.

Figure 6 shows the carbon abundance by mass fraction at the center of a grid of massive stars at a time when helium has all burned but carbon has not yet ignited. The expected gradual decrease of carbon abundance with increasing mass (decreasing density) is apparent. The evolution of helium cores (stars whose calculation is begun at helium burning rather than followed through the main-sequence evolution and whose mass is assumed constant) will give different results for the carbon-to-oxygen ratio. Growth of the helium core by hydrogen-shell burning is appreciable in massive stars, so the nucleosynthesis calculated for a helium core of constant mass will be different from that of a helium core of the same final mass evolved inside a star. In particular, the carbon mass fraction will be larger, reflecting

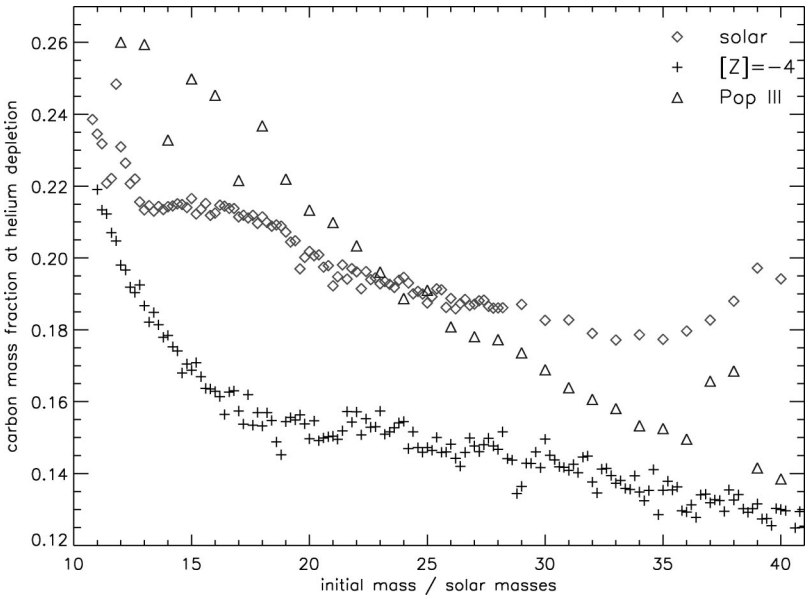


FIG. 6. Central carbon abundance at the end of helium burning ($T_c = 5\times10^8$ K) using a value for the $^{12}C(\alpha,\gamma)^{16}O$ reaction rate equal to 1.2 times that of Buchmann (1996); ◇, solar metallicity stars; +, for early Pop-II star ($10^{-4}$ solar metallicity); △, Pop-III stars ($Z=0$). The differences between points at a given mass reflect the different extent of the helium convection zone in the three populations. Mass loss was included in all calculations, but was important only for the case of solar metallicity.

the fact that a substantial fraction of helium burning occurred at lower mass and entropy.

The total amount of carbon and oxygen produced in a massive star is also sensitive to the treatment of semiconvection, convective boundary layers, and mass loss. If the amount of semiconvection is small or zero, a numerical instability often leads to the formation of semiconvective layers that split the helium convective core into subregions that show only little mixing with each other. The carbon-oxygen core that emerges is much smaller for a given helium-core mass (Langer, El Eid, and Fricke, 1985) and typically has a lower carbon abundance. It is doubtful that this instability exists in real multidimensional stars. It may also be removed by rotation (Heger, Langer, and Woosley, 2000; Maeder and Meynet, 2001). Carbon nucleosynthesis can also be increased by mass loss from the helium core. As the surface of the helium star moves in, the helium convective core shrinks, leaving behind the carbon-rich ashes of partial helium burning. It is possible that even most solar carbon is created in this way, though it is also reasonable to expect a contribution from low-mass stars. Ignoring mass loss, Timmes, Woosley, and Weaver (1995) find that about 1/3 of solar carbon is made in stars more massive than $8M_\odot$. Certainly most of the oxygen in the universe comes from helium and neon burning in massive stars.

### 2. $^{18}$O, $^{19}$F, and $^{21,22}$Ne

The neutron-rich isotope of oxygen, $^{18}$O, is made in massive stars by the reaction sequence $^{14}N(\alpha,\gamma)^{18}F(e^+\nu)^{18}O$ and is also destroyed at higher temperature by $^{18}O(\alpha,\gamma)^{22}Ne$. Its production is sensitive to $\alpha$-capture rates and to the treatment of semiconvection. Use of the Ledoux criterion tends to give larger $^{18}$O production, perhaps too much (Weaver and Woosley, 1993). On the other hand, the reaction rate for $^{18}O(\alpha,\gamma)^{22}Ne$ may be much larger than the Caughlan and Fowler (1988) value (Giesen *et al.*, 1993), and this may reduce the $^{18}$O yield (Aubert, Prantzos, and Baraffe, 1996). Woosley and Weaver (1995), using the Caughlan and Fowler rate and moderate semiconvection, find agreement with the solar abundance (Timmes, Woosley, and Weaver, 1995).

A portion of fluorine is also made during helium burning in massive stars by the reaction $^{15}N(\alpha,\gamma)^{19}F$ with $^{15}$N from $^{18}O(p,\alpha)^{15}N$ and protons from $^{14}N(n,p)^{14}C$ (Meynet and Arnould, 1993, 2000). However, most of the $^{19}$F is probably made by the neutrino process (Sec. VIII.B.4).

The neutron-rich isotopes of neon, $^{21}$Ne and $^{22}$Ne, are produced in helium burning, though $^{21}$Ne is also made in carbon burning. The abundances of $^{18}$O, $^{19}$F, and $^{22}$Ne all scale with the initial metallicity of the star since they are derived from nitrogen.

## E. The *s* process

The *s* process is one of nucleosynthesis by slow neutron capture—slow compared to the beta-decay lifetimes of nuclei near the line of stability (Burbidge *et al.*, 1957). Analysis of the solar abundances shows that two kinds of *s* processes have contributed to the synthesis of elements heavier than iron (Ulrich, 1973; Ward and Newman, 1978; Käppeler *et al.*, 1982; Walter, Beer, Käppeler, and Penzhorn, 1986; Walter, Beer, Käppeler, Reffo, and Fabbri, 1986), one characterized by a relatively weak neutron irradiation at relatively low temperature and the other stronger and hotter. The neutron density and temperature of the two components can be determined by an analysis of branching points along the *s*-process path where a beta decay is sensitive to the excited-state population of the parent nucleus. The results indicate a typical neutron density of 0.5–1.3 $\times10^8$ cm$^{-3}$ (Walter, Beer, Käppeler, and Penzhorn, 1986; Walter, Beer, Käppeler, Reffo, and Fabbri 1986) and temperature of about $3\times10^8$ K for the weak component associated with massive stars (Couch, Schmiede-

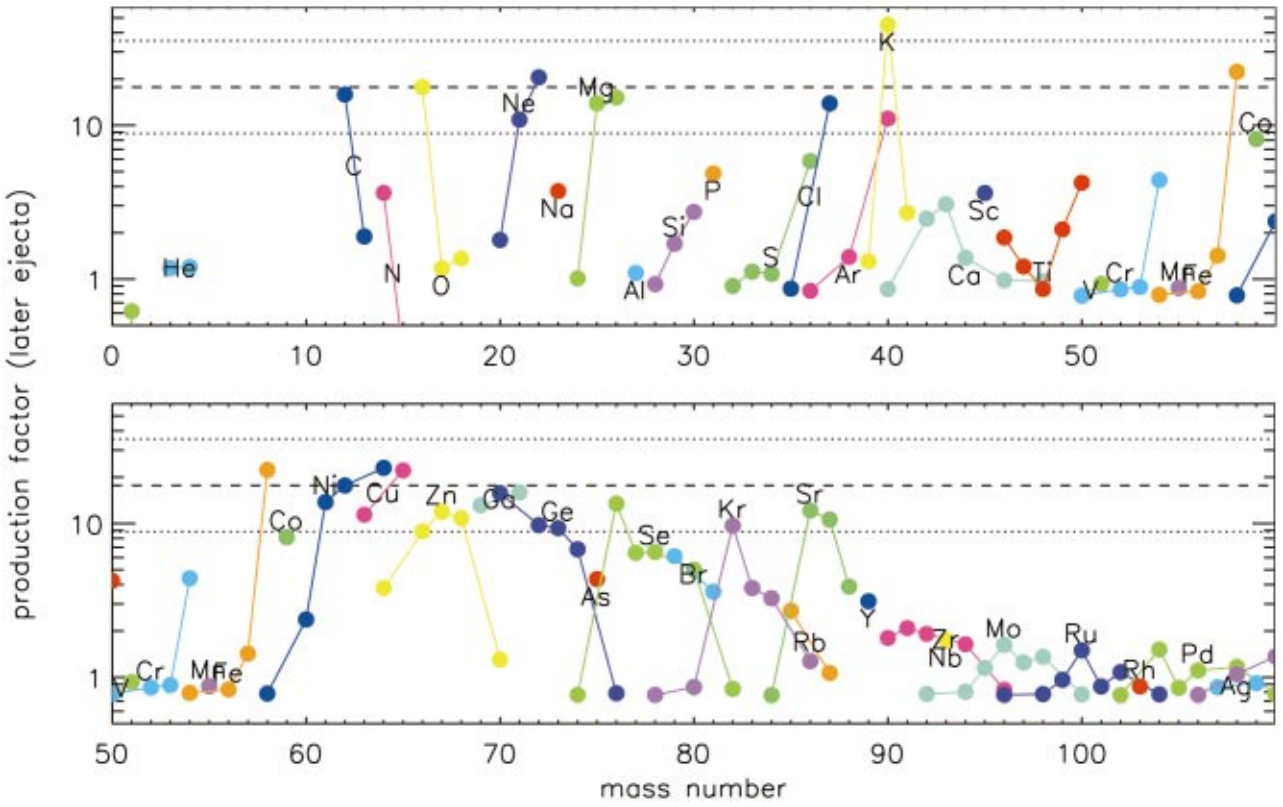


FIG. 7. Composition of a $25M_{\odot}$ star of solar metallicity at the end of helium burning compared with solar abundances (Rauscher *et al.*, 2002). The edit includes all mass outside the collapsed remnant mass including fallback ($1.96M_{\odot}$; see also Fig. 27) and all mass lost by stellar winds. Isotopes of a given element have the same color and are connected by lines. The plot is truncated at $A=100$. Little modification has occurred to species heavier than this. The prominent *s*-process production between $A=60$ and 88 is sensitive to the choice of key reaction rates, especially $^{22}\mathrm{Ne}(\alpha,n)^{25}\mathrm{Mg}$. Here the recent results of Jaeger *et al.* (2001) were employed. All values greater than unity indicate net production in hydrogen and helium burning [Color].

kamp, and Arnett 1974; Lamb *et al.*, 1977). The stronger *s* process is believed to occur in lower-mass stars found on the asymptotic giant branch (AGB) during a series of helium-shell flashes. It can be shown that these flashes give conditions that not only allow the production of *s*-process isotopes up to lead, but also naturally give a quasiexponential distribution of exposures (with only a small amount of material experiencing the strongest exposure), as is essential if the solar abundances are to be replicated (Ulrich, 1973).

The weak *s*-process component from massive stars, responsible for synthesizing isotopes up to $A\approx 88$, occurs chiefly during helium burning. Carbon and neon burning add a small additional exposure, perhaps of order 10%, and oxygen burning destroys whatever *s*-process nuclei its convective shell encompasses (Sec. VIII.B.3), so a completely accurate calculation of the *s*-process yield can be complicated. However, the helium-burning *s* process in massive stars has been studied many times (see, for example, Prantzos, Hashimoto, and Nomoto, 1990; Käppeller *et al.*, 1994; The, El Eid, and Meyer, 2000; Hoffman, Woosley, and Weaver, 2001), and the yields, for a given set of reaction cross sections are well determined. A recent calculation is shown in Fig. 7.

The reaction that produces neutrons for the *s* process in massive stars is $^{22}\mathrm{Ne}(\alpha,n)^{25}\mathrm{Mg}$ with the $^{22}$Ne coming from two $\alpha$ captures on the $^{14}$N left over from the CNO cycle. The amount of $^{22}$Ne thus scales linearly with the initial metallicity of the star. So, too, does the abundance of seed nuclei that capture neutrons, so the neutron-to-seed ratio is approximately constant independent of metallicity. The reaction $^{22}\mathrm{Ne}(\alpha,n)^{25}\mathrm{Mg}$ is, to an appreciable extent, "self-poisoning" in that most of the neutrons it produces are captured by $^{25}$Mg. The remainder capture on other nuclei having appreciable abundances and neutron capture cross sections. Of these $^{56}$Fe is most important, but other nuclei also participate and, given the rapid decline in natural abundances that occurs above mass number $A=60$, it turns out that even this weak exposure can produce most of the solar *s*-process abundances up to mass number 88.

Because the $^{22}\mathrm{Ne}(\alpha,n)^{25}\mathrm{Mg}$ reaction requires high temperature, the *s* process occurs late during helium burning, almost at the end, and full consumption of $^{22}$Ne occurs only in the more massive stars. An alternate way of converting $^{22}$Ne into $^{26}$Mg exists by $^{22}\mathrm{Ne}(\alpha,\gamma)^{26}\mathrm{Mg}$ that does not liberate free neutrons. The rates for these two reactions are uncertain and comparable during the conditions under which the *s* process occurs. Thus the

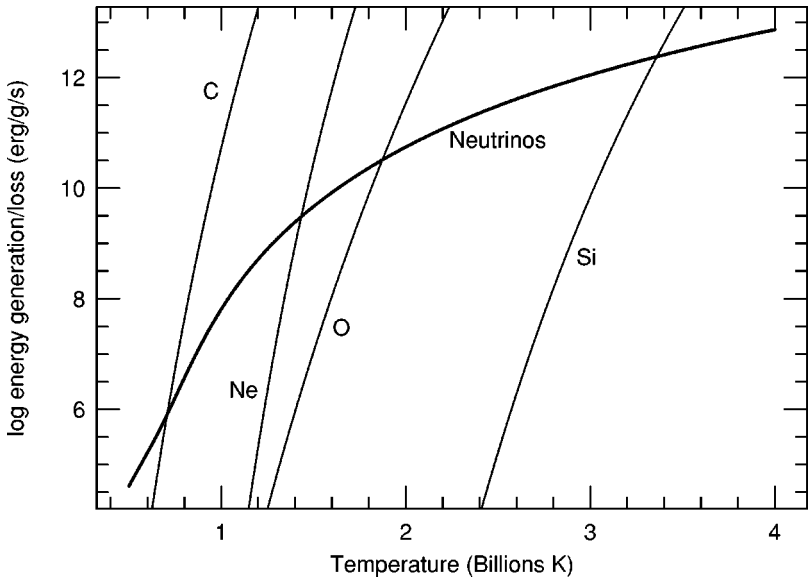


FIG. 8. Logarithm of the energy generation during the advanced burning stages of a massive star. The center of the star is assumed to follow a typical adiabat, $\rho = 10^6 T_9^3$ (Fig. 1). Neutrino losses (Munakata *et al.*, 1985) as a function of temperature are given as the dark line labeled "Neutrinos." The four steeper lines are simple approximations to the nuclear energy generation during carbon (C), neon (Ne), oxygen (O), and silicon (Si) burning that are discussed in the text. The intersections of these lines define the burning temperature for the given fuel—$T_9 = 0.7$ (C), 1.45 (Ne), 1.9 (O), and 3.4 (Si). The slopes of the lines near the intersection give the power of the temperature to which the burning is sensitive—$n = 32$ (C), 50 (Ne), 36 (O), and 49 (Si). These include the assumed temperature scaling of the density and are for assumed mass fractions C = 0.2, O = 0.7, Ne = 0.2, and Si = 0.5. Combustion of each gram of these four fuels yields a relatively constant energy, $q/10^{17}$ erg g$^{-1}$ = 4.0 (C), 1.1 (Ne), 5.0 (O), and 1.9 (Si). The lifetime of the burning stage is approximately $q$ times the mass fraction divided by the energy generation at balanced power, i.e., from thousands of years for C to less than a day for Si (Table I).

strength of the *s* process is sensitive to poorly determined nuclear quantities. Of particular interest is the 633-keV resonance in the $^{22}$Ne + $\alpha$ channel (Käppeller *et al.*, 1994). Various choices for the parameters of this resonance can give quite different strengths for the *s* process, though none so powerful as to move the *s*-process peak much above $A = 90$. Recent studies by Jaeger *et al.* (2001) suggest a diminished role for this resonance and a reaction rate no larger than the "lower bound" recommended by Käppeler *et al.* (1994). Figure 7 used the Jaeger *et al.* rate for $^{22}$Ne$(\alpha,n)^{25}$Mg and other recent reaction rates as described by Rauscher *et al.* (2001).

For stars with significantly less than solar metallicity, $^{12}$C and $^{16}$O can become significant poisons, resulting in a still weaker *s* process than the low seed abundances might suggest (Nagai *et al.*, 1995). For lower-mass stars in which $^{22}$Ne$(\alpha,n)^{25}$Mg is deferred until carbon burning, other poisons produced by carbon burning (Sec. IV.A.1) can also weaken the *s* process. The final *s* process ejected by a $15M_\odot$ supernova is significantly weaker than that for a $25M_\odot$ supernova (Rauscher *et al.*, 2001).

While the *s* process is often thought of as a way of making elements heavier than iron, a number of lighter isotopes are also made mostly by the *s* process in massive stars. These include $^{36}$S, $^{37}$Cl, $^{40}$Ar, $^{40}$K, and $^{45}$Sc. Appreciable amounts of $^{43}$Ca and $^{47}$Ti are also made by the *s* process in massive stars, though probably not enough to account for their solar abundance.

## IV. ADVANCED NUCLEAR BURNING STAGES

Because of the importance of neutrino losses, stellar evolution after helium burning is qualitatively different. Once the central temperature exceeds $\sim 5 \times 10^8$ K, neutrino losses from pair annihilation dominate the energy budget. Radiative diffusion and convection remain important to the star's structure and appearance, but it is neutrino losses that, globally, balance the power generated by gravitational contraction and nuclear reactions (Arnett, 1972a; Woosley, Arnett, and Clayton, 1972). Indeed, the advanced burning stages of a massive star can be envisioned overall as the neutrino-mediated Kelvin-Helmholtz contraction of a carbon-oxygen core (Fig. 1), punctuated by occasional delays when the burning of a nuclear fuel provides enough energy to balance neutrino losses. Burning can go on simultaneously in the center of the star and in multiple shells, and the structure and composition can become quite complex. Owing to the extreme temperature sensitivity of the nuclear reactions, however, each burning stage occurs at a nearly unique value of temperature and density (Fig. 8).

Nucleosynthesis in these late stages is characterized by a great variety of nuclear reactions made possible by the higher temperature, the proliferation of trace elements from previous burning stages, and the fact that some of the key reactions, like carbon and oxygen fusion, liberate free neutrons, protons, and $\alpha$ particles. It is impossible to keep track of all these nuclear transmuta-

tions using closed analytic expressions, and one must resort to "nuclear reaction networks," coupled linearized arrays of differential rate equations, to solve for the evolution of the composition. As we shall see, these late burning stages, both before and during the explosion of massive stars, account for the synthesis of most of the heavy elements between atomic mass 16 and 64, as well as the $p$ process and probably the $r$ process.

Except for a range of transition masses around $8-11M_\odot$, each massive star ignites a successive burning stage at its center using the ashes of the previous stage as fuel for the next (see Table I). Four distinct burning stages follow helium burning, characterized by their principal fuel—carbon, neon, oxygen, and silicon. Only two of these—carbon burning and oxygen burning—occur by binary fusion reactions. The other two require the partial photodisintegration of the fuel by thermal photons.

Because the late stages transpire so quickly (Table I; Fig. 8), the surface evolution fails to keep pace and "freezes out." If the star is a red supergiant, then the Kelvin-Helmholtz time scale for its hydrogen envelope is approximately 10 000 years. Once carbon burning has started, the luminosity and effective emission temperature do not change until the star explodes. Wolf-Rayet stars, the progenitors of type-Ib supernovae, continue to evolve at their surface right up to the time of core collapse.

### A. General nuclear characteristics

#### 1. Carbon burning

The principal nuclear reaction during carbon burning is the fusion of two $^{12}$C nuclei to produce compound nuclear states of $^{24}$Mg (here "*" indicates highly excited nuclear states of the nucleus), which then decay through three channels:

$$\begin{aligned} {}^{12}\mathrm{C}+{}^{12}\mathrm{C} \rightarrow {}^{24}\mathrm{Mg}^* &\rightarrow {}^{23}\mathrm{Mg}+n-2.62\ \mathrm{MeV} \\ &\rightarrow {}^{20}\mathrm{Ne}+\alpha+4.62\ \mathrm{MeV} \\ &\rightarrow {}^{23}\mathrm{Na}+p+2.24\ \mathrm{MeV}. \end{aligned} \tag{17}$$

The probability of decay through the proton channel is approximately the same as that for decay through the $\alpha$ channel, hence $B_p \approx B_\alpha \approx (1-B_n)/2$ (Caughlan and Fowler, 1988). The neutron branching ratio is temperature sensitive since the reaction is endoergic. At $T_9 = 0.8$, 1.0, 1.2, and 5, $B_n$ is 0.011%, 0.11%, 0.40%, and 5.4%, respectively (Dayras, Switkowski, and Woosley, 1977). Though small, the production of $^{23}$Mg is important since it may frequently decay [in competition with $^{23}\mathrm{Mg}(n,p)^{23}\mathrm{Na}$ at higher temperature] to $^{23}$Na with a consequent change in the neutron excess. Other reactions that significantly increase the neutron excess during carbon burning are (Arnett and Truran, 1969) $^{20}\mathrm{Ne}(p,\gamma)^{21}\mathrm{Na}(e^+\nu)^{21}\mathrm{Ne}$ and $^{21}\mathrm{Ne}(p,\gamma)^{22}\mathrm{Na}(e^+\nu)^{22}\mathrm{Ne}$. Owing to these reactions, even a star having zero initial metallicity develops, in those regions experiencing carbon burning and more advanced stages, an excess of neutrons (i.e., $Y_e < 0.50$) that is critical to its nucleosynthesis. In $15M_\odot$ and $25M_\odot$ stars of solar metallicity, $\eta = 1-2Y_e = 2.24\times10^{-3}$ and $1.96\times10^{-3}$ at the end of central carbon burning. Here the neutron excess is due chiefly to the production of $^{22}$Ne from $^{14}$N during helium burning. In $15M_\odot$ and $25M_\odot$ stars of zero initial metallicity, the neutron excesses are $1.24\times10^{-3}$ and $6.80\times10^{-4}$.

Since the neutrons, protons, and $\alpha$ particles released by carbon fusion may react on the principal products as well as with subsequent daughters, a host of reactions is possible, especially when one considers the large assortment of heavy nuclei left over from star formation, helium burning, and the helium-burning $s$ process. The final nucleosynthesis can only be determined using a nuclear reaction network of at least several hundred nuclei. The principal nuclei produced by carbon burning are (see, for example, Arnett and Thielemann, 1985) $^{16}$O (a survivor from helium burning), $^{20,21,22}$Ne, $^{23}$Na, $^{24,25,26}$Mg, and $^{26,27}$Al, with smaller amounts of $^{29,30}$Si and $^{31}$P. The production of species having $N>Z$ is sensitive to the neutron excess. There is also a milder $s$ process than in helium burning (Cameron, 1959; Acoragi, Langer, and Arnould, 1991; Raiteri *et al.*, 1991).

The specific energy from carbon burning for a typical mix of neon and magnesium product nuclei is $4.0\times10^{17}$ erg g$^{-1}$ and the nuclear energy generation rate is (Woosley, 1986)

$$\dot{S}_{nuc}(^{12}\mathrm{C}) \approx 4.8\times10^{18} Y^2(^{12}\mathrm{C})\rho\lambda_{12,12}\ \mathrm{erg\,g^{-1}\,s^{-1}}, \tag{18}$$

where $Y(^{12}\mathrm{C})$ is the carbon mass fraction divided by 12 and $\lambda_{12,12}$ is the rate factor for carbon fusion as given, for example, by Caughlan and Fowler (1988). In the relevant temperature range for carbon burning, $T_9 = 0.6$ to 1.2, neglecting electron screening, $\lambda_{12,12} \approx 4\times10^{-11} T_9^{29}$ to within a factor of 2. Equating this to neutrino losses implies a carbon-burning temperature in balanced power of $T_9 = 0.7$ to 0.8 (Fig. 8; Arnett, 1972b) and a carbon-burning lifetime, $\tau_{12} = (\rho Y_{12}\lambda_{12,12})^{-1}$, of a few hundred years. Convection can lengthen this value (Table I). The specific energy released by carbon burning is $q_{\mathrm{nuc}}(^{12}\mathrm{C}) = 4.0\times10^{17}\, X(^{12}\mathrm{C})$ erg g$^{-1}$.

#### 2. Neon burning

Following carbon burning, the composition consists chiefly of $^{16}$O, $^{20}$Ne, and $^{24}$Mg. Oxygen has the smallest Coulomb barrier, but before the temperature required for oxygen fusion is reached, $^{20}\mathrm{Ne}(\gamma,\alpha)^{16}\mathrm{O}$ becomes energetically feasible using high-energy photons from the tail of the Planck distribution. The $\alpha$-particle separation energies of $^{16}$O (doubly magic), $^{20}$Ne, and $^{24}$Mg are 7.16, 4.73, and 9.32 MeV, respectively, so $^{20}$Ne is the more fragile nucleus. The $\alpha$ particle released by the disintegration of $^{20}$Ne initially adds back onto $^{16}$O restoring $^{20}$Ne, but soon this reaction reaches equilibrium $[Y_\alpha Y(^{16}\mathrm{O})\rho\lambda_{\alpha\gamma}(^{16}\mathrm{O}) \approx Y(^{20}\mathrm{Ne})\lambda_{\gamma\alpha}(^{20}\mathrm{Ne})]$ and the $\alpha$ particles begin to add onto $^{20}$Ne to produce $^{24}$Mg. The net result is that for each two $^{20}$Ne nuclei that disappear, one $^{16}$O nucleus and one $^{24}$Mg nucleus appear.

Other secondary reactions of interest to nucleosynthesis (but not to energy generation) are $^{24}\mathrm{Mg}(\alpha,\gamma)^{28}\mathrm{Si}$, $^{25}\mathrm{Mg}(\alpha,n)^{28}\mathrm{Si}$, $^{26}\mathrm{Mg}(\alpha,n)^{29}\mathrm{Si}$, $^{26}\mathrm{Mg}(p,n)^{26}\mathrm{Al}$, $^{26}\mathrm{Mg}(\alpha,\gamma)^{30}\mathrm{Si}$, $^{27}\mathrm{Al}(\alpha,p)^{30}\mathrm{Si}$, and $^{30}\mathrm{Si}(p,\gamma)^{31}\mathrm{P}$. Thus the final composition is enhanced in $^{16}$O, all the isotopes of magnesium, aluminum, silicon, and phosphorus as well as additional quantities of $^{36}$S, $^{40}$K, $^{46}$Ca, $^{58}$Fe, $^{61,62,64}$Ni, and traces of the radioactivities $^{22}$Na and $^{26}$Al, important for $\gamma$-line astronomy.

Energy generation comes mostly from the rearrangement reaction

$$2\ ^{20}\mathrm{Ne}\rightarrow{}^{16}\mathrm{O}+{}^{24}\mathrm{Mg}+4.59\ \mathrm{MeV}. \tag{19}$$

An analytic solution for the energy generation can be found using the steady-state $\alpha$-particle abundance implied by the condition $Y_\alpha Y(^{16}\mathrm{O})\rho\lambda_{\alpha\gamma}(^{16}\mathrm{O}) \approx Y(^{20}\mathrm{Ne})\lambda_{\gamma\alpha}(^{20}\mathrm{Ne})$ in the rate equation

$$\frac{dY(^{16}\mathrm{O})}{dt}=\frac{dY(^{24}\mathrm{Mg})}{dt}=-\frac{1}{2}\frac{dY(^{20}\mathrm{Ne})}{dt} = Y_\alpha Y(^{20}\mathrm{Ne})\rho\lambda_{\alpha\gamma}(^{20}\mathrm{Ne}). \tag{20}$$

The energy generation is then

$$\dot{S}_{nuc}(^{20}\mathrm{Ne})\approx 2.5\times10^{29}T_9^{3/2}\left(\frac{Y^2(^{20}\mathrm{Ne})}{Y(^{16}\mathrm{O})}\right)\lambda_{\alpha\gamma}(^{20}\mathrm{Ne}) \times\exp(-54.89/T_9)\ \mathrm{erg\,g^{-1}\,s^{-1}}. \tag{21}$$

In the temperature range near $1.5\times10^9$ K the rate factor $\lambda_{\alpha\gamma}(^{20}\mathrm{Ne})$ is approximately (Caughlan and Fowler, 1988) $3\times10^{-3}T_9^{10.5}$ cm$^3$ mol$^{-1}$ s$^{-1}$. The actual energy generation is sensitive to a much higher power of the temperature ($\sim T_9^{50}$) owing to the exponential dependence on temperature of the $\alpha$-particle mass fraction. The balanced power condition gives a neon-burning temperature of about $T_9=1.5$ and a lifetime of a few months—lengthened again, where appropriate, by convection. The energy yield is $q_{nuc}(^{20}\mathrm{Ne})=1.10\times10^{17}X(^{20}\mathrm{Ne})$ erg g$^{-1}$, or about 1/4 that of carbon burning.

Owing to this small energy yield, the importance of neon burning was overlooked for some time (Arnett, 1974a), but it is important for nucleosynthesis and for altering the entropy structure of some (lower-mass) presupernova stars.

### 3. Oxygen burning

Following neon burning one has $^{16}$O, $^{24}$Mg, and $^{28}$Si with traces of $^{25,26}$Mg, $^{26,27}$Al, $^{29,30}$Si, $^{31}$P, $^{32}$S, and the *s*-process elements. Oxygen is lightest and the next to burn (Arnett, 1972a, 1974b). For temperatures at which oxygen will burn in a massive star ($T_9\sim2$), oxygen fusion is favored over its photodisintegration. During explosive oxygen burning ($T_9\sim3$–4) both the photodisintegration of $^{16}$O [by $^{16}\mathrm{O}(\gamma,\alpha)^{12}\mathrm{C}$] and the oxygen fusion reaction can occur at comparable rates. Also under explosive conditions the reaction $^{12}\mathrm{C}+{}^{16}\mathrm{O}$ will be of some importance. Even so, the bulk nucleosynthesis and nuclear energy generation will be similar to that which we now describe for oxygen burning in hydrostatic equilibrium.

The oxygen fusion reaction produces compound nuclear states of $^{32}$S that may decay by any of four channels,

$$\begin{aligned}{}^{16}\mathrm{O}+{}^{16}\mathrm{O}\rightarrow{}^{32}\mathrm{S}^*&\rightarrow{}^{31}\mathrm{S}+n+1.45\ \mathrm{MeV}\\ &\rightarrow{}^{31}\mathrm{P}+p+7.68\ \mathrm{MeV}\\ &\rightarrow{}^{30}\mathrm{P}+d-2.41\ \mathrm{MeV}\\ &\rightarrow{}^{28}\mathrm{Si}+\alpha+9.59\ \mathrm{MeV}.\end{aligned} \tag{22}$$

The branching ratios for the neutron, proton, deuteron, and $\alpha$ channels are (Caughlan and Fowler, 1988) 5%, 56%, 5%, and 34%, respectively, at high temperatures when the endoergic deuteron channel is fully open. At lower temperatures the deuteron channel is inhibited and the other channels correspondingly increased. The deuteron produced at the high temperature characteristic of oxygen burning is immediately photodisintegrated into a neutron and a proton.

Once again many secondary reactions are of importance and nucleosynthesis can only be determined with any accuracy by using a reaction network. When all reactions are considered, the chief products of oxygen burning are $^{28}$Si, $^{32,33,34}$S, $^{35,37}$Cl (with $^{37}$Cl produced as $^{37}$Ar), $^{36,38}$Ar, $^{39,41}$K (with $^{41}$K produced as $^{41}$Ca), and $^{40,42}$Ca. Of these, $^{28}$Si and $^{32}$S constitute the bulk ($\sim$90%) of the final composition. Interestingly all the very heavy nuclei (above nickel) that had undergone substantial *s* processing during neon, carbon, and (especially) helium burning now begin to be destroyed by photodisintegration reactions that melt them down into the iron group. During the process some of the *p*-process isotopes are produced (Arnould, 1976), but by the end of oxygen burning the isotopes heavier than the iron group have been destroyed. Some *p*-process isotopes may survive, however, in a shell of incomplete oxygen burning farther out in the star.

Also of importance during *central* oxygen burning is a substantial increase in neutron excess that occurs because of the weak interactions $^{30}\mathrm{P}(e^+\nu)^{30}\mathrm{S}$, $^{33}\mathrm{S}(e^-,\nu)^{33}\mathrm{P}$, $^{35}\mathrm{Cl}(e^-,\nu)^{35}\mathrm{S}$, and $^{37}\mathrm{Ar}(e^-,\nu)^{37}$ Cl. The neutron excess had already begun to increase from its initial value, $\sim0.002(Z/Z_\odot)$, during carbon burning but now, in the center of the star, it assumes values so large ($\eta\gtrsim0.01$) that very nonsolar nucleosynthesis would result from its ejection (Woosley, Arnett, and Clayton, 1972). Thus the products of central hydrostatic oxygen burning are probably never ejected into the interstellar medium. Oxygen (as well as carbon, neon, and silicon) can also burn in a shell, however, and there the temperature is higher and the density lower. Less electron capture occurs. As a result the nucleosynthesis outside what will subsequently become the "iron core" retains memory of its initial neutron excess.

Energy generation during oxygen burning can be estimated by assuming, as is energetically approximately

correct, that the net result of the fusion of two oxygen nuclei is $^{32}$S (Woosley, 1986),

$$\dot{S}_{nuc}(^{16}\mathrm{O}) \approx 8\times 10^{18}\ Y^2(^{16}\mathrm{O})\rho\lambda_{16,16}\ \mathrm{erg\,g^{-1}\ s^{-1}}. \tag{23}$$

Near $2\times 10^9$ K, $\lambda_{16,16}$ is approximately (Caughlan and Fowler, 1988) $2.8\times 10^{-12}\ (T_9/2)^{33}$ (neglecting screening). The specific energy released by oxygen burning is $q_{nuc}(^{16}\mathrm{O}) \approx 5.0\times 10^{17} X(^{16}\mathrm{O})\ \mathrm{erg\,g^{-1}}$. This implies an oxygen-burning lifetime of several months (Fig. 8).

Another interesting occurrence during oxygen burning is the coming into existence of a number of isolated *quasiequilibrium clusters*, groups of nuclei coupled by strong and electromagnetic reactions that are occurring at rates nearly balanced by their inverses. For example, near the end of oxygen burning $^{28}\mathrm{Si}(n,\gamma)^{29}\mathrm{Si}$ is occurring at a rate balanced by $^{29}\mathrm{Si}(\gamma,n)^{28}\mathrm{Si}$ and $^{29}\mathrm{Si}(p,\gamma)^{30}\mathrm{P}$ is balanced by $^{30}\mathrm{P}(\gamma,p)^{29}\mathrm{Si}$. Thus $^{28}$Si, $^{29}$Si, and $^{30}$P are all in equilibrium with one another. Similarly $^{34,35}$S and $^{35,36}$Cl are in equilibrium with one another (but not with $^{28}$Si) and so on. As the temperature rises, more nuclei join in such groups and smaller groups merge into larger ones. By the time silicon burning ignites, there are two large clusters composed on the one hand of nuclei from $A=24$ to 46 and on the other with heavier nuclei in the iron group. After a little silicon burns, these two groups merge into one (Woosley, Arnett, and Clayton, 1973).

#### 4. Silicon burning

Unlike carbon and oxygen burning, silicon burning does not occur predominantly as a fusion reaction. That is, one does not have $^{28}\mathrm{Si}+^{28}\mathrm{Si}\rightarrow{}^{56}\mathrm{Ni}$. Instead silicon burns in a unique fashion resembling, in some ways, the rearrangement that characterized neon burning. A portion of the $^{28}$Si "melts" by a sequence of photodisintegration reactions into neutrons, protons, and especially $\alpha$ particles by the chain $^{28}\mathrm{Si}(\gamma,\alpha)^{24}\mathrm{Mg}(\gamma,\alpha)^{20}\mathrm{Ne}(\gamma,\alpha)^{16}\mathrm{O}(\gamma,\alpha)^{12}\mathrm{C}(\gamma,2\alpha)\alpha$. An equilibrium is further maintained between the $\alpha$ particles and free nucleons by the existence of chains such as $^{28}\mathrm{Si}(\alpha,\gamma)^{32}\mathrm{S}(\gamma,p)^{31}\mathrm{P}(\gamma,p)^{30}\mathrm{Si}(\gamma,n)^{29}\mathrm{Si}(\gamma,n)^{28}\mathrm{Si}$, each reaction being in equilibrium with its inverse. The $\alpha$ particles (and their associated nucleons) released by silicon photodisintegration add onto the big quasiequilibrium group above $^{28}$Si, gradually increasing its mean atomic weight. Eventually most of the material becomes concentrated in tightly bound species within the iron group and the silicon abundance becomes small.

Within the quasiequilibrium group, which includes all nuclei heavier than $^{24}$Mg, the abundance of species $^AZ$ is given (Bodansky, Clayton, and Fowler, 1968) by

$$Y(^AZ) = C(^AZ,\rho,T_9)\,Y(^{28}\mathrm{Si})\,Y_\alpha^{\delta_\alpha}\,Y_n^{\delta_n}\,Y_p^{\delta_p}. \tag{24}$$

Here $\delta_\alpha$, $\delta_n$, and $\delta_p$ are the (integer) numbers of $\alpha$ particles, neutrons, and protons, respectively, in excess of those contained in $^{28}$Si. Additionally, the $\alpha$-particle abundance is related to the free nucleon abundances by

$$Y_\alpha = (\rho N_A)^3 C_\alpha(T_9) Y_n^2 Y_p^2. \tag{25}$$

Expressions for the thermodynamic factors $C$ are given by Bodansky *et al.* (1968). More recent expressions are similar but include the temperature dependence of the partition function, i.e., the contribution of nuclear excited states to the Saha equation.

Examination of Eqs. (24) and (25) shows that the abundance of all species heavier than $^{24}$Mg is uniquely specified by five parameters, $\rho$, $T_9$, $Y_n$, $Y_p$, and $Y(^{28}\mathrm{Si})$. Using mass conservation, $\Sigma A_i Y_i = 1$, and the fact that the abundances of species lighter than $^{24}$Mg are small reduces the number of free parameters to four. These could be, for example, $\rho$, $T_9$, $Y(^{28}\mathrm{Si})$, and $\eta$. As the silicon mass fraction decreases, the mean atomic weight of the quasiequilibrium group increases.

In the simplest case where the neutron excess is small, $\eta \lesssim 0.01$, and the fuel is chiefly $^{28}$Si and $^{32}$S, an approximation to the energy generation can be obtained by assuming that for each two $^{28}$Si nuclei that melt (one making the $\alpha$ particles that "add on" to the other), one $^{56}$Ni nucleus is formed. The critical reaction that allows the photodisintegration of $^{28}$Si is $^{24}\mathrm{Mg}(\gamma,\alpha)^{20}\mathrm{Ne}$ [at higher temperatures in explosive silicon burning it is $^{16}\mathrm{O}(\gamma,\alpha)^{12}\mathrm{C}$]. Thus the rate of destruction of $^{28}$Si is

$$\frac{dY(^{28}\mathrm{Si})}{dt} = -2\ Y(^{24}\mathrm{Mg})\lambda_{\gamma\alpha}(^{24}\mathrm{Mg}). \tag{26}$$

Solution of this equation requires knowledge of the magnesium abundance, which can be determined if the $\alpha$ particle and $^{28}$Si abundances are known. If we assume that only $^{28}$Si and $^{56}$Ni have substantial abundances so that $56Y(^{56}\mathrm{Ni}) = 1 - 28Y(^{28}\mathrm{Si})$, then the $\alpha$-particle abundance, and thus the $^{24}$Mg abundance, can be obtained from the ratio of $^{56}$Ni to $^{28}$Si and will in fact depend only on the 1/7 root of the assumed ratio. Bodansky *et al.* (1968) have given the solution for the energy generation in this situation:

$$\dot{S}_{nuc}(^{28}\mathrm{Si}) \approx 1.8\times 10^{28}\ T_9^{3/2} X(^{28}\mathrm{Si}) e^{-142.07/T_9} \times \lambda_{\alpha\gamma}(^{20}\mathrm{Ne})\mathrm{erg\,g^{-1}\ s^{-1}}. \tag{27}$$

Near $3.5\times 10^9$ K, $\lambda_{\alpha\gamma}(^{20}\mathrm{Ne})$ is approximately $120(T_9/3.5)^5$ and the overall temperature dependence of the energy generation rate is $\sim T^{49}$. The energy release from burning two $^{28}$Si nuclei to $^{56}$Ni is $q_{nuc}(^{28}\mathrm{Si}) \approx 1.9\times 10^{17} X(^{28}\mathrm{Si})\ \mathrm{erg\,g^{-1}}$, considerably less than from oxygen burning.

For silicon burning in the core of a massive star, substantial electron capture will already have occurred so that the fuel consists of a mixture of $^{28}$Si and $^{29,30}$Si in comparable amounts. The burning then is not governed entirely by the photodisintegration of $^{24}$Mg, but also by $(p,\alpha)$ and $(n,\alpha)$ reactions on $^{25}$Mg and $^{26}$Mg. Furthermore, the dominant product is not $^{56}$Ni, but $^{54}$Fe or even $^{56}$Fe. The real situation must be followed carefully with a large quasiequilibrium group coupled with a reaction network to describe the evolution of those species lighter than magnesium that have not attained equilibrium. The evolution of the neutron excess by way of weak interactions must also be followed carefully, as it affects not only the nucleosynthesis but the structure of

the star. Indeed, silicon burning is the most computationally intensive and potentially numerically unstable stage in the computer modeling of the evolution of a massive star. The coupling of silicon burning to convection is particularly problematic because the nuclear rearrangement time for nuclei in the quasiequilibrium cluster is almost instantaneous and the energy generation rate is very stiff in the temperature. A stable model requires implicit coupling of the nuclear burning to the equation-of-state routine, multiple schemes for recovery when the stiff quasiequilibrium equations do not converge, and convection not of individual nuclei but of equilibrium parameters—$\eta$ and $Y(^{28}\mathrm{Si})$. Several groups have different approaches to silicon burning. Weaver, Zimmerman, and Woosley (1978 and subsequent work) carry a 128-isotope quasiequilibrium network coupled to a small reaction network below magnesium. Nomoto and Hashimoto (1988) use tables to give energy generation and the evolution of $Y_e$, and Chieffi, Limongi, and Straniero (1998) carry a large reaction network and do not assume quasiequilibrium.

Following silicon burning, the composition consists of the most tightly bound iron-group nuclei allowed at the given temperature, density, and neutron excess. In the case of explosive silicon burning, the ejected composition depends upon how much silicon was burned in the explosion and agrees with solar abundances only for a very limited range of neutron excess, $\eta \lesssim 0.006$. For this neutron excess, near solar abundances are produced of $^{48,49}$Ti, $^{51}$V, $^{50,52,53}$Cr, $^{55}$Mn, $^{54,56,57}$Fe, and, if they are not consumed in the explosion, $^{28}$Si, $^{32}$S, $^{36}$Ar, and $^{40}$Ca.

#### 5. Nuclear statistical equilibrium

As the abundance of $^{28}$Si becomes very small at the end of silicon burning, the nonequilibrated reactions linking magnesium with neon, carbon with oxygen, and carbon with $\alpha$ particles finally become balanced by their inverses. The very last reaction to achieve equilibrium is the triple-alpha reaction, which eventually occurs at a rate balancing carbon photodisintegration. Once this happens, the silicon abundance can be expressed in terms of the $\alpha$-particle abundance by a Saha equation. This additional constraint allows all abundances to be specified by only three independent parameters: temperature, density, and neutron excess. All strong and electromagnetic reactions are occurring at rates balanced by their inverses and the abundances are given by the nuclear Saha equation:

$$Y(^AZ) = C(^AZ,\rho,T_9)\, Y_n^N\, Y_p^Z,$$

$$C(^AZ,\rho,T_9) = (\rho N_A)^{A-1} C'(^AZ,T_9),$$

$$C(^AZ,T_9) = \frac{G(^AZ,T_9)A^{3/2}}{2^A}\,\theta^{1-A}\exp[BE(^AZ)/kT],$$

$$\theta = 5.943\times 10^{33}\; T_9^{3/2}. \tag{28}$$

These equations have the interesting property of favoring, for low temperatures (say, $T_9 \lesssim 10^{10}$ K), the most tightly bound nuclei of the given neutron excess $\eta$. For compositions having near neutron-proton equality, that species is $^{56}$Ni, a fact that has important consequences for both nucleosynthesis and the light curves of supernovae. For neutron excesses more characteristic of matter near the valley of $\beta$ stability, $\eta \approx 0.07$, the most tightly bound nucleus is $^{56}$Fe, and for compositions containing still greater neutron-to-proton ratios the equilibrium shifts to heavier isotopes (Aufderheide, Fushiki, Woosley, and Hartmann, 1994). The most tightly bound nucleus of all is, in fact, $^{62}$Ni.

As the temperature of an equilibrium composition is raised, the binding energy becomes of decreasing importance relative to both the partition function (that must account for all the bound excited states of the nucleus) and the phase space available to free $\alpha$ particles and nucleons. Thus, for a given density, as the temperature is raised, an increasing fraction of the composition resides in lighter particles. This photodisintegration is of great importance, both for triggering the collapse of the iron core of a massive evolved star and for causing losses to the shock wave generated by core bounce. In tearing $^{56}$Fe to free $\alpha$ particles and neutrons, for example, $1.7\times 10^{18}$ erg must be provided. In fact this photodisintegration does not go to completion during the collapse of the iron core.

For a Fermi-gas representation of the nuclear level density, the nuclear partition function will be given approximately at high temperatures by (see, for example, Fowler, Woosley, and Engelbrecht 1978)

$$G(T_9) \approx \frac{\pi}{6akT}\exp(akT), \tag{29}$$

with $a$ the nuclear level-density parameter, approximately given by $A/9$. Thus at very high temperature the partition function will be as important as the nuclear binding energy in determining the abundances.

It can also be shown by integration of the energy-weighted partition function that at high temperature the total energy stored in the excited states of a bound nucleus is about

$$E_{ex} \approx a(kT)^2. \tag{30}$$

At a temperature of $5\times 10^{10}$ K, for example, the excitation energy of an average iron nucleus is about 115 MeV, or $2.0\times 10^{18}$ erg g$^{-1}$. This is an important sink of energy during core collapse. Indeed, as Bethe *et al.* (1979) first pointed out, it is this storage of energy in excited states coupled with the large partition function assigned to those states that allows discrete bound nuclei to persist and remain relatively cool until the core has collapsed to nuclear density.

### B. Stellar models

#### 1. $8M_\odot$ to $11M_\odot$

Stars below a certain mass, $M_1$, develop a degenerate core and do not ignite carbon burning. Above $M_2$, on the other hand, carbon and neon both ignite nondegenerately near the center of the star. The exact values of

$M_1$ and $M_2$ depend upon the assumed helium abundance, metallicity, and especially the treatment of convection and convective overshoot. Iben and Renzini (1983) gave a value $M_1 = 8-9M_\odot$ depending upon composition, and $8M_\odot$ is commonly adopted. However, a large postulated degree of overshoot beyond the edge of the convective core during the main-sequence phase can reduce $M_1$ significantly. For example, assuming mixing by half of a pressure scale height beyond the formal edge of the convective core, Bressan *et al.* (1993) find that, for $Z=0.02$ and $Y=0.28$, $M_1$ is in the range $5-6M_\odot$. $M_2$ is also uncertain, but generally thought to be $11-12M_\odot$ in those models that do not employ much overshoot mixing. Woosley and Weaver (1995) found that a $12M_\odot$ model ($3.2M_\odot$ helium core) ignited neon (and oxygen and silicon) burning centrally. There are also indications that bare helium cores do not experience the growth in convective core mass and nonmonotonic behavior in final carbon abundance seen by their full star counterparts, while an $11M_\odot$ model ($2.9M_\odot$ helium core) ignited off center. A similar helium-core mass ($3.3M_\odot$) for $M_2$ was also found by Nomoto and Hashimoto (1988).

Between $M_1$ and $M_2$ stellar evolution during carbon and neon burning is quite complicated, with the residual effects of degeneracy playing a major role and off-center ignition being the rule rather than the exception. The carbon-oxygen core, and later the oxygen-neon core, is surrounded by a steep density gradient wherein lies a thermally pulsing thin helium shell. These are high-mass equivalents to asymptotic giant branch stars and, as such, may be endowed with "superwinds" of up to $10^{-4}M_\odot\,\mathrm{y}^{-1}$. If so, then in most cases the final evolutionary state will not be a supernova, but an oxygen-neon white dwarf. In any case, because of the steep density gradient, such stars will not contribute appreciably to the galactic nucleosynthesis of abundant nuclei like oxygen, silicon, and iron.

The existence of this interesting branch of stellar evolution was pointed out by Barkat, Reiss, and Rakavy (1974). Miyaji *et al.* (1980) and Woosley, Weaver, and Taam (1980) first studied the late evolution of $10M_\odot$ stars and found seemingly discrepant results. Miyaji *et al.*, who did not follow hydrogen, helium, or carbon burning, but accreted neon and oxygen onto a core of the same composition, found that neon ignited owing to electron capture at about $2.5\times10^{10}\,\mathrm{g\,cm^{-3}}$. A degenerate runaway ensued in which the loss of pressure to electron capture more than compensated for the rising temperature and the core collapsed to a neutron star. Woosley *et al.*, who followed an entire $10M_\odot$ star, but used coarse zoning in the helium-burning shell, found that neon ignited off-center in a series of strong flashes that propagated to the center of the star, turning it into silicon and other oxygen-burning products. Continued evolution thru silicon burning produced an iron core in the usual way, which collapsed. Interestingly the strong neon flashes in this (poorly zoned) model were sufficient to eject the hydrogen envelope about ten years before the final explosion, with interesting consequences for the light curve. Modern calculations now call into question all these conclusions.

Nomoto (1984, 1987), Habets (1986), Miyaji and Nomoto (1987), and Nomoto and Hashimoto (1988) followed the evolution of helium cores in the mass range $2.0-4.0M_\odot$ through helium and carbon burning, assuming that they would mimic the evolution of full stars of four times that mass, and uncovered some interesting systematics. For helium cores in the range $2.2-2.5M_\odot$ (main-sequence stars of about $9-10M_\odot$), neon never burned stably in hydrostatic equilibrium. The core grew to the Chandrasekhar mass and neon ignited by electron capture at $\sim5\times10^9\,\mathrm{g\,cm^{-3}}$. The ensuing deflagration to nuclear statistical equilibrium was accompanied by such copious electron capture that the core collapsed to a neutron star (Bruenn, 1972). Bounce and shock propagation were studied by Hillebrandt, Nomoto, and Wolff (1984), Burrows and Lattimer (1985), and Mayle and Wilson (1988), who, after some initial confusion, determined that the presence of unburned nuclear fuel in the collapsing core caused only a minor perturbation. The explosion mechanism was essentially the same as in collapsing iron cores of the same mass—neutrino powered.

However, Nomoto (1984) observed that his $2.6M_\odot$ helium core ignited neon in a series of strong off-center flashes that did not lead immediately to core collapse, i.e., the same behavior observed by Woosley, Weaver, and Taam (1980) in their $10M_\odot$ ($2.7M_\odot$ helium core) star. Later Nomoto and Hashimoto (1988) revised their estimate for neon ignition in a stable star upwards from $2.6M_\odot$ to $2.8M_\odot$. Clearly this is a range of masses in which the final evolution is sensitive to moderate changes in the degeneracy. Nomoto (1984) also determined that the critical mass for neon ignition lies above $1.37M_\odot$ (compare to $1.06M_\odot$ for carbon ignition).

All of the calculations by Nomoto *et al.* and Woosley *et al.* in this mass range neglected mass loss and used zoning that was inadequate to follow the thin helium-shell flashes surrounding the degenerate core that develops for helium cores of less than about $2.5M_\odot$ (though see Fig. 1 of Nomoto, 1987). More recently calculations by Garcia-Berro and co-workers (Garcia-Berro and Iben, 1994; Ritossa, Garcia-Berro, and Iben, 1996, 1999; Garcia-Berro, Ritossa, and Iben, 1997; Iben, Ritossa, and Garcia-Berro, 1997) have addressed these deficiencies in a study of the post-helium-burning evolution of main-sequence stars of $9.0M_\odot$, $10.0M_\odot$, $10.5M_\odot$, and $11.0M_\odot$. All of these stars except the $11M_\odot$ model ignited carbon off-center and a convectively bounded carbon fusion flame conveyed burning to the center of each (see also Timmes, Woosley, and Taam, 1994). Each star ended its life as a thermally pulsing AGB star with a superwind. The $9.0M_\odot$, $10.0M_\odot$, and $10.5M_\odot$ models ejected their hydrogen envelopes and ended up as oxygen-neon white dwarfs of $1.16M_\odot$, $1.25M_\odot$, and $1.31M_\odot$, respectively. However, the $11.0M_\odot$ model had an oxygen-neon core of $1.368M_\odot$ and presumably will finish its life collapsing as an electron-capture supernova as described by Miyaji *et al.* before losing its entire en-

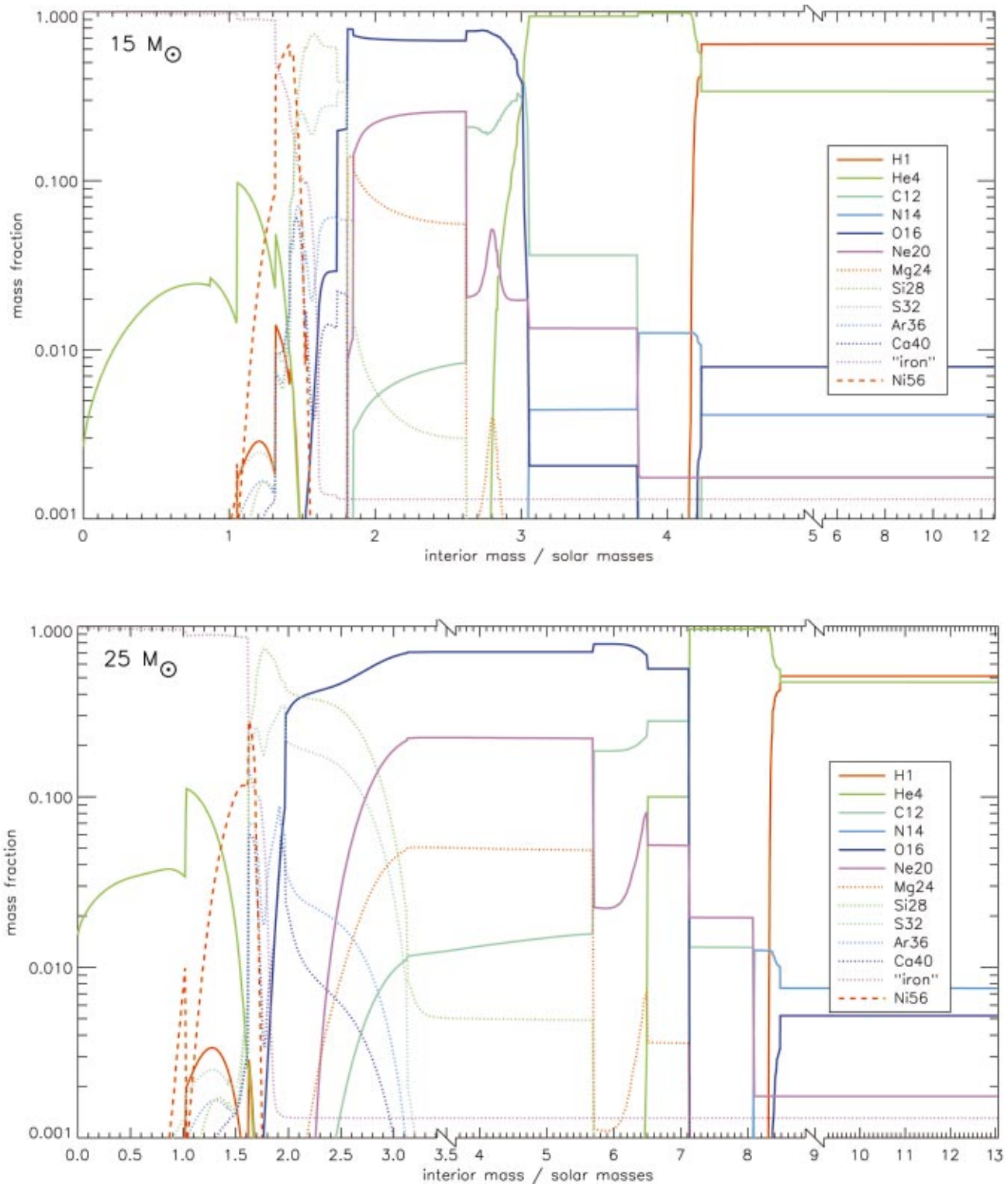


FIG. 9. Final composition by mass fraction of two presupernova stars of mass $15M_\odot$ (top) and $25M_\odot$ (bottom). Both stars were evolved from the main sequence, including mass loss (Heger, Woosley, Rauscher, and Hoffman, 2002). The notation "iron" refers to the sum of neutron-rich isotopes in the iron group, especially $^{54}$Fe, $^{56}$Fe, and $^{58}$Fe [Color].

velope. It seems, though, that in realistic models the mass range for electron-capture supernovae is quite nar row.

There are some indications that the Crab supernova had a progenitor star in the $8-11M_\odot$ range (Nomoto *et al.*, 1984).

### 2. $11M_\odot$ to $100M_\odot$

While the effects of partial degeneracy and the consequent off-center ignition of fuels, especially oxygen, may persist on up to $15M_\odot$, all stars heavier than about $11M_\odot$ complete all the advanced burning stages, includ-

ing silicon burning, in hydrostatic equilibrium prior to collapse. The presupernova star is thus characterized by an iron core of roughly the Chandrasekhar mass (Sec. V.A) surrounded by active burning shells and the accumulated ashes of oxygen, neon, carbon, and helium burning (Fig. 9). If the star has not lost its hydrogen envelope along they way, most of the radius and an appreciable part of the mass may still consist of unburned hydrogen and helium.

Because of the comparative simplicity of the nuclear physics, many groups have studied the evolution of stars in this mass range through carbon burning (e.g., Lamb *et al.* 1977; Acoragi, Langer, and Arnould, 1991; Schaller *et al.*, 1992; Mowlavi *et al.*, 1998), but relatively few have followed the star through oxygen and silicon burning to obtain presupernova models.[2]

In addition to the complex interplay among thermal neutrino losses, degeneracy, and nuclear energy generation discussed in Sec. IV.A, the core structure is sensitive to the location and timing of numerous episodes of convective burning (Fig. 10). Each stage of core or shell burning redistributes the entropy in such a way as to create regions where its radial derivative is small. Since the burning typically ignites at the bottom of a region of unburned fuel where the entropy is initially the least, the greatest rises in entropy occur at the bottoms of convective shells. These discontinuities serve as barriers to the outward penetration of subsequent convection zones. Since a typical star (e.g., $15M_{\odot}$; Woosley and Weaver, 1995; Fig. 10) may have four stages of convective carbon burning (core burning plus three stages of shell burning) and two or three stages each of neon, oxygen, and silicon burning, the distribution of the composition becomes complicated. Indeed the location of the bases of convective shells and even the masses of iron cores in presupernova stars of variable mass may be quite nonmonotonic (Barkat and Marom, 1990; Fig. 17 below). Moreover, the use of mixing-length theory during oxygen and silicon burning is particularly problematic (Bazan and Arnett, 1994, 1998) since the nuclear and convective time scales become comparable.

The late stages of evolution in these stars are also governed by (a) the tendency of more massive stars to have higher entropy at all stages of their evolution and (b) the tendency (though not absolute) of the core to lose entropy, particularly during carbon burning. Neutrinos carry away both energy and entropy; nuclear burning, locally at least, generates both. However, nuclear burning coupled to convection can actually lead to an overall decrease in the entropy (Fig. 11), and the presence of an active burning shell within the core of a star lends support and stability while the matter interior to that shell cools off. Globally, burning can act to decrease the entropy.

This helps to explain the remarkable behavior of the iron-core mass as a function of stellar mass. Above about $19M_{\odot}$ for current choice of the reaction rate for $^{12}C(\alpha,\gamma)^{16}O$, the central carbon abundance following helium burning is too small ($\lesssim 15\%$) ever to generate energy in excess of the neutrino losses powered by core contraction. The carbon burns, as do its products neon and magnesium, but the net energy generation including neutrinos does not become positive. The central part of the star is not convective during carbon and neon burning. There are several reasons for the small carbon abundance. One is the well-known tendency of entropy to be higher in stars of higher mass. Another is the existence of so-called "breathing modes" that mix helium into the helium-depleted core, reducing the final carbon abundance appreciably (Sec. III.D.1).

We note that the final evolution of massive stars will also be sensitive to metallicity (Sec. VIII.D) and particularly the larger presupernova masses at low metallicity (Fig. 12), especially above $30M_{\odot}$.

### C. Role of weak interactions

Though the stars are powered chiefly by fusion reactions (i.e., the strong interaction) from start to finish, weak interactions play an important role in determining both the presupernova stellar structure and the nucleosynthesis. They affect the structure because, at all times, the pressure is mostly due to electrons—at first, nonrelativistic and nondegenerate, but later neither—and weak reactions change $Y_e$ [Eq. (4)]. They affect the nucleosynthesis because the synthesis of all nuclei except those with equal numbers of neutrons and protons is sensitive to the neutron excess, $\eta = 1 - 2Y_e$. The neutrinos lost in weak interactions also affect the energy and entropy budgets of the star, losses that are especially important in the final collapse of the star (Sec. V.B).

For the weak-interaction rates prior to oxygen burning, one can use the measured decay rates of unstable nuclei prone to beta decay, electron capture, and positron emission. In some cases where low-lying levels exist with known *ft* values for weak decay, a thermal distribution of excited states is assumed and an effective rate is computed. There are, of course, special cases like $^{26}Al$ in which the states may not achieve a thermal population at all temperatures of interest. In such cases the individual levels must be followed explicitly, but in any case the change in neutron excess prior to oxygen burning has only a slight effect on the stellar structure.

After oxygen burning, though, weak interactions take on a different character. Such a large number of excited states with uncertain properties become populated that their decay must be dealt with statistically. Early attempts in this direction were made by Hansen (1968), Mazurek (1973), Mazurek, Truran, and Cameron (1974), and Takahashi, Yamada, and Kondo (1973). However, it

[2]Exceptions are Arnett (1974b, 1977); Weaver, Zimmerman, and Woosley (1978); Nomoto and Hashimoto (1988); Hashimoto *et al.* (1993); Woosley and Weaver (1995); Chieffi, Limongi, and Straniero (1998); Heger, Langer, and Woosley (2000); and Rauscher *et al.* (2002).

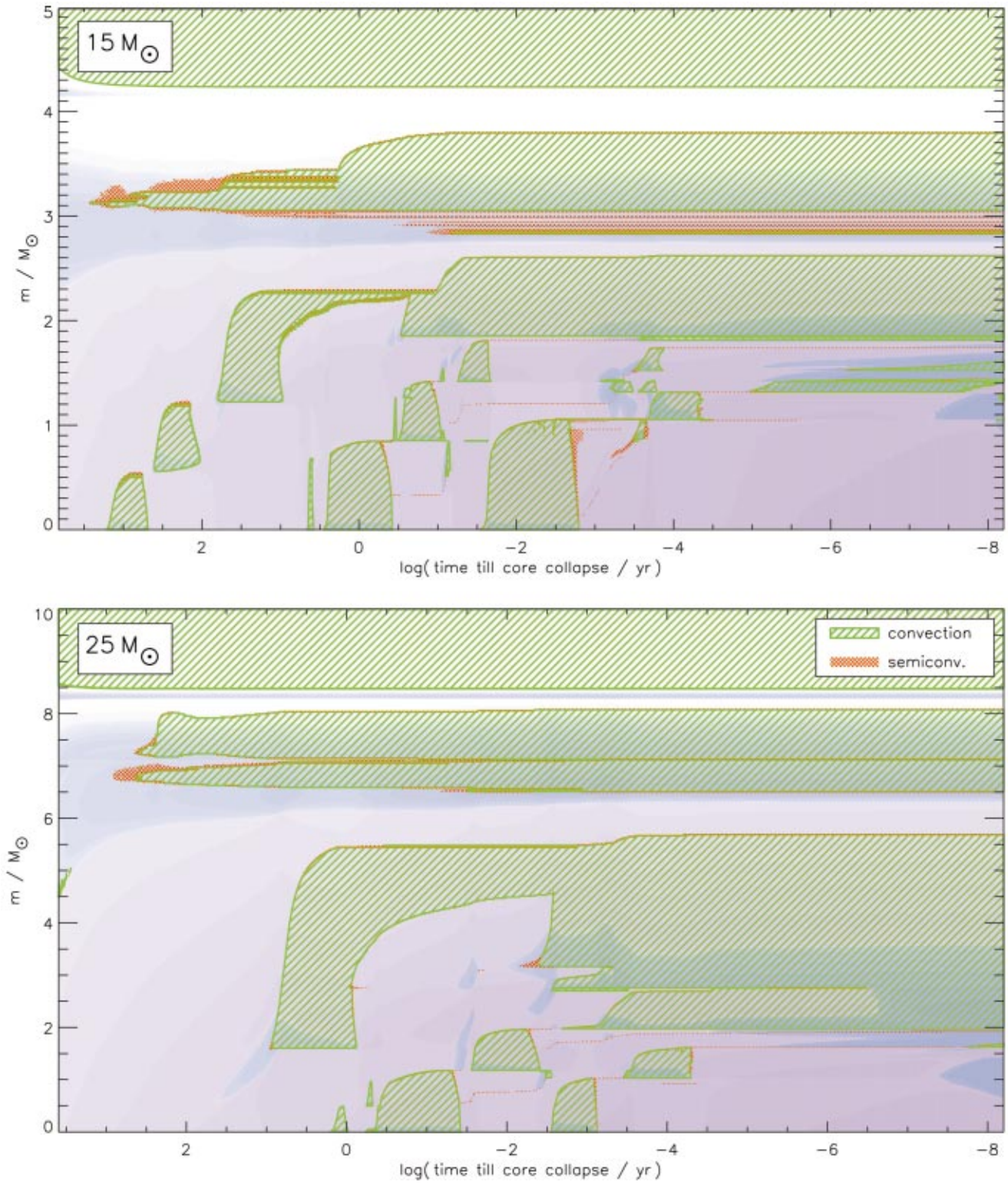


FIG. 10. Convective history during carbon, neon, oxygen, and silicon burning for stars of $15M_\odot$ (top) and $25M_\odot$ (bottom). Time is measured logarithmically in years until collapse. Shading and hatching have the same meaning as in Fig. 3, with darker blue indicating higher positive net energy generation and darker pink showing larger losses. Note the existence of well-developed convective carbon burning at the center of the $15M_\odot$ star that is absent in the $25M_\odot$ model. The final iron-core masses in these two stars were $1.45M_\odot$ and $1.62M_\odot$, respectively [Color].

was Fuller, Fowler, and Newman (1980, 1982a, 1982b, 1985) who recognized the key role played by the Gamow-Teller resonance and noted that measured decay rates exploited only a small fraction of the available strength. More recently new shell-model calculations of the distribution of Gamow-Teller strength have resulted in an improved—and often reduced—estimate of its strength (Langanke and Martínez-Pinedo, 1999, 2000).

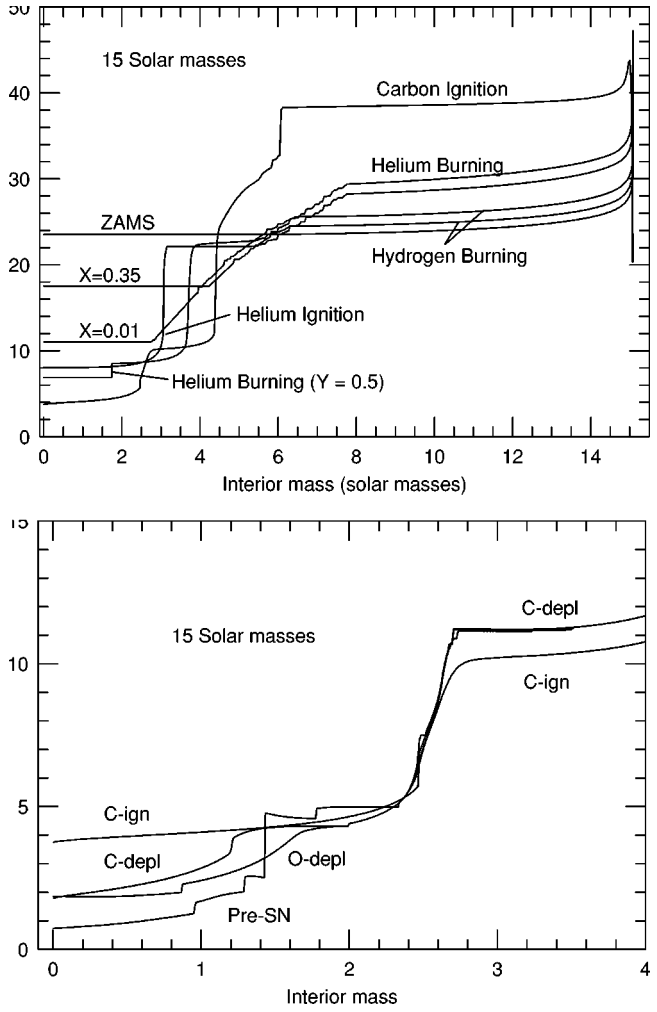


FIG. 11. Evolution of the entropy in the interior of a $15M_\odot$ star. The total entropy per baryon, $S/N_A k$, is given on the main sequence, following helium burning, at the end of carbon burning, at the end of oxygen burning, and for the presupernova star. Neutrino losses during the late stages of evolution lead to a dramatic increase in the core entropy and convergence upon a common, degenerate structure for the iron core.

The alteration in some important rates, such as electron capture on $^{60}$Co, is as large as two orders of magnitude in important astrophysical circumstances.

The effects of including the new weak-interaction rate set in a $15M_\odot$ model star are shown in Figs. 13 and 14 (Heger, Langanke, *et al.*, 2001; Heger, Woosley, *et al.*, 2001). The most dramatic decline in $Y_e$ occurs early during silicon burning which ignites at about $\log(t_o - t) \approx 6$ in the $15M_\odot$ model shown and lasts until $\log(t_o - t) \approx 5$, but appreciable decreases continue as the iron core sits in hydrostatic equilibrium surrounded by active shells of silicon burning that impede its collapse. Some of the most important weak flows (using the recent Langanke and Martínez-Pinedo rates) include electron capture on $^{35}$Cl, $^{32,33}$S, $^{53}$Fe, $^{55}$Co, and $^{56}$Ni early on. Later electron capture on $^{54,55,56}$Fe and $^{61}$Ni becomes important, as does the beta decay of $^{32}$P, $^{52}$V, $^{54,55,56,58}$Mn, and $^{62,64}$Co. The final value of $Y_e = 0.43$ is not particularly sensitive to the weak rates or to the stellar mass.

Interestingly, as Fig. 14 shows, there is a period, beginning about the time that silicon disappears from the center of the star, when the weak interactions reach a state of dynamic equilibrium (see also Aufderheide, Fushiki, Fuller, and Weaver, 1994). This is not true equilibrium in the sense that every weak rate occurs at a rate balanced by its inverse, and certainly neutrino capture is not balancing electron capture, but the sum of all weak flows that increase $Y_e$, i.e., beta decay, balances the sum of flows that decrease it, i.e., electron capture. For a given set of weak rates, then, $Y_e$ takes on a value at a given temperature and density that is independent of its previous evolution. For heavier-mass stars, 25 and $40M_\odot$ evolved without mass loss, Heger *et al.* find that this beta equilibrium is approached but not quite reached to the extent shown here for the $15M_\odot$ star. As the iron core contracts during the last 1000 s of the star's life, weak equilibrium is again lost as the filled phase space hinders beta decay and favors electron capture. But by this point the final value of $Y_e$ has almost been determined.

### D. Effects of rotation in the late stages

As discussed in Sec II.F, the effects of rotation on compositional mixing are known to be important during hydrogen and helium burning, but what about the later stages? Will rotation be dynamically important in core collapse? Is it possible to predict, from first principles, the rotation rate of pulsars?

Calculations by Heger, Langer, and Woosley (2000) suggest that rotation is still important in causing additional mixing during the advanced burning stages, especially by shear instabilities. There is also a cumulative effect because the larger helium cores obtained from calculations that include rotation affect the nucleosynthesis and structure through all phases.

With regard to angular momentum, early numerical studies of rotating massive stars found that the stellar core would reach breakup rotation before carbon ignition (Kippenhahn, Meyer-Hofmeister, and Thomas, 1970; Endal and Sophia, 1976). In more recent models, additional angular momentum is lost from the core before carbon burning (Heger, Langer, and Woosley, 2000; Maeder and Meynet, 2001), but presupernova core rotation rates that would lead to neutron stars of breakup velocity are still predicted. These studies imply that rotation will become an important dynamic effect during core collapse (Fig. 15; Fryer and Heger, 2000). They also predict that neutron stars will be born with angular momentum $j \sim 10^{16}$ cm$^2$ s$^{-1}$ and periods $\sim 1$ ms. Such large rotation rates are inconsistent with the currently observed slow rotation rate of pulsars, but gravitational radiation owing to the $r$-mode instability could rapidly brake the rotation of young neutron stars (Lindblom *et al.*, 2001; Stergioulas and Font, 2001; though see Arras *et al.*, 2002).

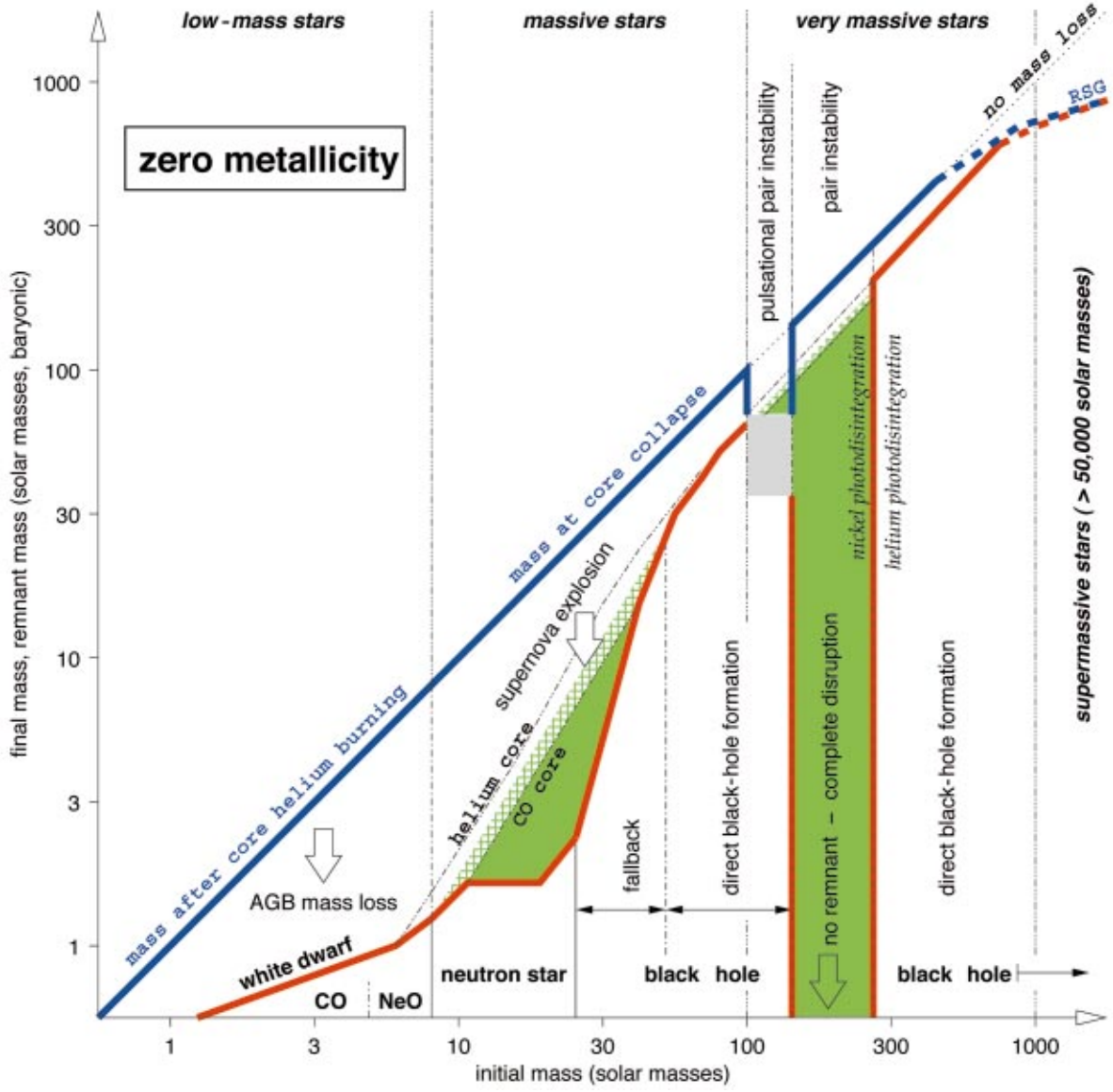


FIG. 12. Initial-final mass function of nonrotating primordial stars ($Z=0$). The $x$ axis gives the initial stellar mass. The $y$ axis gives both the final mass of the collapsed remnant (thick red curve) and the mass of the star when the event that produces that remnant begins [e.g., mass loss in asymptotic giant branch (AGB) stars, supernova explosion for those stars that make a neutron star, etc.; thick blue curve]. Dark green indicates regions of heavy-element ($Z>2$) synthesis and cross-hatched green shows regions of partial helium burning to carbon and oxygen. We distinguish four regimes of initial mass: *low-mass stars* below $\sim 10M_{\odot}$ that form white dwarfs; *massive stars* between $\sim 10M_{\odot}$ and $\sim 100M_{\odot}$; *very massive stars* between $\sim 100M_{\odot}$ and $\sim 1000M_{\odot}$; and *supermassive stars* (arbitrarily) above $\sim 1000M_{\odot}$. Since no mass loss is expected for $Z=0$ stars, the blue curve corresponds approximately to the (dotted) line of no mass loss, except for $\sim 100$–$140M_{\odot}$ where the pulsational pair instability ejects the outer layers of the star before it collapses, and above $\sim 500M_{\odot}$ where pulsational instabilities in red supergiants may lead to significant mass loss. Since the magnitude of the latter is uncertain, lines are dashed. In the low-mass regime we assume, even in $Z=0$ stars, that mass loss on the asymptotic giant branch removes the envelope of the star, leaving a CO or NeO white dwarf (though the mechanism and thus the resulting initial-final mass function may differ from solar composition stars). Massive stars are defined as stars that ignite carbon and oxygen burning nondegenerately and do not leave white dwarfs. The hydrogen-rich envelope and parts of the helium core (dash-double-dotted curve) are ejected in a supernova explosion. Below initial masses of $\sim 25M_{\odot}$ neutron stars are formed. Above that, black holes form, either in a delayed manner by fallback of the ejecta or directly during iron-core collapse (above $\sim 40M_{\odot}$). The defining characteristic of very massive stars is their electron-positron pair instability after carbon burning. This begins as a pulsational instability for helium cores of $\sim 40M_{\odot}$ ($M_{\mathrm{ZAMS}} \sim 100M_{\odot}$). As the mass increases, the pulsations become more violent, ejecting any remaining hydrogen envelope and an increasing fraction of the helium core itself. An iron core can still form in hydrostatic equilibrium in such stars, but it collapses to a black hole. Above $M_{\mathrm{He}}=63M_{\odot}$ or about $M_{\mathrm{ZAMS}}=140M_{\odot}$, and on up to $M_{\mathrm{He}}=133M_{\odot}$ or about $M_{\mathrm{ZAMS}}=260M_{\odot}$, a single pulse disrupts the star. Above $260M_{\odot}$, the pair instability in nonrotating stars results in complete collapse to a black hole [Color].

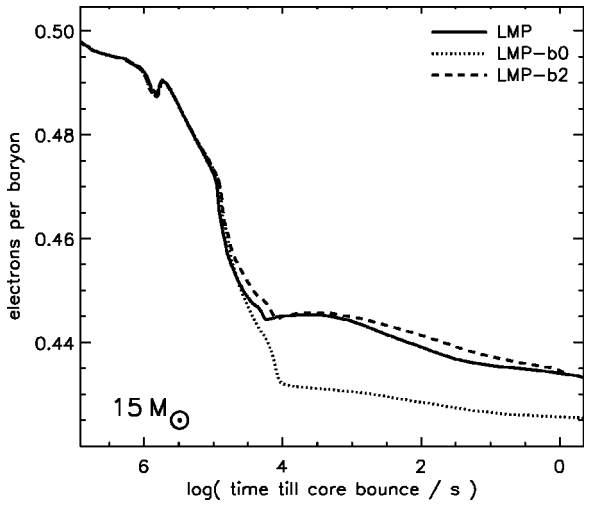


FIG. 13. Evolution of $Y_e$ in the center of a $15M_\odot$ star using three choices of weak interaction rate sets followed from central oxygen depletion until the onset of core collapse. LMP uses the weak rate set of Langanke and Martínez-Pinedo (2000); LMP-b0 and LMP-b2 are the results using the same rates with beta decay multiplied by zero and two. While the increase does not change the result much, neglecting beta decays makes a significant difference. For more details see Heger, Langanke, *et al.* (2001) and Heger, Woosley, *et al.* (2001).

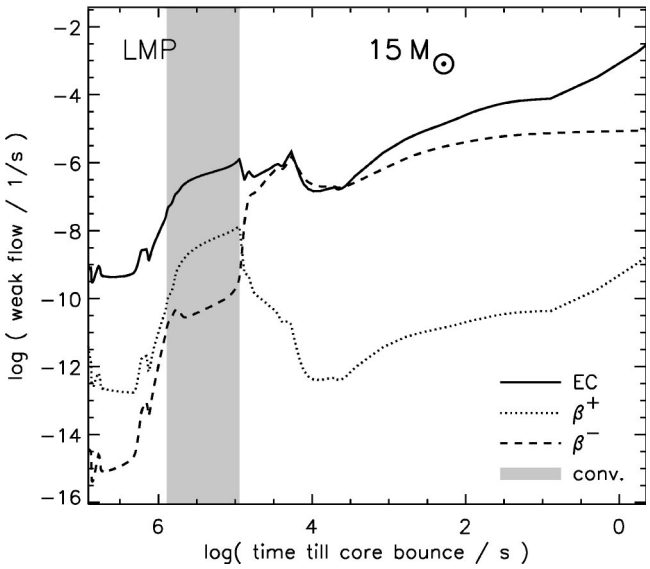


FIG. 14. Partial contributions to the evolution of the central electron mole number $Y_e$ as a function of time until collapse in a $15M_\odot$ star using the Langanke and Martinez-Pinedo rates. Note the initial dominance of electron capture, but a period around $\log(t_b - t) = 3.5$ to 4.5 when beta decay balances electron capture. Still later, the increasing density in the contracting core favors electron capture again and beta decay cannot keep up. However, time has become so short that $Y_e$ changes very little in these last few hours (Fig. 10). The shaded region is the epoch of convective silicon-core burning. For more details see Heger, Langanke, *et al.* (2001) and Heger, Woosley, *et al.* (2001).

What is bad news for pulsars may be good news for gamma-ray bursts (and vice versa) since all current gamma-ray-burst models that invoke massive star progenitors require considerably higher angular momenta than exist in the surfaces of most pulsars (Sec. VI.B).

### E. Magnetic fields

If rotation is as important as models suggest, a self-consistent depiction of angular momentum transport should include the magnetic torques that exist between differentially rotating shells. Widely varying estimates of the importance of these magnetic torques can be found in the literature. Spruit and Phinney (1998) concluded that the magnetic interaction between the rapidly rotat-

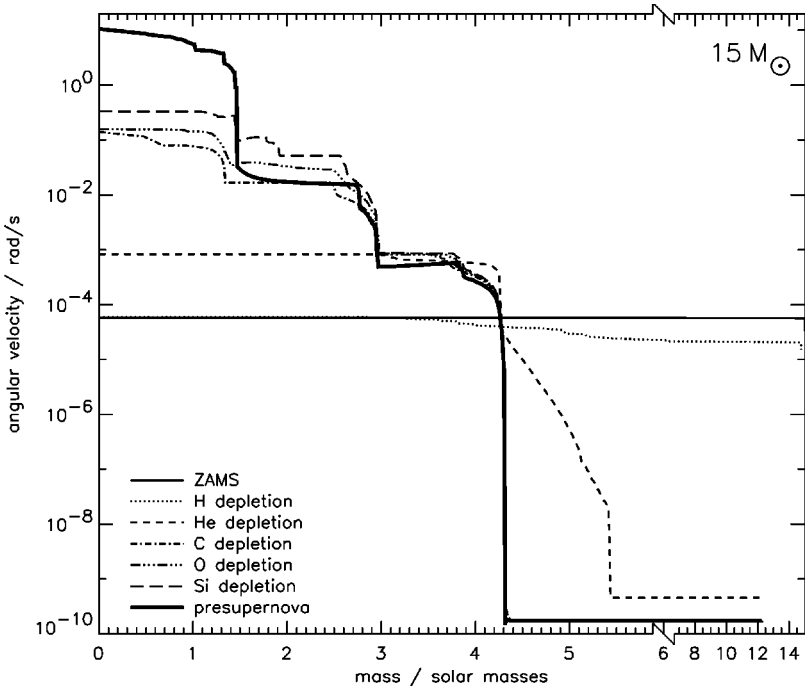


FIG. 15. Angular velocity as a function of mass coordinates at different stages of evolution for a rotating $15M_\odot$ star of solar composition with an initial surface rotation rate of 200 km s$^{-1}$ on the zero-age main sequence (ZAMS). Beyond helium depletion the angular velocity profile in the envelope (outside of $4.3M_\odot$) coincides with that of the presupernova model. The star has a fully convective hydrogen-rich envelope. The presupernova model is defined as the point where the core of the star reaches an infall velocity of 900 km s$^{-1}$. Note that the scale on the $x$ axis changes at an enclosed mass of six solar masses (Heger, Langer, and Woosley, 2000). Magnetic fields were not included in this calculation.

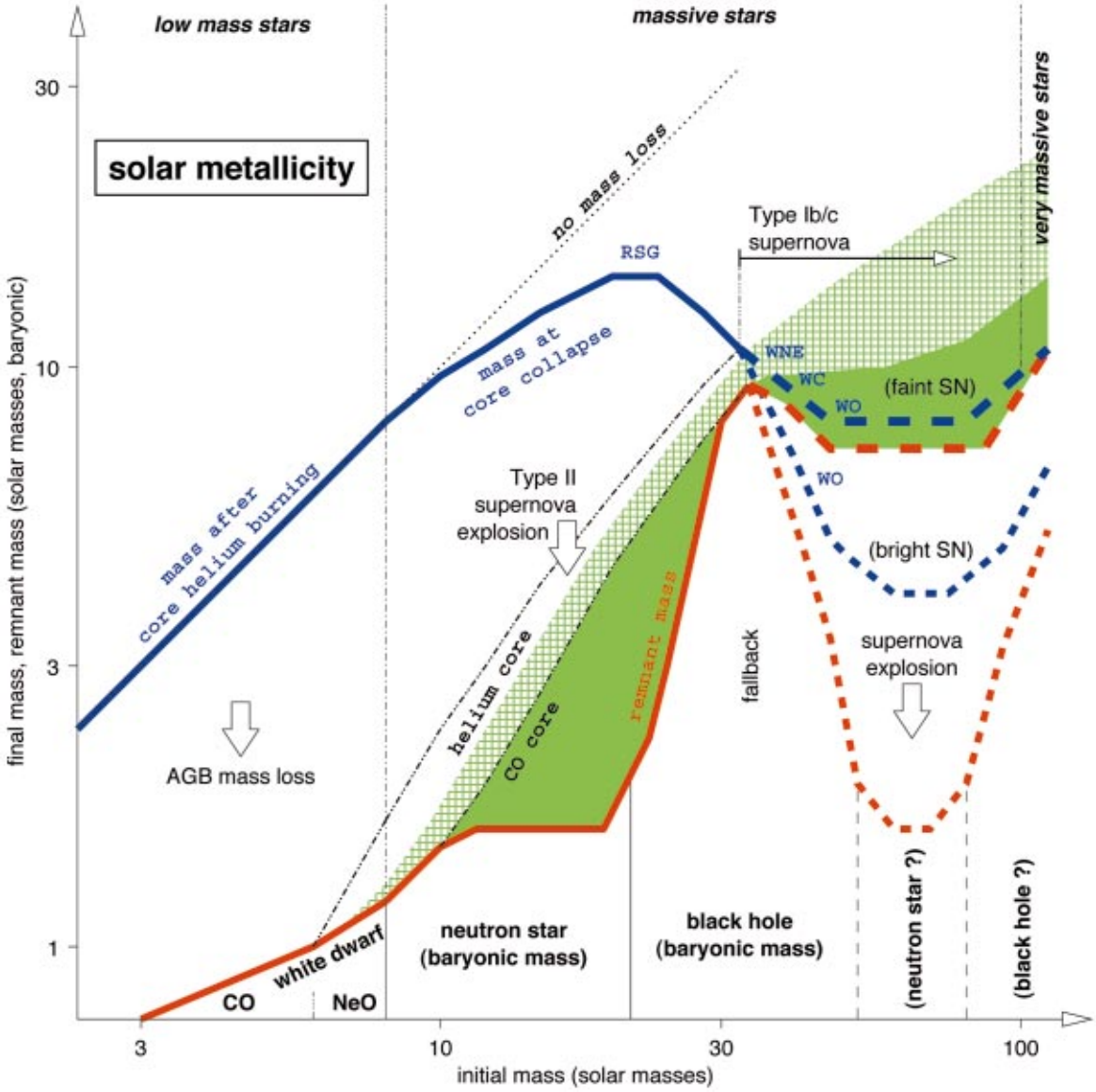


FIG. 16. Initial-final mass function of nonrotating stars of solar composition, similar to Fig. 12. Mass loss reduces the mass of the envelope (blue curve) until, for a mass above $\sim 33 M_{\odot}$ the helium core is uncovered before the star reaches core collapse. At this point the star becomes a Wolf-Rayet star and the strong Wolf-Rayet mass loss sets in. We give two scenarios for the uncertain strength of the Wolf-Rayet-mass-loss rate: The short-dashed red and blue lines are for a high mass-loss rate. Here a "window" of initial masses may exist around $50 M_{\odot}$, where neutron stars are still formed (bound by higher- and lower-mass stars that make black holes). For a low Wolf-Rayet mass-loss rate (long-dashed red and blue lines) the final mass at core collapse is higher and the "neutron star window" may not exist. Then only black boles are formed above $\sim 21 M_{\odot}$. "RSG," "WE," "WC," and "WO" indicate the type of the last mass-loss phase and also the (spectral) type of the star when it explodes. The heavy-element production (green and green cross hatched) is given only for the low-mass-loss case [Color].

ing helium core and an essentially stationary red giant envelope would halt the rotation of the former in far less than a helium-burning lifetime. The iron cores of massive stars, for them, collapsed without rotation, and pulsars acquired whatever spin they have from asymmetries in the explosion mechanism. The magnetic torque is proportional to the product of the radial component of the field $B_r$ and the poloidal component $B_\phi$. The latter can become quite large owing to differential winding, but will still reach a maximum given by instabilities and reconnection. The radial field, on the other hand, is given almost entirely by instabilities. Spruit and Phinney took $B_r \sim B_\phi$.

More recent work by Spruit (1999, 2002), which uses a physical model to estimate $B_r$, suggests an important but diminished role for magnetic torques. Using Spruit's new prescription, Heger, Woosley, and Spruit (2002) find angular momenta in their presupernova models corresponding to pulsar rotation rates that, though rapid ($\sim 10$ ms), are well below breakup. Clearly this is an area of rapid development and current great uncertainty. Unfortunately it is difficult to say today whether

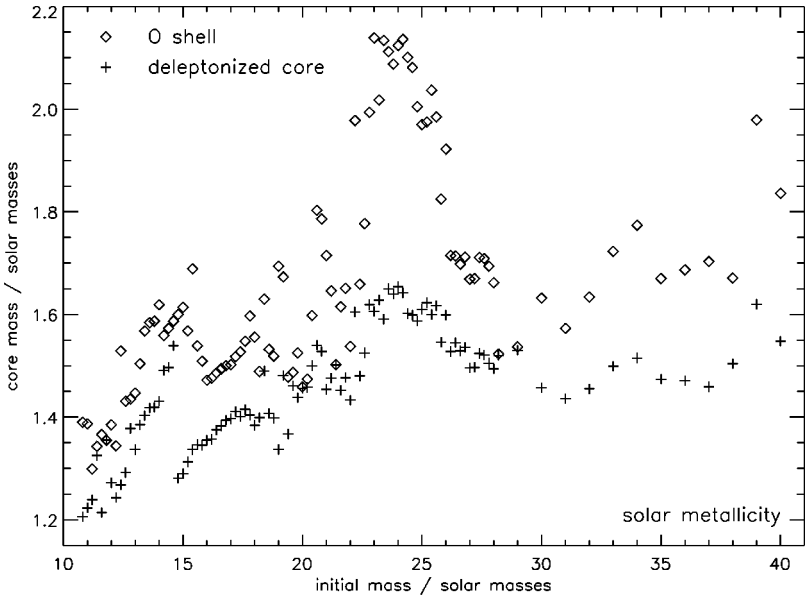


FIG. 17. The mass of the final iron cores and location of the oxygen-burning shells in a large number of presupernova stars of solar metallicity (Heger, Woosley, Rauscher, and Hoffman, 2002). The baryonic mass of the neutron star remnant might lie between these two masses.

rotation (and possibly magnetic fields) are overwhelmingly important or quite unimportant in the explosion.

### F. Effect of metallicity on the presupernova model

The principal effects of low metallicity on the presupernova structure come about because of the diminished mass loss. For solar metallicity, the helium core at death reaches a maximum of $\sim 12 M_\odot$, corresponding to an initial main-sequence mass of $35 M_\odot$ (Fig. 16). This does not preclude the existence of more massive Wolf-Rayet stars at an earlier stage in their evolution, but for higher-mass main-sequence stars of solar metallicity, the presupernova mass decreases rapidly above $35 M_\odot$ because of efficient mass loss from Wolf-Rayet stars [Eq. (15)]. This saturation of the core mass manifests itself in a variety of ways directly relevant to the explosion mechanism. Since the helium-core mass of the presupernova star ceases to grow, the iron-core mass and especially the location of the oxygen-burning shell quit increasing at around $30 M_\odot$ (Fig. 17). The binding energy of all matter outside the iron core also ceases to increase and even decreases a little. This suggests that the final products of extremely massive solar metallicity stars ($30 M_\odot$ to $>100 M_\odot$) may be no more difficult to explode than their lower-mass counterparts. We believe that such stars have their counterparts in nature as type-Ib/Ic supernovae and (if $M_{\rm preSN} \gtrsim 4 M_\odot$) subluminous type-Ib supernovae.

Presupernova stars of lower metallicity have significantly different characteristics, at least at high mass. Because of the metallicity dependence of mass loss (Sec. II.G), the mass of the lightest single star to lose its hydrogen envelope increases with declining metallicity and, along with it, the mass of its helium core at death.

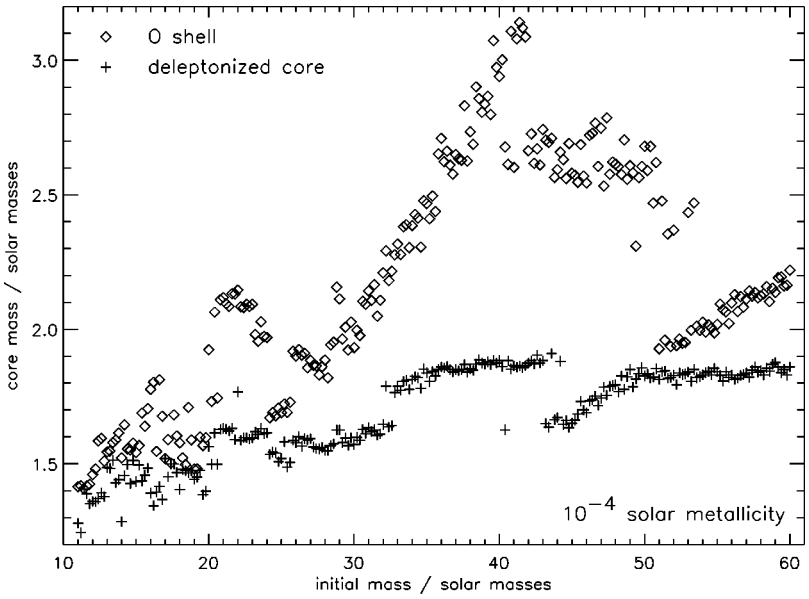


FIG. 18. The mass of the final iron cores and location of the oxygen-burning shells in a large number of presupernova stars of $10^{-4}$ solar metallicity (Heger, Woosley, Rauscher, and Hoffman, 2002).

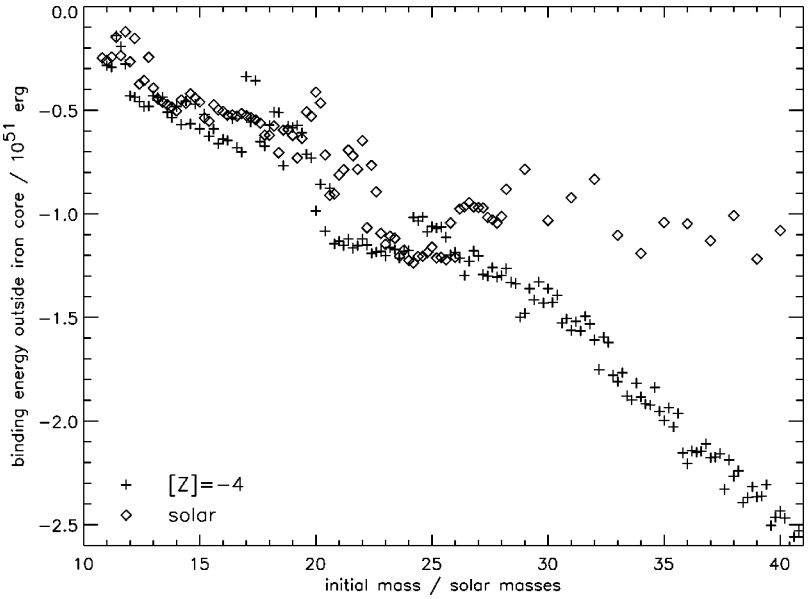


FIG. 19. Binding energy of the star outside of the iron core in a large number of presupernova stars of solar metallicity and $10^{-4}$ solar metallicity. Above about $35M_\odot$, the presupernova mass of solar metallicity stars decreases due to mass loss, along with the binding energy.

In fact, for zero-metallicity stars, the helium core increases without bound in near proportion to the main-sequence mass (Fig. 12). Consequently, the iron cores and oxygen shell masses also increase (Fig. 18) along with the binding energy (Fig. 19). A comparison at $50M_\odot$ is educational. For a solar metallicity star, the final helium-core mass is in the range 3.6–7.5 for a range of mass-loss rates equal to one to three times Eq. (15). The corresponding iron-core masses are $1.45–1.51M_\odot$ and the binding energy outside the iron core is $0.51–0.79\times10^{51}$ erg. This core should be no more difficult to blow up than similar cores that develop from the $15M_\odot$ to $25M_\odot$ main-sequence stars thought responsible for common supernovae.

Using the same physics, but with mass loss reduced by $Z^{1/2}$, the supernova progenitor coming from a $50M_\odot$ star of $10^{-4}$ solar metallicity is very different. For one thing it still has a hydrogen envelope (presupernova mass is $49.8M_\odot$); the iron-, silicon-, and helium-core masses are $2.0M_\odot$, $4.2M_\odot$, and $20.2M_\odot$, respectively, and the binding energy outside of the iron core is $2.8\times10^{51}$ erg. It is difficult to believe that this star will avoid becoming a black hole. One conclusion, then, is that black-hole formation may have occurred much more frequently, or at least in larger stars in the early universe than now. See also Secs. VI.B, VI.A, and VII. The $Z$ dependence of mass loss, however, is clearly a major uncertainty.

## V. CORE COLLAPSE AND EXPLOSION

### A. The iron core

During carbon and oxygen burning, pair neutrino losses lead to a sufficient decrease in the central entropy of a massive star that the concept of Chandrasekhar mass becomes, in an approximate sense, meaningful. Traditionally (Chandrasekhar, 1938)

$$M_{\rm Ch0}=5.83Y_e^2, \tag{31}$$

which for $Y_e=0.50$ is $1.457M_\odot$. Typical iron cores at collapse have a central $Y_e$ of 0.42, which rises gradually to 0.48 at the edge (Fig. 20). Taking $Y_e=0.45$ as an average, one might expect a Chandrasekhar mass of $1.18M_\odot$. But there are numerous corrections (Timmes, Woosley, and Weaver, 1996), some of which are large. These corrections take into account the thermal structure of the core, in particular that its entropy is not zero, the fact that the particles responsible for the pressure have charge (Coulomb corrections), the fact that the iron core is surrounded by matter (and thus has a surface boundary pressure), and the usual special and general relativistic corrections (Shapiro and Teukolsky, 1983) that, by themselves, reduce $M_{\rm Ch0}$ to $1.42M_\odot$ for $Y_e=0.50$ and $1.15M_\odot$ for $Y_e=0.45$.

The loss of entropy can facilitate the collapse of a core that is already near the Chandrasekhar mass. To a first approximation

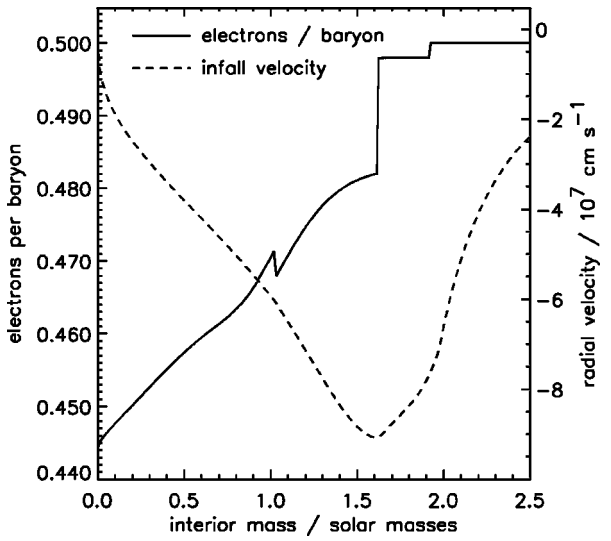


FIG. 20. Distribution of $Y_e$ (solid line) and collapse velocity (dashed line) in the inner $2.5M_\odot$ of a $15M_\odot$ presupernova star.

$$M_{\rm Ch} \simeq M_{\rm Ch0}\left[1+\left(\frac{\pi^2 k^2 T^2}{\epsilon_{\rm F}^2}\right)\right], \tag{32}$$

where $\epsilon_{\rm F}$ is the Fermi energy for the relativistic and partially degenerate electrons

$$\epsilon_{\rm F} = 1.11(\rho_7 Y_e)^{1/3}\ {\rm MeV}. \tag{33}$$

The effective Chandrasekhar mass may also be expressed in terms of the electronic entropy per baryon

$$M_{\rm Ch} \approx M_{\rm Ch0}\left[1+\left(\frac{s_e}{\pi Y_e}\right)^2\right], \tag{34}$$

where $s_e$ in units of the Boltzmann constant $k$ is (Cooperstein and Baron, 1990)

$$s_e = \frac{S_e}{N_A k} = \frac{\pi^2 T Y_e}{\epsilon_{\rm F}} \simeq 0.50\rho_{10}^{-1/3}\left(\frac{Y_e}{0.42}\right)^{2/3} T_{\rm MeV}. \tag{35}$$

At the time the iron core in a $15M_\odot$ star collapses, the electronic entropy typically ranges from 0.4 in the center to 1 at the edge of the iron core. Taking 0.7 as a rough average (and again $Y_e \approx 0.45$), one has an "effective Chandrasekhar mass" of $1.34M_\odot$, which is in fact close to calculated values (Timmes, Woosley, and Weaver, 1996). For a $25M_\odot$ star, the presupernova core entropy ranges from 0.5 to 1.8, suggesting a Chandrasekhar mass of $1.79M_\odot$. More massive stars have more entropy and, on average, produce larger iron cores and possibly more massive neutron stars. However, that general tendency is modulated (Fig. 17) by the loss and redistribution of entropy that occurs during the late burning stages.

The presence or lack of exoergic, convective carbon burning at the center of the star and the number and intensity of carbon convective shells have an important impact especially visible around $20M_\odot$ [for the current choice of $^{12}{\rm C}(\alpha,\gamma)^{16}{\rm O}$]. Below $20M_\odot$ carbon burns convectively at the middle of the star (Fig. 10); above it burns radiatively. In fact, for stars heavier than $20M_\odot$, neither carbon nor neon burning ever achieves energy generation in excess of neutrino losses at the middle of the star. Carbon still burns convectively in exoergic shells (cf. the $25M_\odot$ star in Fig. 10), but above $20M_\odot$, the number and location of these shells shift abruptly, going from four convective carbon-burning episodes in a $19M_\odot$ star to two in a $21M_\odot$ star. During these convective shell-burning phases, the center of the star sheds entropy by neutrino emission. This accounts for the abrupt change in central entropy in the presupernova models (Fig. 21), which is in turn reflected in the iron-core masses.

However, central entropy is not the whole story. The growth of the last silicon shell (whose extent determines the size of the iron core) is dependent upon the location of the oxygen-burning shell above, whose location may in turn have been influenced by the carbon and neon burning before. So long as there is an active burning shell within the core, it will not collapse; contraction leads to accelerated nuclear burning and expansion.

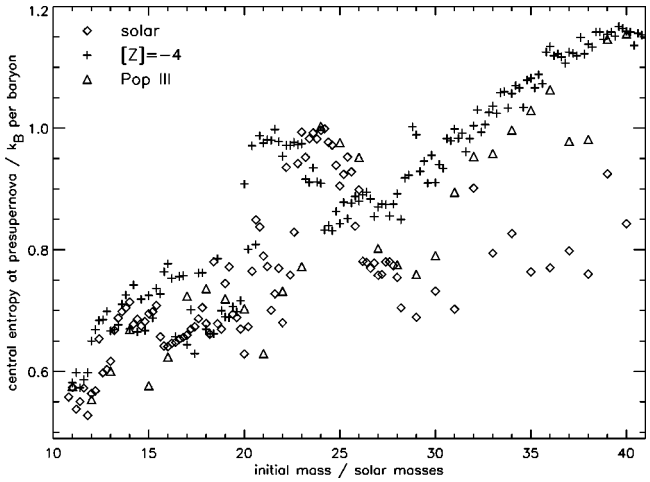


FIG. 21. Final central entropies for a large number of presupernova stars of solar metallicity (diamonds) and $10^{-4}$ solar metallicity (crosses; Heger, Woosley, Rauscher, and Hoffman, 2002). In general the entropy increases with stellar mass but with significant scatter and structure imposed by the number of burning shells. This distribution of central entropies is also reflected in the iron-core masses (Figs. 17 and 18).

However, the iron core does not grow by radiative diffusion, but by a series of convective shell-burning episodes, the last of which overshoots the (generalized) Chandrasekhar mass (usually there are just one or two such episodes). How far each silicon-burning shell extends is sensitive both to the previous entropy history in the inner regions of the star (i.e., its entire life history, especially the location of the previous oxygen-burning shells) and to how convection is treated (e.g., semiconvection or no semiconvection). This leads to some aspects of chaos and uncertainty in the presupernova iron-core mass: chaos in the sense that two stars separated by only a small mass on the main sequence can have iron-core masses that differ appreciably if one of them requires an additional shell-burning episode; uncertainty in the sense that mixing-length convection theory during oxygen and silicon burning is not very accurate (Bazan and Arnett, 1994, 1998).

### B. Collapse and bounce

A degenerate iron core in excess of the Chandrasekhar mass, appropriately adjusted for $Y_e$, entropy, boundary pressure, etc., will collapse. The core does not cross this transition abruptly, however, but on a thermal time scale, as copious neutrinos carry away the binding energy of the core. Collapse is accelerated by two instabilities. First, as the density rises, electrons capture onto iron-group nuclei, leading to a composition that is increasingly neutron rich. As $Y_e$ goes below about 0.41, the mean atomic weight of the dominant nuclei begins to increase well above mass 70. This removes electrons that were contributing to the pressure and reduces the structural adiabatic index. A second instability, dominant in the more massive stars, is photodisintegration. Continuing to follow a path of approximately $\rho_{\rm c} \propto T_{\rm c}^3$ carries the

star into a region where nuclear statistical equilibrium favors a large abundance of free $\alpha$ particles. The nuclear binding energy of this new composition is less, so the core does not gain sufficient thermal energy in the contraction to keep pace with gravity. Considered from an entropy point of view, the production of alpha particles increases the ionic entropy (one nucleus becomes 14) but, since the overall contraction is approximately adiabatic (neglecting neutrino losses), the electronic entropy must decrease (Cooperstein and Baron, 1990). This reduces the effective Chandrasekhar mass and favors collapse. However, full dissociation into $\alpha$ particles does not occur.

Prior to about 1980, it was thought that the iron core might photodisintegrate not only into $\alpha$ particles but completely into nucleons. Electrons would then capture on free protons, not bound nuclei, and the supernova core might experience a thermal bounce at a density well below nuclear. Bethe *et al.* (1979) emphasized the role of the nuclear partition function—especially the exponential growth of the number of excited nuclear states populated at high temperature—in keeping the matter from totally disintegrating. As a result, it was understood that the bounce would be relatively cold, with heavy bound nuclei persisting until they touched and merged at just below nuclear density. The resulting ensemble, essentially one gigantic stellar mass nucleus, would then bounce, overshooting nuclear density by a factor of several. Here the repulsive hard-core potential of the nucleus acts as a stiff spring storing up energy in the compressive phase, then rebounding as the compression phase ends. That portion of the collapsed, neutronized core that stays in sonic communication, the sonic mass, and the so-called "homologous core mass," that part of the core that collapses with $v \propto r$, are approximately equal. Just outside of these, a shock wave initially forms as the rebounding core encounters matter that is continuing to fall in. The impact is supersonic; the bouncing core has positive velocity, the infalling material is negative. In a perfectly elastic collision, the infalling outer core could bounce back to the radius from which it fell, even if the inner core were stationary. The outward motion of the inner core thus gives rise to the possibility of a "superelastic bounce."

For a time it was thought that this bounce shock would successfully explode the star (Baron, Cooperstein, and Kahana, 1985; Baron *et al.*, 1987). Now we know that, for models with realistically sized iron cores, it does not (Bruenn, 1989a, 1989b; Myra and Bludman, 1989; Baron and Cooperstein, 1990; Cooperstein and Baron, 1990). Two effects act to prohibit the development of the prompt explosion. The first is photodisintegration. As the shock moves through infalling bound nuclei, it heats them and tears them apart to neutrons and protons (despite the large partition function). The shock spends roughly $10^{51}$ erg for each $0.1 M_\odot$.

The second effect is neutrino emission from behind the shock, especially as it moves to lower-density regions below $10^{12}\ \mathrm{g\,cm^{-3}}$ where neutrinos can diffuse out ahead of the shock. $\mu$ and $\tau$ neutrinos participate in this shock-wave cooling, as do electron neutrinos. The scattering of neutrinos of all flavors with electrons behind the shock is also important. Unlike the coherent scattering off of nuclei and nucleons that provides the major source of neutrino opacity, electron scattering does not conserve neutrino energy. By reducing the mean neutrino energy, electron scattering makes it easier for neutrinos to escape. The successful prompt shock explosions of Baron, Cooperstein, and Kahana (1985) neglected $\mu$ and $\tau$ neutrinos and electron scattering and thus gave unrealistic explosions.

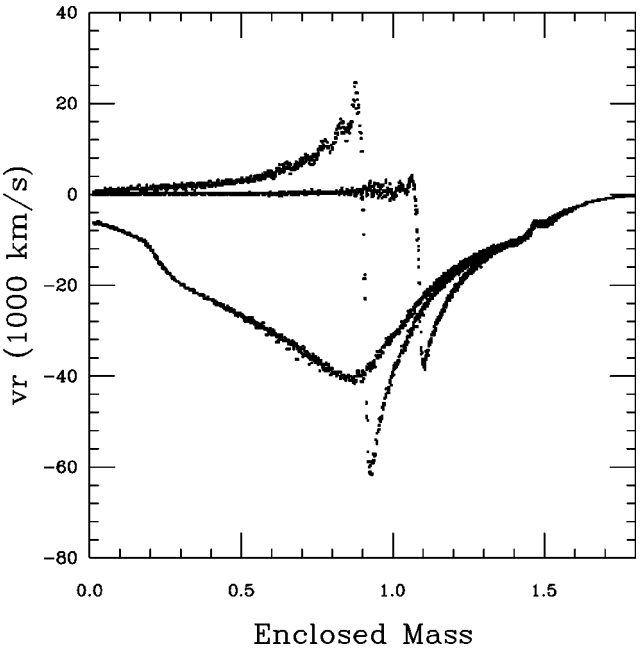


FIG. 22. Collapse and bounce of the iron core in a $13 M_\odot$ supernova. Radial velocity vs enclosed mass at $-0.5$ ms, $+0.2$ ms, and 2.0 ms with respect to bounce. The blip at $1.5 M_\odot$ is due to the explosive nuclear burning of oxygen in the infall (Herant and Woosley, 1996).

And so one is left, about 10 ms after the core has bounced, with a hot dense proto-neutron star accreting matter at its outer boundary at a high rate ($1-10 M_\odot\ \mathrm{s^{-1}}$; Fig. 22).

### C. Neutrino energy deposition and convection; the shock is launched

A successful explosion then requires a new energy source. This is now thought to be neutrino energy deposition (Colgate and White, 1966; Bethe and Wilson, 1985; Mayle, 1985, 1990; Wilson, 1985; Wilson *et al.*, 1986; Bethe, 1990; Mayle and Wilson, 1991). The shock wave is revived on a time $\sim 0.1$ s, long compared to the hydrodynamic time scale, a few ms for the shock to reach the edge of the core, but short compared to the 3–10 s Kelvin-Helmholtz time scale for the neutron star

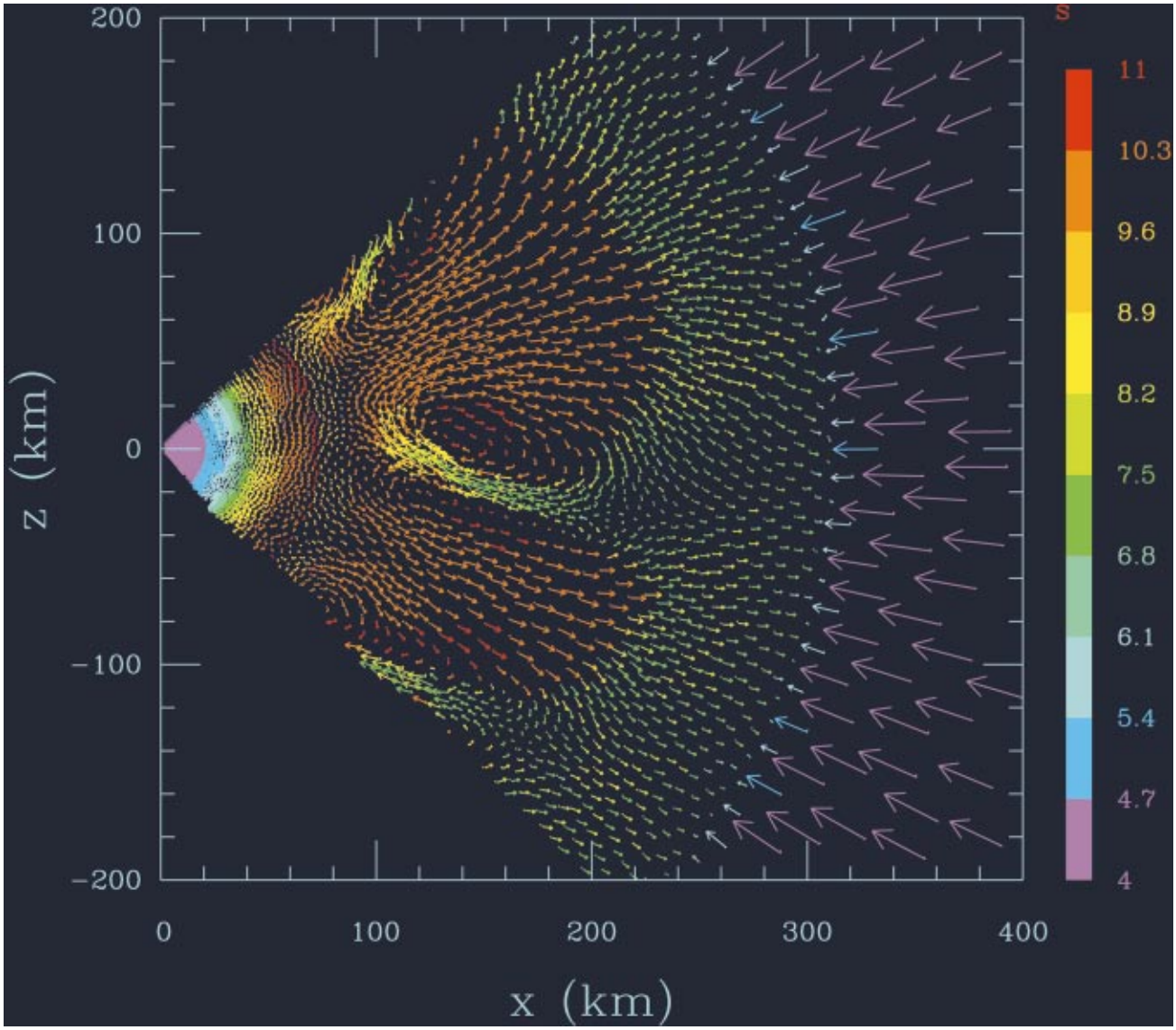


FIG. 23. Neutrino-driven convection 50 ms after the bounce of the core of a $13M_{\odot}$ supernova. The entropy is color coded (Herant and Woosley, 1996) [Color].

to emit its binding energy. Considerable progress has been made in the last decade in simulating this event in two dimensions.[3]

Multidimensional calculations (or at least a parametric representation of multidimensional effects) are essential in order to reveal the convective flow responsible for boosting the neutrino luminosity of the proto-neutron star. This flow also increases the efficiency of neutrino absorption (by cooling the region where neutrinos deposit their energy) and carries neutrino-deposited energy out to the shock (Fig. 23). Most of the calculations cited above have found successful explosions in two dimensions when these convective effects are included.

Not all agree, however. Bruenn and Mezzacappa find that convection does not lead to explosion. Moreover, all of these exploratory calculations were done for a very limited range of stellar masses ($13M_{\odot}$ and $15M_{\odot}$) and metallicities (solar) and with overly simple prescriptions for neutrino energy transport. Two-dimensional (2D) calculations of turbulent flow are also known to misrepresent the turbulent cascade. Work is underway by all the groups listed above for their 2D work to rectify these problems, and we may expect progress in the near future.

Those two-dimensional models that *do* explode so far share common problems when compared to observation. Because neutrino interactions with nucleons in the convective hot bubble lead to a significant lowering of $Y_e$,

[3]See the work of Herant, Benz, and Colgate, 1992; Burrows and Fryxell, 1993; Herant *et al.*, 1994; Bruenn and Mezzacappa, 1994; Burrows, Hayes, and Fryxell, 1995; Janka and Müller, 1995, 1996; Mezzacappa *et al.*, 1998; Fryer and Heger 2000.

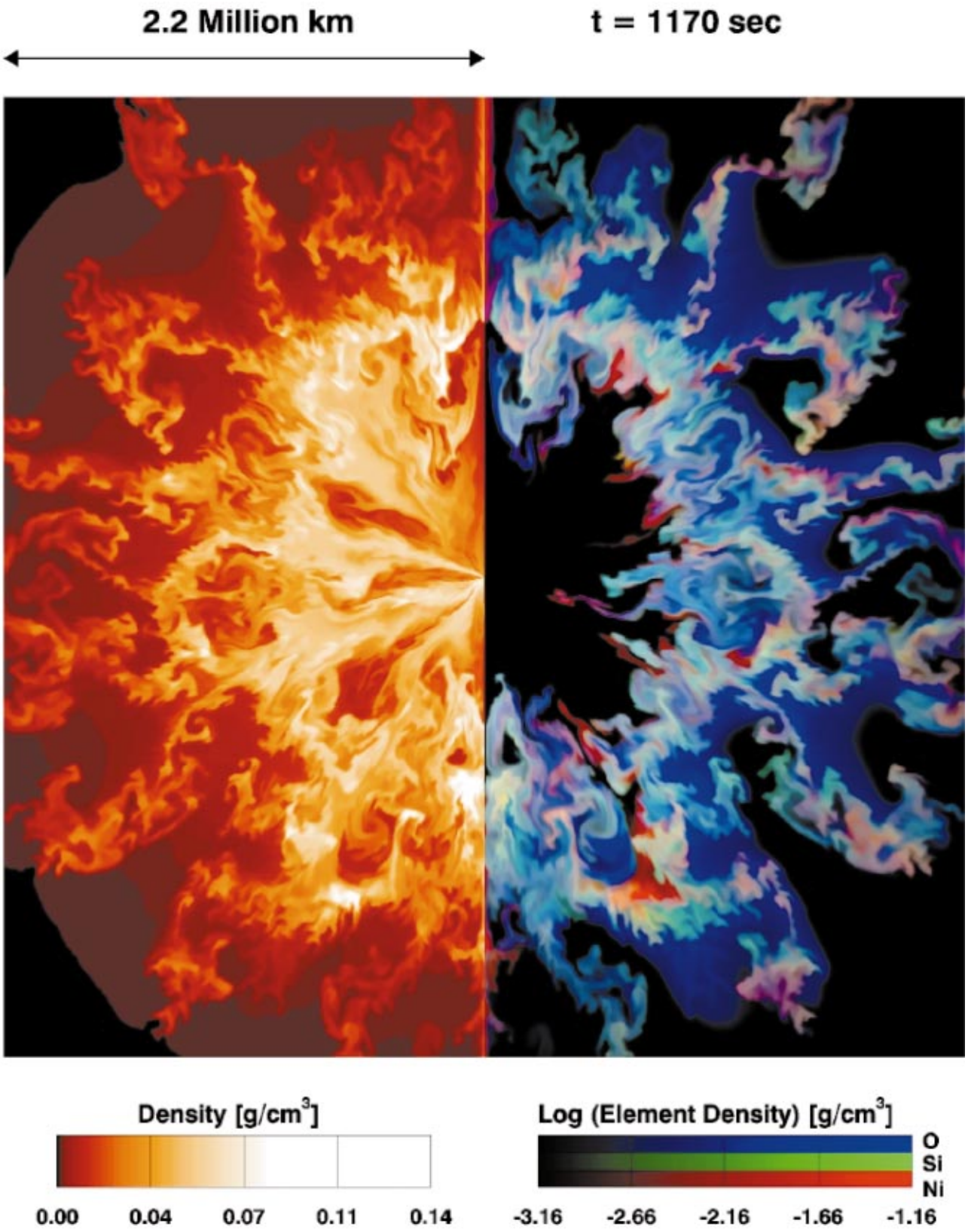


FIG. 24. Mixing in the explosion of a $15M_{\odot}$ red supergiant. From Kifonidis *et al.*, 2000 [Color].

they eject too much neutron-rich nucleosynthesis. Most of the calculations so far follow the explosion for a very limited time and it is not known with any accuracy how the kinetic energy produced by the supernova depends on the initial stellar mass (though see Fryer, 1999). Those calculations that do produce an explosion tend to blow away a portion of the neutron star and leave remnant masses that are too small. The degree of fallback

(Sec. VI.A) also remains uncertain.

### D. Shock propagation and mixing

Given an outgoing shock, there are instabilities that will affect its propagation and, even for initially spherically symmetric explosions, produce mixing and irregular structure. Falk and Arnett (1973) and Chevalier and Klein (1978) pointed out that passage of the shock leaves behind regions of inverted gravitational and density gradients subject to Rayleigh-Taylor instability. Numerous multidimensional calculations since that time[4] have shown the importance of this instability and its dependence upon stellar mass and density structure. In general, stars with more massive extended envelopes, that is, red supergiants that have not lost a lot of mass, experience the greatest degree of mixing and clumping. Stars that have lost much of their hydrogen envelope experience less, but even stars with no hydrogen envelope experience some mixing at the interfaces between the silicon core, the carbon-oxygen core, and the helium core (Kifonidis *et al.*, 2000; Fig. 24). Such mixing may be necessary in supernovae without hydrogen in order to explain the light curves and spectra of type-Ib and type-Ic supernovae (Shigeyama *et al.*, 1990; Woosley and Eastman, 1997). Without mixing, the heating from $^{56}$Ni and $^{56}$Co decay is concentrated in too small a volume and the photosphere recedes rapidly with time, producing a supernova that is overly blue. The rise time of the light curve is also affected. Lacking the nonthermal excitation of gamma rays from radioactive decay, distinctive lines in the spectrum, especially He I [5876A], are absent.

The criterion for mixing is that the outgoing shock slow down in a region where the density is declining. The Sedov solution shows that the shock will decelerate when passing through a region where the quantity $\rho r^3$ increases (Herant and Woosley, 1994; Fig. 22). Of course appreciable mixing can also be introduced if the central engine powering the explosion inputs its energy in an asymmetric way. Calculations to study this are still in an early stage (Burrows, Hayes, and Fryxell, 1995; Nagataki, Shimizu, and Sato, 1998; Fryer and Heger, 2000). Seeds for the mixing may already be present in the convective shells prior to shock-wave passage (Bazan and Arnett, 1998).

One of the principal lessons of SN 1987A was the importance of mixing for understanding even the qualitative shape of the light curve (Shigeyama, Nomoto, and Hashimoto, 1988; Woosley, 1988; Arnett and Fu, 1989; Shigeyama and Nomoto, 1990) as well as details of the spectrum (Utrobin, Chugai, and Andronova, 1995), the high velocity of heavy elements (Witteborn *et al.*, 1989), and the early appearance of x rays and gamma rays from radioactive decay (Itoh *et al.*, 1987; Kumagai *et al.*, 1988, 1989; Pinto and Woosley, 1988a, 1988b).

## VI. NEUTRON STARS AND BLACK HOLES

Given the uncertainties surrounding the explosion mechanism (Sec. V.C), it is difficult to say with any precision just what the mass of the collapsed remnant will be for a given presupernova model. However, some general restrictions and tendencies can be noted. First, on nucleosynthetic grounds, the average supernova cannot eject more than about $0.01M_\odot$ of its presupernova iron core. Material inside the last silicon convective shell is quite neutron rich and limits on $^{54}$Fe production—if not rarer, more neutron-rich species—limit its ejection (Weaver, Zimmerman, and Woosley, 1978). It may thus be safely assumed that the iron-core mass is a lower limit to the baryonic mass of the remnant. For stars between about $8M_\odot$ and $10M_\odot$, the falloff of density outside the iron core is so rapid that any successful explosion should eject it all. For these stars, the iron-core mass is also approximately an upper limit on the remnant mass. No such upper bound exists for heavier stars unless one imposes information about the engine—for example, that it provide a certain energy (Woosley and Weaver, 1995). However, there is a jump in entropy at the base of the oxygen-burning shell that signals a rapid falloff in density outside. A neutrino-powered explosion that accretes matter up to this point will experience a rapid decline in ram pressure from the infalling material.

In the absence of definitive explosion models, one may then assume that the remnant will have a baryonic mass between the iron-core and oxygen-shell masses given in Figs. 17 and 18. For progenitor stars between $11M_\odot$ and $20M_\odot$ this gives remnant masses in the range $1.3–1.6M_\odot$. The explosion physics of larger stars is even more uncertain, but the plots indicate that they may make either larger neutron stars or, at some point, black holes. After radiating away its binding energy as neutrinos, a neutron star loses $\sim$10–15 % of its rest mass, with the larger stars radiating a larger fraction. One therefore expects gravitational masses (for the most frequent events) in the range $1.2–1.4M_\odot$. The average gravitational mass for 26 neutron stars observed in binary systems is $1.35\pm0.04M_\odot$ (Thorsett and Chakrabarty, 1999). Given all the uncertainties in the stellar and supernova models, this is remarkable agreement and suggests that in many events the mass cut has not occurred far outside the oxygen shell. However, the dispersion about the mean is much smaller in the observations than theory would suggest (Fig. 17). A possible explanation is that the observed neutron star masses are all obtained from binary systems (accurate masses are thus far impossible to obtain elsewhere) which may have experienced mass exchange prior to producing supernovae. Removing the hydrogen envelopes from massive stars results in the convergence upon a narrow range of presupernova masses (Fig. 5), around $3–4M_\odot$. This same small range is necessary to explain the near uniformity and narrow peaks of the light curves of type-Ib supernovae. Any

[4]See, for example, Arnett, Fryxell, and Müller, 1989; Müller, Fryxell, and Arnett, 1991; Herant and Benz, 1992; Hachisu *et al.*, 1994; Herant and Woosley, 1994; Iwamoto *et al.*, 1997; Nagataki, Shimisu, and Sato, 1998; Kifonidis *et al.*, 2000.

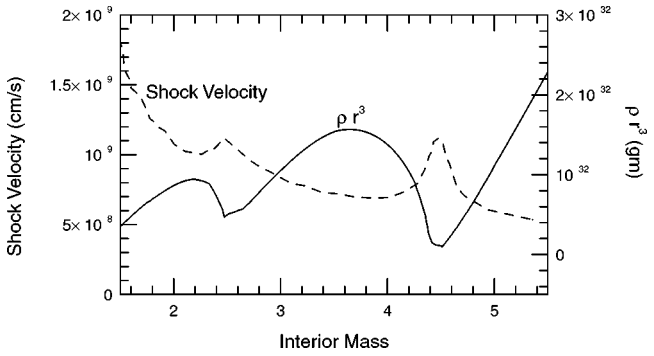


FIG. 25. The distribution of $\rho r^3$ in the interior of a $15M_\odot$ presupernova star (right-hand axis) and the shock speed (left-hand axis) as a function of mass for an explosion of $1.2 \times 10^{51}$ erg. The $15M_\odot$ progenitor is a red supergiant. Note the correlation between shock acceleration and declining $\rho r^3$. When the shock decelerates it leaves behind a region that is unstable to mixing. The edge of the helium core is at $4.2M_\odot$ so a large degree of mixing occurs as the helium core runs into the hydrogen envelope. From Woosley and Weaver, 1995.

$4M_\odot$ core mass resembles in structure, though not necessarily in composition, the helium core of a $\sim 15M_\odot$ supernova (Fig. 4). From $13M_\odot$ to $17M_\odot$ the mass of the silicon core (interior to the oxygen-burning shell) varies little and is almost always between $1.5M_\odot$ and $1.6M_\odot$ (gravitational mass $1.3–1.4M_\odot$).

Above $25M_\odot$, for solar metallicity, the iron-core mass stops rising, reflecting the diminished mass of the star by mass loss (Table I; Fig. 16). The gravitational binding energy of the star outside the iron core also stops increasing. Whether such stars leave black holes depends upon an uncertain equation of state for the neutron star and unresolved details of the explosion (see especially Sec. VI.A).

### A. Fallback during the explosion

Even if a successful shock is launched and a stable neutron star is left behind, the story of the compact remnant is not over. The shock must have sufficient energy (and maintain sufficient pressure at the origin) to eject all the rest of the star. Since the shock's energy is determined on a time scale of about 0.1 s, but it takes tens of seconds to sample the mass and binding energy of the overlying matter, the shock cannot know ahead of time how hard it will be to explode the star. Obviously if the shock energy is less than the binding energy of the star outside the iron core, some matter must fail to achieve escape velocity, but actually the criterion for fallback is more complicated and restrictive due to the nonmonotonic behavior of the shock velocity in the overlying star (Sec. V.D; Fig. 25).

Woosley and Weaver (1995) and MacFadyen, Woosley, and Heger (2001) have shown that the amount of mass that falls into the collapsed remnant is very sensitive to the explosion energy and the presupernova mass of the star. In their (1D) calculations many supernovae leave black holes formed a few hours after launching successful shocks that make bright optical events. In some cases the radioactive $^{56}$Ni falls back, which removes its contribution to the light curve and nucleosynthesis. In others, the entire heavy-element core implodes. One expects the effect to be even more important in stars of low metallicity because of both the larger binding energy of such stars (Fig. 19) and the enhanced fallback expected for blue supergiants as compared with red ones (Chevalier, 1989).

The type-II supernova atlas of Patat *et al.* (1993, 1994) shows that many type-II supernovae have exponential tails compatible with what is expected from the decay of $^{56}$Co. One possible signature of black-hole formation would be a bright optical supernova that lacked the radioactive tail because all the $^{56}$Ni fell into the remnant. A low $^{56}$Ni mass might also be produced in supernovae around $10M_\odot$ (Wilson and Mayle, 1988), and mixing could result in some $^{56}$Ni's being ejected even in events that make black holes, so this is not a unique diagnostic, but the larger the black hole the more likely that no $^{56}$Ni was ejected at all (Turatto *et al.*, 1998).

### B. Fate of "failed" supernovae

It is to be emphasized that black-hole production and supernovae are not mutually incompatible outcomes. Even without rotation, a metastable proto-neutron star could form, launch a successful shock, and collapse after some delay to a black hole (Bethe and Brown, 1995; Ellis, Lattimer, and Prakash, 1996; Pons *et al.*, 1999). This can occur only if the remnant core mass is only slightly above the maximum stable neutron star mass. A more likely pathway for making black holes in supernovae is fallback (Sec. VI.A).

With rotation, the possibilities become richer. Nuclear burning cannot, by itself, reverse the implosion of a massive star that has formed a neutron star or black hole at its center (Woosley and Weaver, 1982; though see Sec. VII). But if the "braking action of rotation" (Fowler and Hoyle, 1964) is included, a thermonuclear supernova is possible (Bodenheimer and Woosley, 1983). The amount of angular momentum required is large, however (MacFadyen and Woosley, 1999), over $10^{17}$ erg s in the mantle, in order that centrifugal stagnation occurs deep enough for explosive oxygen burning ($T_9 \gtrsim 3$), but not so deep as to cause photodisintegration ($T_9 \gtrsim 5$). The actual rotation rates are likely to be slower so that the infalling material does photodisintegrate but still has sufficient angular momentum to pile up in an accretion disk outside the event horizon ($j \gtrsim 10^{16}$ erg s). What follows then depends on the uncertain physics of magnetohydrodynamics accretion into a rapidly rotating black hole.

Based upon both theory (see, for example, Blandford and Znajek, 1977; MacFadyen and Woosley, 1999) and observations of jets in active galactic nuclei, it seems likely that some fraction, of order 1–10 %, of the mass that accretes through the disk will be converted into the energy of twin jets propagating along the rotational axes. The mechanism for converting disk energy to jet energy could be neutrino transport, magnetic-field dissi-

pation in the disk, extraction of part of the black hole's rotational energy, or other more exotic processes. For 1% efficiency, over $10^{52}$ erg of jet energy would be provided by the accretion of only $1M_\odot$ of mantle material. The accretion would take $\sim 10$ s, the free-fall time scale for a mantle with average density $\sim 10^4$ g cm$^{-3}$. This jet would explode the rest of the star (MacFadyen, Woosley, and Heger, 2001), but would still maintain a large fraction of its initial energy after breaking out (Aloy *et al.*, 2000; Zhang, Woosley, and MacFadyen, 2002). Interaction of this relativistic jet with the circumstellar matter would produce a cosmic gamma-ray burst (Woosley, 1993; Jaroczynski, 1996; MacFadyen and Woosley, 1999). It is important in this gamma-ray-burst model that the star have lost its hydrogen envelope prior to iron core collapse, otherwise the jet dissipates its energy prior to breaking out. Though detrimental for gamma-ray bursts, a star with an extended envelope might still make a very powerful, bright supernova.

MacFadyen (2001) and MacFadyen and Woosley (1999) have also pointed out that, even in the absence of jets, the disk itself produces a strong "wind," composed initially of nucleons and later of $^{56}$Ni, that carries over $10^{51}$ erg of kinetic energy. This wind alone could power a supernova. The relation between gamma-ray bursts and supernovae is an area of rapid progress in which one can expect significant revisions in the near future. For now we merely point out that there may be more than one way to explode a massive star and a "fail-safe" mechanism that operates even when the ordinary neutrino energy paradigm fails (see also Wheeler *et al.*, 2000).

Of course in the absence of rotation, and without an outgoing shock produced by neutrino energy deposition, there is no supernova. The star simply disappears.

## VII. PAIR-INSTABILITY SUPERNOVAE

Thus far our discussions have focused on main-sequence stars of under $100M_\odot$. If the presupernova star has a helium core in excess of $40M_\odot$ a new kind of explosion mechanism becomes accessible, one powered by nuclear burning. This is the domain of the *pair-instability supernova*. Following helium burning, the star contracts at an accelerated rate. Energy that might have gone into raising the temperature and providing more pressure support is diverted to the production of electron-positron pairs. The creation of these particles' rest mass temporarily drives the structural adiabatic index below 4/3 and a runaway collapse develops—higher temperature makes more pairs and accelerates the implosion. Nuclear energy generation from carbon and neon burning is insufficient to halt this contraction, but, in some cases, oxygen burning can. By this point, though, the collapse has already become dynamic and the star overshoots the temperature and density that might have provided hydrostatic equilibrium. The energy release from very temperature-dependent fusion reactions eventually halts the infall if the collapse velocity is not too high or the star already too tightly bound, but it is more than that necessary for an elastic bounce. Implosion becomes explosion. The more massive the helium core, the deeper the bounce, the higher the bounce temperature, and the greater the amount of oxygen burned. For quite high stellar masses, oxygen burning is inadequate to reverse the implosion and, in the absence of rotation, the star becomes a black hole.

Explosions of this sort have been studied for many years (Rakavy, Shaviv, and Zinamon, 1967; Bond, Arnett, and Carr, 1984; Glatzel, Fricke, and El Eid, 1985; Woosley, 1986), but there has been a recent resurgence of interest because such massive stars may have been an important component of Population III, the first stars to form in the universe (Bromm, Coppi, and Larson, 1999; Abel, Bryan, and Norman, 2000; Nakamura and Umemura, 2000). In order to die with a helium-core mass over $40M_\odot$, not only must main-sequence stars be considerably over $100M_\odot$ (El Eid and Langer, 1986; Langer and El Eid, 1986), but mass loss must not erode the helium core. Mass loss may be driven either by radiation or by nuclear pulsations, and it has long been known that stars in this mass range would be subject to both (Schwarzschild and Härm, 1959; Appenzeller, 1970; Talbot, 1971a, 1971b; Papaloizou, 1973a, 1973b). Probably pair-instability supernovae do not exist at solar metallicity.

However, the situation changes again at low metallicity, where it is possible not only to make such stars but to preserve them. Radiative winds depend on the metallicity and can be neglected in very metal-deficient stars. Recent studies by Baraffe, Heger, and Woosley (2001) also suggest that very massive stars, up to at least several hundred solar masses, may be stable to the usual epsilon instability on the main sequence.

Recent studies by Heger and Woosley (2002) have helped to clarify both the behavior of pair-instability supernovae as a function of progenitor mass and their nucleosynthesis. For helium cores between about $40M_\odot$ and $65M_\odot$, corresponding to main-sequence masses in the range $100–140M_\odot$, the pair instability leads to violent mass-ejecting pulsations, but not the complete disruption of the star. Multiple pulses, each with supernovalike energy, eject sufficient material that the instability is relieved and the star ends its life eventually, producing an iron core that collapses much like those in the lighter stars (Woosley, 1986). If collapse of the iron core leads to another strong explosion, collision among the shells could produce a very bright light curve, though this remains to be explored in any detail. The first pulse ejects what remains of the hydrogen envelope, and subsequent pulsations may continue for years (for helium cores near $40M_\odot$) or even centuries (for helium cores near $65M_\odot$).

Above $65M_\odot$ and below $133M_\odot$ (or main-sequence masses $\sim 140–260M_\odot$), the core of helium and heavier elements is completely disrupted by a single thermonuclear explosion of increasing violence. The peak temperature achieved during the thermal bounce increases with mass, and heavier elements are produced. The kinetic energy of the explosion also increases with mass.

In the explosion of a $70M_\odot$ helium core, only $0.1M_\odot$ of $^{56}$Fe is produced (made as $^{56}$Ni), but by the time the core mass reaches $130M_\odot$, $40M_\odot$ of iron is made in a single explosion that reaches a bounce temperature of $6.2\times10^9$ K. The net kinetic energies in the $70M_\odot$ and $130M_\odot$ core explosions are $4.9\times10^{51}$ erg and $8.7\times10^{52}$ erg, respectively, possibly making these the biggest stellar explosions in the universe. Those stars that make tens of solar masses of $^{56}$Ni are brighter than several type-Ia supernovae put together and stay that bright for many months (Heger, Pinto, and Woosley, 2002). Sometimes they are referred to as hypernovae (Woosley and Weaver, 1982).

Above $133M_\odot$ (main-sequence mass $260M_\odot$), without rotation, helium cores collapse directly to black holes. Nuclear burning is unable to reverse the momentum of the implosion before a large fraction of the core encounters the photodisintegration instability. This suggests that if many stars were born in the early universe with mass over $260M_\odot$, black-hole production may have been a common occurrence. With rotation, the mass limit for black-hole formation increases and still more violent explosions can occur. Possibly these stars too make black holes with transient accretion disks and may also produce some form of energetic electromagnetic display (Fryer, Woosley, and Heger, 2001).

In terms of nucleosynthesis, depending on the initial mass function, pair-instability supernovae can produce a nearly solar distribution of elements from oxygen through nickel, but with a large deficit of nuclei with odd nuclear charge (N, F, Na, Al, P, etc.). This reflects the lack of appreciable weak interactions during the explosion in all but the most massive events (Heger and Woosley, 2002), hence $Y_e$ remains very close to 0.50. Pair-instability supernovae make no elements by the $r$, $s$, or $p$ processes and eject no elements heavier than zinc.

## VIII. NUCLEOSYNTHESIS RESULTING FROM GRAVITATIONALLY POWERED EXPLOSIONS

Nucleosynthesis in both the preexplosive and explosive phases of massive stellar evolution has been extensively reviewed.[5] Here we present both a summary of conditions and processes, difficult to find in any single reference thus far, as well as some recent results using the latest stellar models and nuclear physics.

### A. Conditions for explosive nucleosynthesis

The conditions for explosive nucleosynthesis in massive stars are characterized primarily by the peak temperature achieved in the matter as the shock passes and

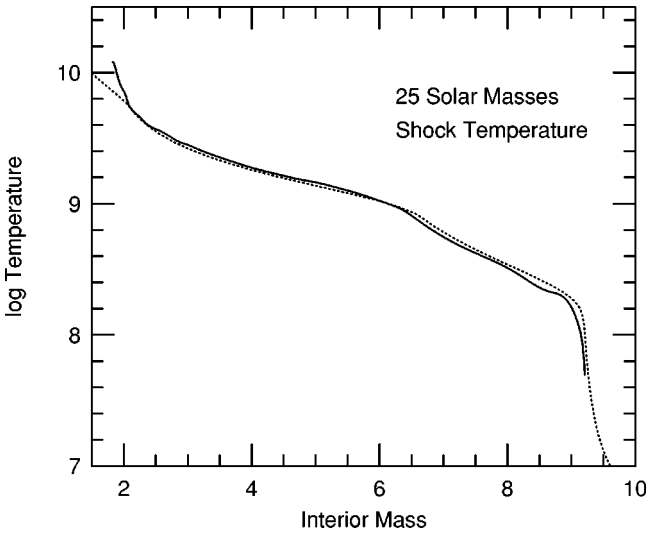


FIG. 26. Shock temperature as a function of mass for a $25M_\odot$ supernova of final kinetic energy at infinity of $1.2\times10^{51}$ erg. The dashed line is an approximation [Eq. (37)] discussed in the text.

the time for which that temperature persists. A typical time for the density to $e$-fold is the hydrodynamic time

$$\tau_{\rm HD}\approx\frac{446}{\rho^{1/2}}\ {\rm s}, \tag{36}$$

where $\rho$ is the mean density interior to $r$, or very approximately, the local density. Except for small radii near the origin of the shock, the peak temperature at radius $r$ can be obtained by setting $(4/3)\pi r^3 a T_s^4 \approx KE_{\rm inf}\approx10^{51}$ erg. This assumes that the heat capacity of the material behind the shock is in the radiation field and that expansion and pressure waves behind the shock are capable of maintaining nearly isothermal conditions. The shock temperature at radius $r$ is then given to good accuracy (Fig. 26) by

$$T_s(r)=1.33\times10^{10}\left(\frac{KE_{\rm inf}}{10^{51}\ {\rm erg}}\right)^{1/4}\left(\frac{r}{10^8\ {\rm cm}}\right)^{-3/4}{\rm K}. \tag{37}$$

Temperatures greater than 5 billion K will be achieved interior to $\sim$3700 km. At such high temperatures, any initial composition is processed into nuclear statistical equilibrium on a hydrodynamic time scale. Consequently any part of the presupernova star ejected from the interior to 3700 km will be iron-group elements. At a radius of 5000 km the shock temperature falls below 4 billion K and at 13 000 km to 2 billion K. At this point explosive nuclear processing ceases for all fuels heavier than helium.

In fact the necessary condition for explosive modification of the preexplosive composition is that the burning lifetime at the shock temperature be less than the hydrodynamical time scale. Defining $\tau_{\rm nuc}$ as $q_{\rm nuc}/\dot{S}_{\rm nuc}$ and using Eqs. (18), (21), (23), and (27), one finds that silicon will burn explosively between 4 and 5 billion K; oxygen

[5]See Burbidge *et al.* (1957), Trimble (1975), Arnett and Thielemann (1985), Thielemann and Arnett (1985), Woosley (1986), Arnett (1995, 1996), Woosley and Weaver (1995), Thielemann, Nomoto, and Hashimoto (1996), and Wallerstein *et al.* (1997).

between 3 and 4; neon between 2.5 and 3; and carbon between 1.8 and 2.5. The products of explosive nucleosynthesis are more sensitive to the peak temperature than the initial composition. Material heated to 5 billion K will become iron whether it started as silicon or carbon. Of course, if explosive processing is negligible the initial composition is ejected without appreciable modification. This is the case for most elements lighter than silicon.

One other parameter to which explosive nucleosynthesis is sensitive is the neutron excess. Except very near the neutron star, the explosion happens too quickly for $\eta$ to be changed, so the ejecta are characterized by the neutron excess of the preexplosive composition.

### B. Explosive processes

#### 1. Explosive oxygen and silicon burning

The products of explosive oxygen and silicon burning are similar to those made by burning the same initial composition in hydrostatic equilibrium, though the isotopic patterns are altered somewhat by the higher freeze-out temperature (Truran and Arnett, 1970; Woosley, Arnett, and Clayton, 1973; Meyer, Krishnan, and Clayton, 1998). An important distinction is the fact that stable oxygen or silicon burning in the middle of a massive star is accompanied by a lot of electron capture. Typically, at the end of oxygen burning in the center of a $15M_\odot$ star, $\eta \approx 0.01$. By the time silicon ignites, this has increased to 0.024, and by the time silicon is depleted at the center, $\eta \approx 0.05$. In the shells of oxygen, silicon, and neon that will experience explosive oxygen and silicon burning and be ejected, however, $\eta$ is still approximately constant at 0.002–0.004 for solar metallicity stars. In a $15M_\odot$ presupernova star of initially solar metallicity, for example (Woosley and Weaver, 1995), for the silicon and oxygen shells, $1.29–1.77M_\odot$, 1200–6400 km, $\eta = 0.002–0.004$ (increasing inwards). In a star of 0.01 times solar metallicity, the silicon and oxygen shells are found between $1.54M_\odot$ and $1.78M_\odot$, 2200–4100 km. Despite the smaller radii, the neutron excess ranges from $2\times10^{-4}$ to 0.001. Thus the products of explosive oxygen and silicon burning do retain some sensitivity, albeit less than linear, to the initial metallicity.

For the relevant values of $\eta$, the chief products of explosive silicon burning that goes to completion ($T_{9s} \gtrsim 5$) are $^{48,49}$Ti (as $^{48,49}$Cr), $^{50}$Cr, $^{51}$Mn (as $^{51}$V), $^{52,53}$Cr (as $^{52,53}$Fe), $^{54}$Fe, $^{55}$Mn (as $^{55}$Co), and $^{56,57}$Fe (as $^{56,57}$Ni), all in approximately solar proportions. If the density is low and the expansion time fast, free $\alpha$ particles will exist in abundance and be unable to reassemble to heavier elements on a hydrodynamic time scale. This gives rise to the "$\alpha$-rich freeze-out" (Woosley, Arnett, and Clayton, 1973) which makes $^{44}$Ca (as $^{44}$Ti), $^{56,57}$Fe (as $^{56,57}$Ni), $^{59}$Co (as $^{59}$Cu), $^{58}$Ni, $^{60,61,62}$Ni (as $^{60,61,62}$Zn), and traces of $^{43}$Ca and $^{64,66}$Zn (as $^{64,66}$Ge). Some of these same species are produced by the *s* process in massive stars, especially $^{59}$Co, $^{60,61,62}$Ni, and $^{66}$Zn. In more extreme versions of the $\alpha$-rich freeze-out, still heavier nuclei are produced until, for the very high entropies and large neutron excesses characterizing the neutrino-powered wind, one merges into the *r* process (Woosley and Hoffman, 1992; Sec. VIII.B.5).

For incomplete silicon burning ($T_{9s} \approx 4$ to 5), the products include those listed above for complete silicon burning as well as important amounts of $^{28}$Si, $^{32}$S, $^{36}$Ar, and $^{40}$Ca, i.e., the same as silicon burning in hydrostatic equilibrium (Sec. IV.A.4). Similarly the products of explosive oxygen burning resemble those of ordinary oxygen burning (Sec. IV.A.3). The ejected iron-group elements are only made explosively, but the intermediate mass elements Si–Ca have appreciable contributions from both hydrostatic and explosive burning.

For common supernovae below $25M_\odot$, typical amounts of $^{56}$Ni ejected in the models of Woosley and Weaver (1995) are consistent with the empirical values of $0.07\pm0.01M_\odot$ for SN 1987A (Arnett, Bahcall, *et al.*, 1989; Arnett, Fryxell, *et al.*, 1989) and $0.08\pm0.02M_\odot$ for SN 1993J (Woosley, Eastman, *et al.*, 1994; Shigeyama *et al.*, 1994). Other type-IIp supernovae have radioactive tails on their light curves that suggest similar amounts of $^{56}$Ni (Patat *et al.*, 1993, 1994).

Explosive oxygen burning, between $T_9$ of 3 and 4, is responsible for producing most of the intermediate-mass elements from $^{28}$Si to $^{42}$Ca, at least those isotopes not already made in hydrostatic neon and carbon burning or by the *s* process. These include $^{28}$Si, $^{32,33,34}$S, $^{35,37}$Cl, $^{36,38}$Ar, $^{39,41}$K, $^{40,42}$Ca, $^{46}$Ti, and part of $^{47}$Ti, $^{51}$V, and $^{53}$Cr (Woosley, Arnett, and Clayton, 1973). Some of these isotopes are produced in oxygen shell burning prior to core collapse, and just which dominates—hydrostatic or explosive burning—depends on details of convection (do the carbon, oxygen, and neon shells link up?) and varies from mass to mass.

#### 2. Explosive neon and carbon burning

Between roughly 2 and $3\times10^9$ K—7000–13 000 km from the blast—part, but usually not all of the carbon and neon convective shells are reprocessed in the explosion (Arnett, 1969). The primary products resemble carbon and neon burning before the explosion (Secs. IV.A.1 and IV.A.2), but because of the high temperature, a brief burst of protons and neutrons is generated that leads to interesting synthesis of many rare isotopes (Howard *et al.*, 1972; Lee *et al.*, 1979; Wefel *et al.*, 1981). Thus, in addition to important yields of $^{23}$Na, $^{24,25,26}$Mg, $^{27}$Al, $^{29,30}$Si, and $^{31}$P, explosive carbon and neon burning produce many neutron-rich isotopes from sulfur through zirconium ($A = 36–88$; Fig. 27). Production occurs as sort of a "mini-*r* process" as neutrons are copiously liberated from $^{22}$Ne and $^{25,26}$Mg. The neutrons are released by $(\alpha,n)$ reactions with $\alpha$ particles from the main neon- and carbon-burning reactions. Among these neutron-rich isotopes is $^{60}$Fe, a potential candidate for $\gamma$-ray astronomy.

Not all of the interesting products are neutron rich. The neon-carbon shell is also the principal site for the production of $^{26}$Al, another favorite target of $\gamma$-ray as-

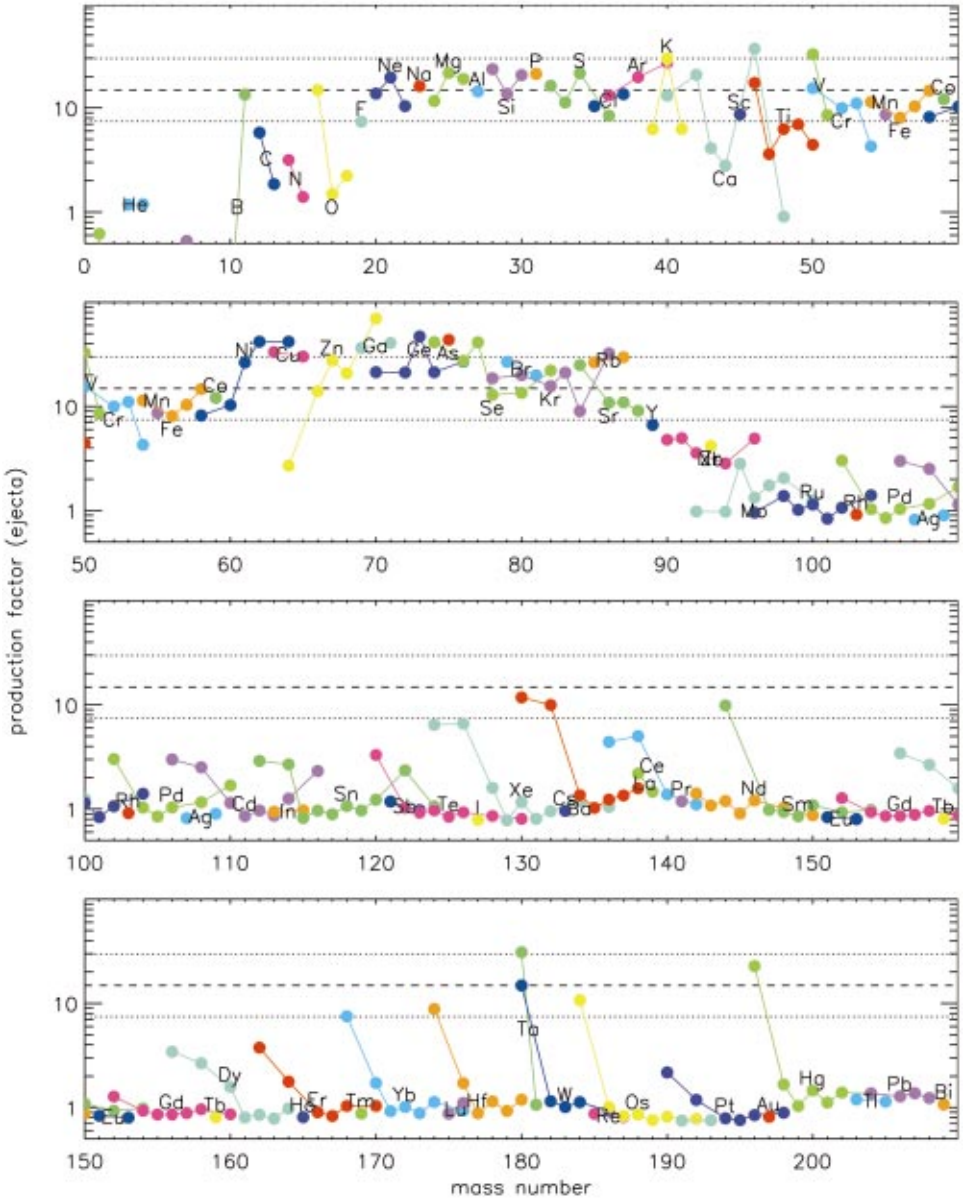


FIG. 27. Final nucleosynthesis from a $25M_{\odot}$ supernova compared to solar abundances (Heger, Woosley, Rauscher, and Hoffman, 2002). Isotopes of a given element are all the same color and are connected by lines. All ejecta, including the wind, are included. A possible *r* process in the neutrino wind is not taken into account here. The production factor is the ratio of the mass fraction in the ejecta divided by the mass fraction in the sun [Color].

tronomers (Woosley and Weaver, 1980). This isotope is produced by proton reactions on $^{25}$Mg and is partly destroyed by the neutron flux [$^{26}$Al$(n,p)^{26}$Mg].

In fact, there is some ambiguity in separating the products of explosive neon and carbon burning from preexplosive burning. In many massive stars the carbon and neon convective burning shells (and sometimes even the oxygen-burning shell) merge in the last hours of the star's life (Fig. 9). Temperatures are so high at the base of the convective shell that carbon and neon burn while being convected downwards. Since the convective speeds are not too much less than the sound speed (and the sound speed is comparable to the escape velocity), the condition $\tau_{\rm nuc} \approx \tau_{\rm conv}$ is not so different from the classic condition for explosive nucleosynthesis, $\tau_{\rm nuc} \approx \tau_{\rm HD}$ with $\tau_{\rm HD}$ given by Eq. (35).

### 3. The *p* process

Between roughly 2 and $3\times10^9$ K the *s*-process nuclei produced in helium and carbon burning, as well as those incorporated into the original star, experience a partial meltdown to the iron group. Along the way, chiefly by a combination of $(\gamma,n)$, $(\gamma,p)$, and $(\gamma,\alpha)$, the *p* process nuclei are produced (Arnould, 1976; Woosley and Howard, 1978; Rayet *et al.*, 1995).

Figure 27 shows the production of a large number of *p*-process nuclei in our fiducial $25M_{\odot}$ supernova explosion. The *p*-process isotopes of Hg, Os, W, Hf, Yb, Sm, Ce, Ba, and Xe are particularly well produced with a yield consistent with other major productions in the same star. More problematic are the *p* isotopes of Pt, Er, Dy, Gd, and all the elements below Te and heavier than Zr ($Z$ between 40 and 52). Especially disturbing are the small productions of $^{92,94}$Mo and $^{96,98}$Ru, which have relatively large abundances in the sun (doubtless related to the closed neutron shell at $N=50$). Of course this is but one star and the relevant reaction rates are more uncertain here than for the lighter nuclei. Still, these deficiencies are difficult to explain away. Production would be improved, especially for Mo and Ru, if the

preexplosive *s* process were stronger (Costa *et al.*, 2000). Unfortunately this may require larger cross sections for $^{22}$Ne$(\alpha,n)^{25}$Mg than the laboratory allows (Jaeger *et al.*, 2001). Hoffman *et al.* (1996) have suggested that $^{92,94}$Mo at least might be produced in neutrino-powered winds (Sec. VIII.B.5), and Howard, Meyer, and Woosley (1991) have described a possible production site for the *p* process in type-Ia supernovae that can, in certain circumstances, produce Mo and Ru. For now, we have a qualitatively correct model for the *p* process, but there remain many unanswered details.

Rauscher *et al.* (2001) find that in some, but not all, massive stars the oxygen, neon, and carbon convective burning shells merge shortly before core collapse, bringing *s*-process seed and other relatively fragile nuclei into a high-temperature region. In such stars much of the *p* process actually transpires before the explosion as seed nuclei are mixed into and out of regions as hot as $3\times10^9$ K (see also Hoffman, Woosley, and Weaver, 2001).

#### 4. The neutrino process

It was recognized early on (Domogatskii and Nadyozhin, 1977, 1980; Woosley, 1977) that the passage of the huge flux of neutrinos through a star experiencing core collapse would cause interesting transmutation of the elements, even in the relatively cool outer regions. Because of the small cross section, production was restricted to rare species made from abundant targets such as $^2$H from $^1$H (Woosley, 1977), $^{11}$B from $^{12}$C (Domogatskii and Nadyozhin, 1980), or $^{19}$F from $^{20}$Ne (Woosley and Haxton, 1988). The flurry of calculations following SN 1987A led to a better understanding of the neutrino spectra and fluxes, especially for the $\mu$ and $\tau$ neutrinos that carry the bulk of the energy. The first survey to include a realistic presupernova structure, appropriate cross sections for the neutral-current excitation to the giant-dipole resonance (Haxton, 1988), and a description of both neutrino processing and shock reprocessing was carried out by Woosley *et al.* (1990). Those calculations suggested significant production of $^7$Li, $^{11}$B, $^{19}$F, and possibly a dozen other species, including $^{15}$N and $^{26}$Al. The synthesis resulted from the inelastic scattering of $\mu$ and $\tau$ neutrinos, which excited abundant targets to unbound levels that decayed by ejecting nucleons. For example, $^{19}$F was made by $^{20}\mathrm{Ne}(\nu_x,\nu_x'p)^{19}\mathrm{F}$ and $^{20}\mathrm{Ne}(\nu_x,\nu_x'n)^{19}\mathrm{Ne}(e^+\nu)^{19}\mathrm{F}$. Some $^7$Li was made in helium-rich regions by $^4\mathrm{He}(\nu_x,\nu_x'n)^3\mathrm{He}(\alpha,\gamma)^7\mathrm{Be}$, and so on.

Later Woosley and Weaver (1995) included reaction rates provided by Haxton for dozens of neutral- and charged-current neutrino-induced reactions in their survey of supernova nucleosynthesis and confirmed the important production of $^7$Li, $^{11}$B, and $^{19}$F in realistic models of varying metallicity. The results were sensitive to the assumed spectra of $\mu$ and $\tau$ neutrinos, with the best results being obtained for a thermal spectrum with temperature $kT\approx6-8$ MeV. Larger and smaller values overproduced (or underproduced) key species. The neutrino process synthesis is thus a potential thermometer for the $\mu$ and $\tau$ neutrinos. Several authors (e.g., Myra and Burrows, 1990) have pointed out that the real neutrino spectra are likely to be nonthermal and deficient on their high-energy tails, thus lowering the equivalent temperature of the neutrinos in a supernova model to 5–6 MeV. Revised neutrino reaction cross sections have also been provided by Kolbe and Langanke (2001), but neither the new spectra nor cross sections have yet been employed in realistic nucleosynthesis models. It does not appear likely, though, that the basic conclusions will change—neutrinos with equivalent blackbody temperatures of $\sim$6 MeV are responsible for producing $^{11}$B and $^{19}$F from $^{12}$C and $^{20}$Ne and some $^7$Li. These nuclei are thus "primary" and this fact should be reflected in their abundance history in the Galaxy (e.g., Vangioni-Flam *et al.*, 1998). For current choices of cross sections, the production of $^6$Li, $^9$Be, and $^{10}$B by the $\nu$ process is negligible.

#### 5. The *r* process

One of the greatest obstacles remaining in the way of a complete understanding of the origin of the elements is uncertainty in the site of the *r* process. There is general agreement with the original argument of Hoyle and Fowler (1960) that the requisite large neutron densities to produce the solar *r* process are achieved in a region that has been heated to such high temperature that the $\alpha$ particle is at least partly broken down by photodisintegration into nucleons and cooled rapidly so that only a small portion of the nucleons and $\alpha$'s assemble into heavy elements. It also helps if the material initially had an appreciable excess of neutrons over protons (i.e., $Y_e<0.5$).

Many possible sites for the *r* process have been discussed (Hillebrandt, 1978; Mathews and Cowan, 1990; Cowan, Thielemann, and Truran, 1991), but observations of abundances in metal-poor stars suggest an association with first-generation massive stars, especially supernovae (Ryan, Norris, and Beers, 1996; Sneden *et al.*, 1996, 1998, 2000) as originally suggested by Burbidge *et al.* (1957) and Cameron (1957). Three possible sites warrant the most serious consideration. One is the merger of a neutron star with another compact object, originally proposed by Lattimer and Schramm (1974, 1976). Recent calculations (Freiburghaus, Rosswog, and Thielemann, 1999) show that sufficient matter is ejected in such a merger and that, for certain parameters, the abundances agree with solar. Qian (2000), using arguments based upon estimates of mixing, concludes that supernovae are preferred over merging neutron stars because the mass of *r* process produced in the latter is too great and the event rate too low.

The other two sites involve the collapsed iron core of a massive star. A current favorite is the neutrino-powered wind of a young neutron star (Duncan, Shapiro, and Wasserman, 1986) experiencing its Kelvin-Helmholtz evolution ($\tau\approx10$ s). The proto-neutron star contracts, giving up its binding energy, roughly $3\times10^{53}$ erg, to neutrino emission, chiefly from pair anni-

hilation. The deposition of these neutrinos in the atmosphere of the young neutron star drives an outflow of roughly $2\times10^{-5}M_{\odot}L_{52}^{5/3}$ s$^{-1}$, where $L_{52}$ is the total neutrino luminosity in all flavors in units of $10^{52}$ erg s$^{-1}$. Several studies show that this wind could be a good *r*-process site (Woosley and Hoffman, 1992; Woosley, Wilson, *et al.*, 1994; Takahashi, Witti, and Janka, 1994; Wanajo *et al.*, 2001) but that it may be difficult to achieve the necessary high entropy and short time scales (Witti, Janka, and Takahashi, 1994; Qian and Woosley, 1996; Thompson, Burrows, and Meyer, 2001) in the ejecta. To understand the dependence on entropy (essentially $5.2T_{\rm MeV}^3/\rho_8$ for these radiation- and pair-dominated winds), one must consider the physics of the ejection process. The wind orginates from a hot region ($T\gtrsim4$ MeV) where matter is composed of free nucleons. It requires many neutrino interactions to eject each nucleon from the deep gravitational potential (roughly 200 MeV/nucleon), so that dynamic weak equilibrium is achieved, that is, the neutron-to-proton ratio in the wind is set by the fluxes and spectra of $\nu_e$ and $\overline{\nu_e}$ [since $\nu_e(n,p)e^-$ is in steady state with $\overline{\nu_e}(p,n)e^+$]. During the time when most of the neutrinos' energy is emitted, the fluxes of $\nu_e$ and $\overline{\nu_e}$ are very similar (Janka, 1995), but the antineutrinos have a hotter spectrum because they originate from deeper in the neutron star (the outer layers of the neutron star are neutron rich and thus have greater opacity to $\nu_e$). Thus, at late times, the neutrino-powered wind is neutron rich with typical $Y_e\approx0.40$ (Woosley, Wilson, *et al.*, 1994).

As the wind expands and cools, the nucleons reassemble until at $T\approx10^{10}$ K the protons have mostly been absorbed into $\alpha$ particles, leaving behind an excess of neutrons (the inverse of this happens in big-bang nucleosynthesis). From $10^{10}$ K on down to $3\times10^9$ K, some of the $\alpha$ particles reassemble into heavy nuclei, but most do not. If one can reach a temperature of less than $2\times10^9$ K while still burning less than 10% of the $\alpha$'s into heavy seed nuclei ($A\approx100$), one will have a neutron-to-seed ratio of order 100 and a strong *r* process. The higher the entropy the lower the density and the less efficient are reactions like $\alpha(\alpha n,\gamma)^9$Be that limit the conversion of $\alpha$'s to heavies. A fast expansion time scale is also helpful in keeping the neutron-to-seed ratio high (Hoffman, Woosley, and Qian, 1997).

Current supernova models (see, for example, Thompson, Burrows, and Meyer, 2001) give entropies of around 100 when what is needed to make the heaviest *r*-process nuclei is 300 to 400. The following possible solutions to this dilemma have been proposed (Qian and Woosley, 1996):

(a) the neutrino wind does not make all the solar *r* process, but only the lighter nuclei;
(b) there are extra energy inputs into the wind, such as magnetic fields, rotation, and shocks, that have been ignored and that might increase the entropy of the wind or decrease its time scale;
(c) the nuclear equation of state is very soft and the typical neutron star mass involved in making the *r* process is very close to the maximum allowed (not the average neutron star); this raises the gravitational potential, which has the effect of increasing the speed and entropy of the wind (see also Cardall and Fuller, 1997; Otsuki *et al.*, 2000);
(d) important multidimensional effects (clumping?) or general relativistic effects in the neutrino transport have been left out; or
(e) new particle physics, e.g., flavor mixing, might affect $Y_e$ in the wind or its dynamics (Qian *et al.*, 1993; Qian and Fuller, 1995).

In addition to occurring in supernovae, the neutrino wind model for the *r* process has other appealing characteristics. Because it is a wind, the total mass ejected can be small. About $10^{-5}M_{\odot}$ of *r* process ($A\gtrsim100$) per supernova would be produced, and this is in good accord with the demands of galactic chemical evolution (Mathews and Cowan, 1990). In addition, since the properties of the wind are determined by the neutron star and not the presupernova star, the *r* process might have very similar properties from event to event for neutron stars of a constant mass. Finally, unless all of the ejected material eventually falls back onto the neutron star (Sec. VI.A), the neutrino wind is an event that must exist in nature. It is doubtful that its nucleosynthetic contribution is negligible, especially for the lighter *r*-process isotopes (e.g., Sr, Y, Zr).

Early on, the $Y_e$ in the neutrino-powered wind is larger because the spectra of the $\nu_e$ and $\overline{\nu_e}$ are similar. For $Y_e$ close to 0.5, Hoffman *et al.* (1996) and Swift *et al.* (2000) have shown that some of the light *p*-process nuclei, e.g., $^{92,94}$Mo, may be produced. This would imply that a portion but not all of the *p* process is primary and should be correlated with the (light?) *r* process. The remainder of the *p* process would be secondary, made from the *s* process. The nucleus $^{64}$Zn is also abundantly produced in these winds and zinc would also behave like a primary element, i.e., its synthesis would be independent of the initial metallicity of the star.

The second possibility for making the solar *r* process in massive stars relies upon a very asymmetric explosion and jetlike outflows (LeBlanc and Wilson, 1970; Symbalisty, Schramm, and Wilson, 1985; Cameron, 2001). Whether *r*-process synthesis would occur in common supernovae or some particularly energetic subset (those that make gamma-ray bursts?) is not clear, and the details of the synthesis vary from model to model. One could envision a neutron-rich wind from an accretion disk flowing into a black hole or neutron star either during or shortly after core collapse. Or perhaps the jet is energized by a rapidly rotating, highly magnetic neutron star (Wheeler *et al.*, 2000). The strength and weakness of such jet-powered models is that the thermodynamic conditions are at present poorly determined. However, it does seem reasonable that the necessary amount of nucleonic matter might expand and cool on a very rapid time scale. Indeed, it may be too much material for the synthesis to happen in every supernova.

A mild *r* process also occurs in supernovae near the base of the helium shell as the shock wave passes though. This process was originally envisioned as a much stronger event (Hillebrandt and Thielemann, 1978; Truran, Cowan, and Cameron, 1978). The helium shell in modern models is situated too far out (typically $5\times10^{10}$ cm) to become hot enough to generate the sort of neutron fluxes from $^{22}\mathrm{Ne}(\alpha,n)^{25}\mathrm{Mg}$ needed for a strong *r* process. Still a number of neutron-rich species between mass 60 and 90 are produced in considerable abundance using the preexisting *s*-process enhancements in these layers as seed. Examples of such nuclei are $^{70}$Zn, $^{71}$Ga, $^{76}$Ge, and $^{82}$Se. Perhaps most noteworthy in this region is the production of trace radioactivities, especially $^{60}$Fe and $^{60}$Co. Explosive carbon and neon burning also contributes to these same neutron-rich nuclei.

### C. Reaction-rate sensitivity

The results of explosive nucleosynthesis, as contrasted with presupernova nucleosynthesis, are chiefly sensitive to well-determined nuclear binding energies and cross sections that can be calculated using Hauser-Feshbach theory (Hoffman *et al.*, 1999). Weak interactions, except those involved in the neutrino and *r* processes, are negligible in the explosion. The standard set of Hauser-Feshbach rates, which was until recently (depending upon the group doing the calculations) that of either Thielemann, Arnould, and Truran (1987) or Woosley *et al.* (1978) plus Holmes *et al.* (1976), has been improved and revised by Rauscher and Thielemann (2000), which is now the new standard. The new rate set corrects uncertainties in level density and nuclear potential and also incorporates an improved treatment of the photon transmission function for self-conjugate ($Z=N$) nuclei. Errors remain at the factor of 2 level, and more for nuclei in which the level density at the particle separation energy is low; these can be addressed by further experiment, but compared with the effects of $^{12}\mathrm{C}(\alpha,\gamma)^{16}\mathrm{O}$ and $^{22}\mathrm{Ne}(\alpha,n)^{25}\mathrm{Mg}$ on presupernova nucleosynthesis, the uncertainties in rates affecting bulk explosive nucleosynthesis are tolerable.

Exceptions are (a) cross sections, decay rates, and binding energies for the *r* process; (b) neutrino cross sections for the $\nu$ process; and (c) charged particle capture rates (and their inverse photodisintegration rates) for nuclei heavier than the iron group—rates especially important for the *p* process. If nucleosynthesis is to become a precision science with accuracy better than a factor of 2, one also needs further improvements in the photon transmission function for nuclei in the mass range 28–64, especially better rates for $(n,\gamma)$ and $(\alpha,\gamma)$ reactions.

### D. The effects of metallicity

As abundances of increasing precision become available, not only for objects in our Galaxy but for more distant galaxies, it is worth considering how nucleosynthesis at high redshift—and low metallicity—might have differed from what we see in the sun. The work of Timmes, Woosley, and Weaver (1995) included low-metallicity stars but no effects of mass loss and binary membership.

One of the best understood and documented effects of metallicity is its effect on the synthesis of elements with odd nuclear charge and of isotopes with $Z>N$. The production of such nuclei requires an excess of neutrons and is sensitive to the degree by which $Y_e$ [Eq. (4)] differs from 0.5, in particular the neutron excess, $\eta=1-2Y_e$. Helium burning sets an initial value to $\eta$ when it converts $^{14}$N to $^{18}$O and $^{22}$Ne (Sec. III.D.2). This gives

$$\eta\approx 0.0018(Z/Z_\odot). \tag{38}$$

One of the triumphs of nucleosynthesis theory has been the demonstration (Truran and Arnett, 1971; Woosley, Arnett, and Clayton, 1973; Arnett, 1995) that this degree of neutron enrichment is exactly what is needed to explain the abundances of odd-$Z$ elements and isotopes with neutron excesses ($^{25,26}$Mg, $^{29,30}$Si, $^{33,34}$S, etc.). Qualitatively, the predicted trends are seen in observations of metal-deficient stars for intermediate-mass elements like Na and Al (Timmes, Woosley, and Weaver, 1995 and references therein).

Unfortunately, what might have been an unambiguous prediction of nucleosynthesis theory across the periodic chart of intermediate-mass and iron-group elements is muddled by the weak interactions that go on during post-helium-burning evolution. In carbon burning (Arnett and Truran, 1969), the weak interactions $^{12}\mathrm{C}(^{12}\mathrm{C},n)^{23}\mathrm{Mg}(e^+\nu)^{23}\mathrm{Na}$, $^{20}\mathrm{Ne}(p,\gamma)^{21}\mathrm{Na}(e^+\nu)^{21}\mathrm{Ne}$, and $^{21}\mathrm{Ne}(p,\gamma)^{22}\mathrm{Na}(e^+\nu)^{22}\mathrm{Ne}$ create a finite value of $\eta$ even in very metal-deficient stars. During oxygen burning, other reactions, especially $^{33}\mathrm{S}(e^-,\nu)^{33}\mathrm{P}$, increase $\eta$ still further (Woosley, Arnett, and Clayton, 1972) until, by the end of oxygen burning, memory of the initial metallicity has been essentially lost. Thus the metallicity effect on the iron group is essentially indiscernible and the effect on intermediate-mass elements—Si through Ca—is mild.

Heger and Woosley (2002) have recently found that the odd-even abundance signature originally predicted by Truran and Arnett is radically greater in pair-instability supernovae because such stars, which have low metallicity to start with, explode without having experienced stable carbon and oxygen burning.

Many other indirect effects of metallicity on nucleosynthesis are expected because of its role in determining the initial mass function (Sec. VII), the stability of very massive stars (Sec. VII), mass-loss rates (Secs. II.G and IV.F), the mass cut (Sec. VI.A), and the radius of stars in interacting binaries. Working all these out is currently an area of very active research.

### E. Nucleosynthesis summary

#### 1. Processes and products

We have discussed many different processes characteristic of a massive star, both before and during its ex-

TABLE III. The origin of the light and intermediate-mass elements.

| Species | Origin | Species | Origin | Species | Origin |
|---|---|---|---|---|---|
| $^{1}$H | BB | $^{30}$Si | C,Ne | $^{51}$V | $\alpha$,Ia-det,$x$Si,$x$O,$\nu$ |
| $^{2}$H | BB | $^{31}$P | C,Ne | $^{50}$Cr | $x$Si,$x$O,$\alpha$,Ia-det |
| $^{3}$He | BB,L* | $^{32}$S | $x$O,O | $^{52}$Cr | $x$Si,$\alpha$,Ia-det |
| $^{4}$He | BB,L*,H | $^{33}$S | $x$O,$x$Ne | $^{53}$Cr | $x$O,$x$Si |
| $^{6}$Li | CR | $^{34}$S | $x$O,O | $^{54}$Cr | nse-IaMCh |
| $^{7}$Li | BB,$\nu$,L*,CR | $^{36}$S | He(s),C,Ne | $^{55}$Mn | Ia,$x$Si,$\nu$ |
| $^{9}$Be | CR | $^{35}$Cl | $x$O,$x$Ne,$\nu$ | $^{54}$Fe | Ia,$x$Si |
| $^{10}$B | CR | $^{37}$Cl | He(s),$x$O,$x$Ne | $^{56}$Fe | $x$Si,Ia |
| $^{11}$B | $\nu$ | $^{36}$Ar | $x$O,O | $^{57}$Fe | $x$Si,Ia |
| $^{12}$C | L*,He | $^{38}$Ar | $x$O,O | $^{58}$Fe | He(s),nse-IaMCh |
| $^{13}$C | L*,H | $^{40}$Ar | He(s),C,Ne | $^{59}$Co | He(s),$\alpha$,Ia,$\nu$ |
| $^{14}$N | L*,H | $^{39}$K | $x$O,O.$\nu$ | $^{58}$Ni | $\alpha$ |
| $^{15}$N | novae,$\nu$ | $^{40}$K | He(s),C,Ne | $^{60}$Ni | $\alpha$, He(s) |
| $^{16}$O | He | $^{41}$K | $x$O | $^{61}$Ni | He(s),$\alpha$,Ia-det |
| $^{17}$O | novae, L* | $^{40}$Ca | $x$O,O | $^{62}$Ni | He(s),$\alpha$ |
| $^{18}$O | He | $^{42}$Ca | $x$O | $^{64}$Ni | He(s) |
| $^{19}$F | $\nu$,He,L* | $^{43}$Ca | C,Ne,$\alpha$ | $^{63}$Cu | He(s),C,Ne |
| $^{20}$Ne | C | $^{44}$Ca | $\alpha$,Ia-det | $^{65}$Cu | He(s) |
| $^{21}$Ne | C | $^{46}$Ca | C,Ne | $^{64}$Zn | $\nu$-wind,$\alpha$,He(s) |
| $^{22}$Ne | He | $^{48}$Ca | nse-IaMCh | $^{66}$Zn | He(s),$\alpha$,nse-IaMCh |
| $^{23}$Na | C,Ne,H | $^{45}$Sc | $\alpha$,C,Ne,$\nu$ | $^{67}$Zn | He(s) |
| $^{24}$Mg | C,Ne | $^{46}$Ti | $x$O,Ia-det | $^{68}$Zn | He(s) |
| $^{25}$Mg | C,Ne | $^{47}$Ti | Ia-det,$x$O,$x$Si | $r$ | $\nu$-wind |
| $^{26}$Mg | C,Ne | $^{48}$Ti | $x$Si,Ia-det | $p$ | $x$Ne,O |
| $^{27}$Al | C,Ne | $^{49}$Ti | $x$Si | $s$(A$<$90) | He(s) |
| $^{28}$Si | $x$O,O | $^{50}$Ti | nse-IaMCh,He(s) | $s$(A$>$90) | L* |
| $^{29}$Si | C,Ne | $^{50}$V | C,Ne,$x$Ne,$x$O | | |

plosion as a supernova. Table III summarizes our best estimates of where each isotope of the elements lighter than zinc has been created in Nature. We adopt as our standard the composition of the sun.

In this table, "BB" stands for the big bang. Stable isotopes of both hydrogen and $^{3}$He, most of $^{4}$He, and some $^{7}$Li were made there (see, for example Walker *et al.*, 1991; Olive, Steigman, and Walker, 2000). "CR" is for cosmic-ray spallation, responsible for some of the rarest, most fragile isotopes in nature, $^{6}$Li, $^{9}$Be, and $^{10}$B (Fields and Olive, 1999; Fields *et al.*, 2000; Ramaty *et al.*, 2000). Other light isotopes, especially $^{11}$B, $^{19}$F, and some $^{7}$Li, are made by the neutrino process in massive stars (Sec. VIII.B.4). "L" here, means that the isotope is synthesized in stars lighter than $8M_{\odot}$. Notable examples are most of $^{13}$C and $^{14}$N (Renzini and Voli, 1981), half or more of $^{12}$C (Timmes, Woosley, and Weaver, 1995), and the *s* process above mass 90 (Renzini and Voli, 1981; Meyer, 1994; Busso *et al.*, 2001).

Type-Ia supernovae are responsible for making part of the iron group (including about one-half of $^{56}$Fe; Thielemann, Nomoto, and Yokoi, 1986; Timmes, Woosley, and Weaver, 1995). Rare varieties of type-Ia supernovae may be necessary for the production of a few isotopes not adequately made elsewhere. These include neutron-rich isotopes of Ca, Ti, Cr, and Fe made in accreting white dwarfs that ignite carbon deflagration at densities so high that they almost collapse to neutron stars (Woosley, 1997; Iwamoto *et al.*, 1999). We call these "nse-IaMCh" for carbon deflagrations in white dwarfs very near the Chandrasekhar mass. Temperatures near $10^{10}$ K assure nuclear statistical equilibrium and densities near $6\times10^{9}$ g cm$^{-3}$ cause electron capture until $Y_e \approx 0.42$. Another rare variety of type-Ia supernovae are the helium detonations ("Ia-det"; Woosley and Weaver, 1995). These give temperatures of billions of K in helium-rich zones and may be necessary in order to understand the relatively large solar abundance of $^{44}$Ca (made in supernovae as radioactive $^{44}$Ti) only in regions of high temperature and large helium mass fraction. This may also explain the production of a few other rare isotopes like $^{43}$Ca and $^{47}$Ti. Classical novae seem necessary to explain the origin of $^{15}$N (in the beta-limited CNO cycle) and $^{17}$O (Jose and Hernanz, 1998). Prior to 1995, $^{17}$O was regarded as a product of massive stars (Woosley and Weaver, 1995).

All the other labels in Table III refer to burning stages in massive stars: "He" for helium burning, "C" for carbon burning, etc. An "*x*" in front of the elemental symbol indicates that the burning is of the explosive variety, not the presupernova evolution in hydrostatic equilibrium. "$\alpha$" stands for the $\alpha$-rich freeze-out from nuclear statistical equilibrium (Woosley, Arnett, and Clayton, 1973) and $\nu$ wind is the neutrino-powered wind (Sec.

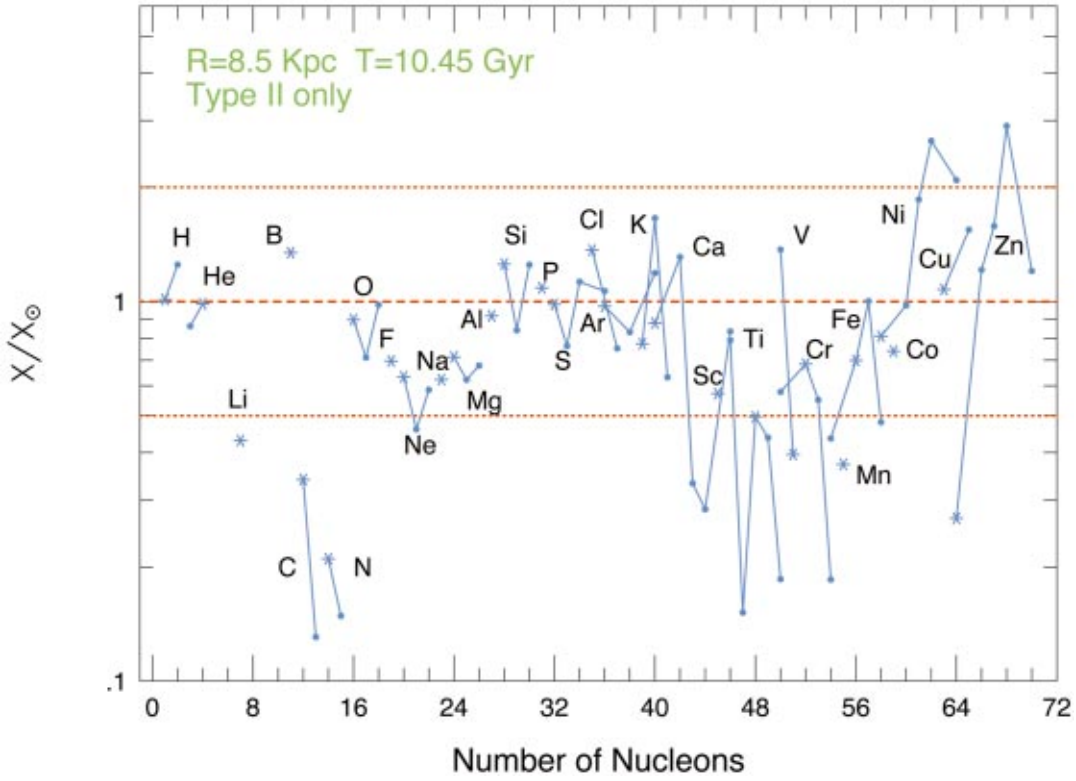


FIG. 28. Integrated nucleosynthesis from a grid of massive stars ($11-40M_\odot$) of various metallicities ($0Z_\odot$, $10^{-4}Z_\odot$, $0.01Z_\odot$, $0.1Z_\odot$, and $1Z_\odot$) compared to the solar abundances (Timmes, 1996). This figure also includes contributions from the big bang (hence $^2$H) but not from low-mass stars (especially $^{12}$C and $^{14}$N) or type-Ia supernovae (especially $^{55}$Mn, $^{54,56}$Fe, and $^{58}$Ni) or novae ($^{15}$N, $^{17}$O). The overproduction of Zn and Ni isotopes may reflect an overly large rate for $^{22}$Ne$(\alpha,n)^{25}$Mg during the *s* process [Color].

VIII.B.5). "He(s)" is the helium-burning *s* process in massive stars (Sec. III.E).

Figure 27 shows the final nucleosynthesis in the supernova explosion of a $25M_\odot$ star ($12.5M_\odot$ at death; Table I). The network included all necessary isotopes through mass 210 and reaction rates current as of 2001. Certainly the solar abundances do not originate from any one mass of star, or even any group of stars with a single metallicity, but the consistent production of so many species in a single model is impressive. With rare exceptions that probably have alternate explanations (Table II), all the isotopes from oxygen through nickel are consistently co-produced in solar proportions with a production factor of about 15 (in this figure, the initial composition of the sun would be a set of points all lying on "1"; a production factor of 15 means that the sun's complement of metals could be understood if 1/15 of its mass passed through conditions like those in this $25M_\odot$ star). The *r*, *s*, and *p* processes are also well produced, perhaps a little overproduced, from nickel to about $A=88$. In a $15M_\odot$ star (not shown here) the *s*-process yield is less. The yield of these "trans-iron" elements is also sensitive to a still poorly determined rate for $^{22}$Ne$(\alpha,n)^{25}$Mg. Above mass 90, nucleosynthesis in massive stars is mostly restricted to the *p* process and possibly the *r* process.

Using a grid of masses and metallicities, Timmes, Woosley, and Weaver (1995) computed the integrated nucleosynthesis of stars above $8M_\odot$. Mass loss was not included in their models, the nuclear physics was that of 1993, the grid of masses was coarse, and species heavier than zinc were not studied. Still, Fig. 28 shows that the good agreement with solar abundances in Fig. 27 is, if anything, improved by considering an ensemble of stars. The slight overproductions of Ni, Cu, and Zn may reflect an overestimate of the $^{22}$Ne$(\alpha,n)^{25}$Mg reaction rate. Better agreement can be achieved by adding sources other than the big bang, massive supernovae, and AGB stars that are in Fig. 29, but then the number of free parameters becomes large.

### 2. Gamma-ray lines and meteorite anomalies

Not obvious in Table III is a variety of moderate- to long-lived radioactive isotopes produced in massive stars. Chief among them are $^{22}$Na (2.6 y), $^{26}$Al ($7.5\times10^5$ y), $^{44}$Ti, (60 y) $^{56,57}$Ni (6.1 d, 1.5 d), $^{56,57,60}$Co (77.1 d, 271 d, 5.27 y), and $^{60}$Fe ($1.5\times10^6$ y), the numbers in parentheses being the half-lives. The observation of characteristic lines from these nuclear decays poses a particular challenge to the gamma-ray astronomer, and their signals can yield important information on many fronts—the rate and distribution of massive star formation and supernovae in the galaxy ($^{26}$Al and $^{60}$Fe); the mass cut and degree of fallback ($^{44}$Ti, $^{56,57}$Ni, $^{56,57}$Co); explosive helium and carbon burning ($^{60}$Fe, $^{60}$Co); and a

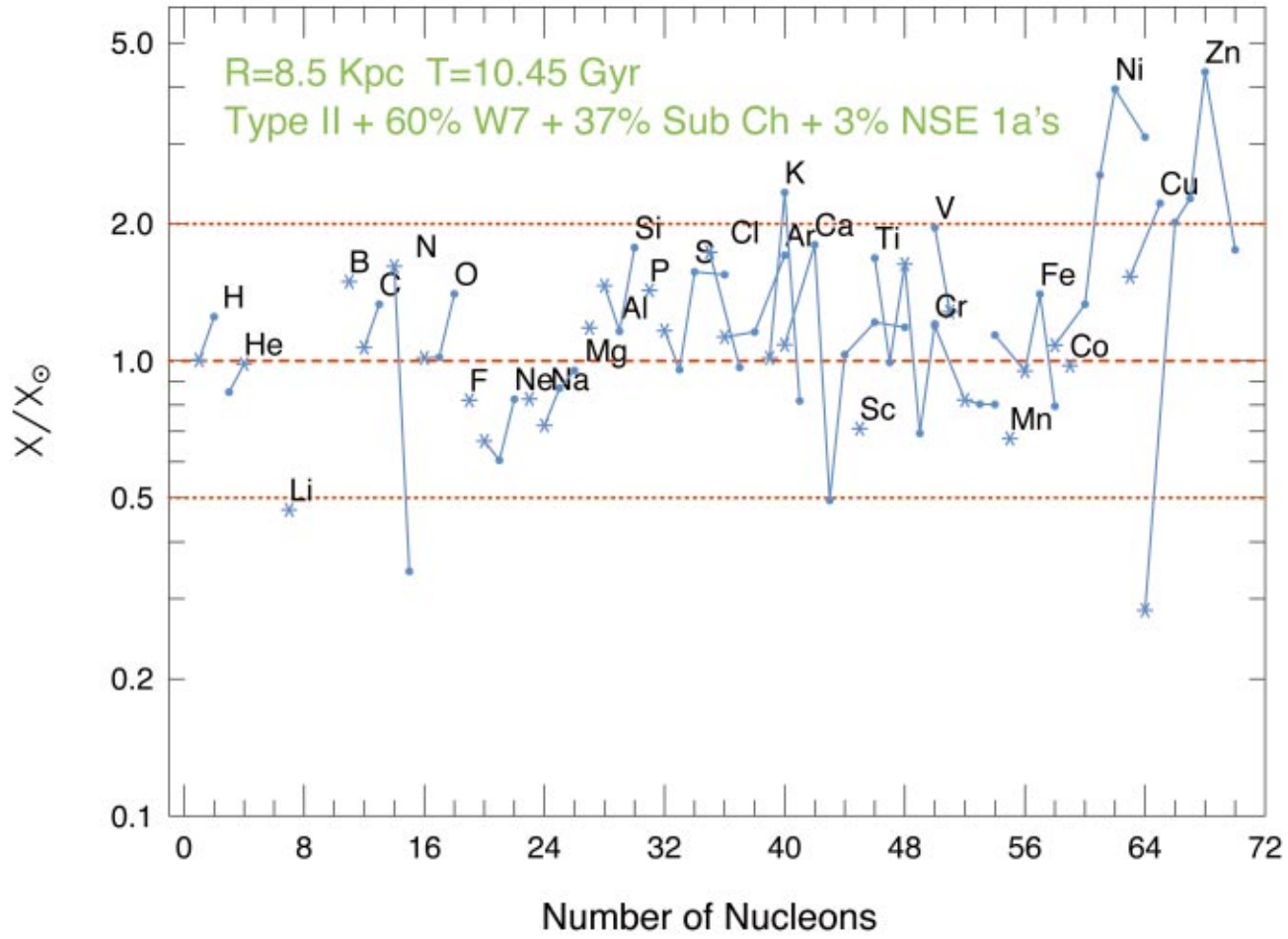


FIG. 29. The agreement in Fig. 28 is greatly improved if one includes the iron-group production from three varieties of type-Ia supernovae (see text and Table III) as well as classical novae (Timmes, 1996) [Color].

variety of other aspects of the supernova progenitor and explosion mechanism (Clayton, Colgate, and Fishman, 1969; Clayton, 1982; Diehl and Timmes, 1998).

Thus far gamma-ray lines of $^{26}$Al have been studied extensively in the disk of the Milky Way (Diehl *et al.*, 1995); $^{56}$Co and $^{57}$Co have been detected in SN 1987A (reviewed by Arnett, Bahcall, *et al.*, 1989) and $^{44}$Ti has been found in the case A supernova remnant (Iyudin *et al.*, 1994). In all cases, the observed fluxes are consistent with theoretical expectations from massive star nucleosynthesis (Timmes *et al.*, 1995, 1996; Meynet *et al.*, 1997) given a reasonable but liberal error bar on the latter, especially for $^{44}$Ti. An active campaign is underway by the INTEGRAL mission to find lines of $^{60}$Fe at the predicted level (Timmes *et al.*, 1995).

Convincing evidence also exists that at least one of the above radioactivities, $^{44}$Ti, along with many other products of massive star nucleosynthesis, found their way into interstellar dust particles and later into meteorites (Travaglio *et al.*, 1999). Interestingly the abundance anomalies resulting from $^{44}$Ti decay are found in carbide grains, whereas the $^{44}$Ti likely formed in regions with a large oxygen excess. Clayton, Liu, and Dalgarno (1999) have explained how this might be possible in a radioactive background where gamma rays dissociate carbon monoxide.

Evidence for $^{26}$Al in meteorites (see, for example, Lee, Papanastassiou, and Wasserburg, 1977) has also been interpreted as implying the injection of radioactive fallout into the primitive solar nebula by a nearby supernova. Other short-lived radioactivities such as $^{36}$Cl, $^{41}$Ca, $^{60}$Fe, and $^{182}$Hf may also have been injected (see, for example, Meyer and Clayton, 2000).

Taken together, the gamma-ray lines and meteoritic anomalies give strong support to a theory in which many isotopes are synthesized in nature explosively with a short time scale.

## IX. LIGHT CURVES AND SPECTRA OF TYPE-II AND TYPE-IB SUPERNOVAE

The light curve of a supernova from a massive star consists of three parts whose relative proportions vary depending upon the mass of the hydrogen envelope (if any), its radius, the explosion energy, and the mass of $^{56}$Ni produced in the explosion.

### A. Shock breakout

The electromagnetic display commences as the shock wave erupts from the surface of the star (Garresberg, Imshennik, and Nadyozhin, 1971; Chevalier, 1976; Falk,

1978; Klein and Chevalier, 1978). The matter is highly ionized and the dominant opacity is electron scattering. As the material expands the diffusing radiation is cooled and the luminosity and temperature decline rapidly.

Ensman and Burrows (1992) did the first two-temperature calculations and found for the specific (and atypical) case of SN 1987A a burst of approximately three minutes' duration with color temperature near $10^6$ K and a luminosity of $5\times10^{44}$ erg s$^{-1}$.

No breakout transient has ever been observed directly for any supernova. Narrow uv and optical emission lines of [C III], [N III], [N IV], and [N V] attest to the brilliance and hardness of this initial transient. Fransson and Lundquist (1989) estimate $2\times10^{46}$ erg of ionizing radiation with temperature in the range $4-8\times10^5$ K. More recent results of Blinnikov *et al.* (2000), who use multigroup radiation transport, are in good accord with the results of Ensman and Burrows.

The breakout transient associated with more common type-IIp supernovae is brighter, longer, and cooler, as one would expect for stars with ten times the radius. The color temperature is about half as great ($4\times10^5$ K) and the transient lasts about 10–15 min. The luminosity is $5-10\times10^{44}$ erg s$^{-1}$ (Blinnikov *et al.*, 2001).

The Sedov solution for a constant-density envelope implies that shock breakout occurs in $7000(M_{\rm env}/E_{51})^{1/2}R_{13}$ s, where $M_{\rm env}$ is the mass of the hydrogen envelope in solar masses, $E_{51}$ is the kinetic energy of the explosion in units of $10^{51}$ erg, and $R_{13}$ is the radius of the presupernova star in units of $10^{13}$ cm. For SN 1987A, $M_{\rm env}\approx10$, $E_{51}\approx1.2$, and $R_{13}\approx0.35$, hence breakout occurs about two hours after the core collapses.

### B. Type-II light curve: The plateau

The plateau commences as hydrogen-rich zones expand and cool below about 5500 K. For typical densities, hydrogen recombines at this point, releasing trapped radiation. This "recombination wave" propagates inwards in mass, though initially outwards in radius, maintaining an approximately constant effective temperature. The radiation is approximately that of a blackbody and the constancy of the temperature thus implies a luminosity that scales as $R_{photo}^2$.

The amount of mass that has recombined by time $t$ is quadratic in $t$. More specifically (Woosley, 1988),

$$M\approx\frac{Lt^2}{q(t_b)t_b}, \tag{39}$$

where $q(t_b)$ is the energy per gram in the hydrogen envelope following shock passage and $t_b$ is the breakout time given above.

The duration is given by Popov (1993):

$$t_p\approx99\frac{\kappa_{0.34}^{1/6}M_{10}^{1/2}R_{0,500}^{1/6}}{E_{51}^{1/6}T_{ion,5054}^{2/3}}\ \text{d}, \tag{40}$$

where $R_{0,500}$ is the radius in units of $500R_\odot$, $M_{10}$ is the mass of the hydrogen envelope in units of $10M_\odot$, $E_{51}$ is the explosion energy divided by $10^{51}$ erg, and $T_{ion,5054}$ is the photospheric temperature divided by 5054 K.

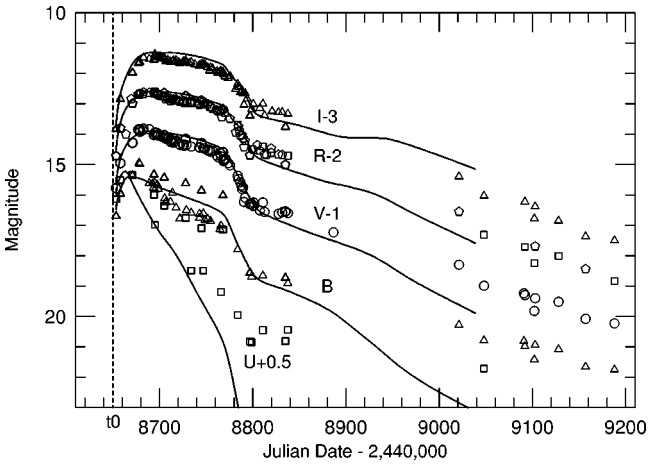


FIG. 30. Five-color photometry of a model $15M_\odot$ supernova compared to observations of type-II-*p* SN 1992H (Eastman *et al.*, 1993; Eastman, Woosley, *et al.*, 1994). The I, R, V, and U magnitudes have been adjusted by the indicated shifts for plotting. The model calculations assume thermal level populations, and the nonlocal thermodynamic equilibrium corrections are appreciable, particularly for the U band. The supernova produced $0.06M_\odot$ of $^{56}$Ni and the assumed distance modulus is 32.0, with no correction for extinction. Data are from Filippenko (1997).

The luminosity on the plateau is

$$L_{bol}\approx1.64\times10^{42}\frac{R_{0,500}^{2/3}E_{51}^{5/6}T_{ion,5054}^{4/3}}{M_{10}^{1/2}\kappa_{0.34}^{1/3}}\ \text{erg s}^{-1}. \tag{41}$$

Clearly stars with smaller radii will have shorter, fainter plateaus. Starting from a smaller radius, a similar amount of shock-deposited internal energy is adiabatically degraded by a larger factor before reaching the recombination radius, a few times $10^{15}$ cm. An example is SN 1987A, a blue supergiant with a radius ten times smaller than the more typical red supergiant, which had a luminosity on the plateau about five times fainter. Indeed the plateau was so faint that the emission of 87A at peak was dominated by radioactive decay.

Figure 30 shows the comparison between theoretical expectations for the explosion of a $15M_\odot$ red supergiant, probably the most common variety of type-II supernova, and observations of SN 1992H. The calculations by Eastman *et al.* (1993) and Eastman, Woosley, and Weaver (1994) did not include the shock breakout phase (which was also unobserved), but used a detailed model for the ionization and level populations and a multifrequency calculation of the radiation transport. Agreement with observations is excellent, except perhaps in the U band, which is affected by nonlocal thermodynamic equilibrium corrections not included in the model.

### C. Type II-light curve: The tail

After the hydrogen has recombined, the display from shock-deposited energy quickly declines. The energy in

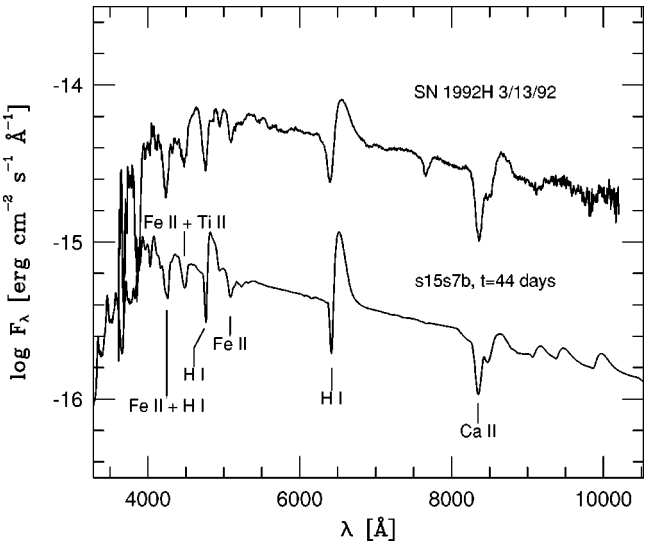


FIG. 31. Spectrum of the type-II-*p* SN 1992H (Filippenko, 1997) compared with a nonlocal thermodynamic equilibrium calculation of a $15M_\odot$ supernova explosion in a red supergiant (Eastman, Woosley, and Weaver, 1994 and Eastman, Schmidt, and Kirshner, 1996).

the helium core is degraded by about $10^5$ in its expansion to a few $\times 10^{15}$ cm and is quite negligible. Once that core is uncovered, the supernova would go out were it not for a new energy source—radioactivity. For progenitor masses over about $12M_\odot$ and yet low enough in mass to avoid significant reimplosion (Sec. VI.A), approximately $0.1M_\odot$ of $^{56}$Ni is ejected in the explosion. Decay of $^{56}$Ni to $^{56}$Co deposits $5.9\times 10^{48}$ erg/$(0.1M_\odot)$ with a half-life of 6.1 d. The further decay of $^{56}$Co to $^{56}$Fe produces $1.3\times 10^{49}$ erg/$(0.1M_\odot)$ with a half-life of 77.3 d. Most of the energy from $^{56}$Ni decay goes into accelerating the expansion of the interior of the supernova; little escapes. However, the energy from $^{56}$Co decay is quite significant. In red supergiants, $^{56}$Co decay gives a "radioactive tail" to the light curve and a bolometric luminosity that tracks its half-life. In blue stars like 87A, $^{56}$Co decay dominates the light curve from an early time (after about 20 d) and is responsible for the peak. In type-Ib and type-Ic supernovae, $^{56}$Co decay powers the entire display. In massive stars that lose most but not all of their hydrogen envelope, a brief plateau merges into a $^{56}$Co powered tail, producing a type II-L ("linear") light curve (Young and Branch, 1989) perhaps augmented by circumstellar shock interaction.

Other radioactivities such as $^{57}$Co ($\tau_{1/2}=272$ d) and $^{44}$Ti ($\tau_{1/2}=60$ y) may also be important to the light curves of type-II supernovae at late times (see, for example, Timmes *et al.*, 1996).

### D. Type-II supernovae—The spectrum and cosmological applications

The spectrum of common type-II plateau supernovae near peak luminosity is given (Fig. 31) by a quasithermal continuum with a superposition of P-Cygni lines. Early on the temperature is high and the lines broad, but within a few weeks it has declined to a value typical of hydrogen recombination—5500 K (Filippenko, 1997). The Balmer series is prominent, with $H_\alpha$ absorption strengthening with time. Lines of Na D and singly ionized metals are prominent and increase in strength with time. After the plateau, emission lines of $H_\alpha$, [Ca II], [O I], and [Fe II] are also prominent. All of these observations are quite consistent with expectations of a model explosion of a red supergiant with envelope mass of order $10M_\odot$ (Fig. 31) and are quite insensitive to the explosion mechanism (provided that there is one).

Given our good understanding of the typical type-II supernova spectrum and light curve, it is natural to try to use these objects for distance determination (Kirshner and Kwan, 1974; Schmidt, Kirshner, Eastman, Hamuy, *et al.*, 1994; Schmidt, Kirshner, Eastman, Phillips, *et al.*, 1994; Eastman *et al.*, 1996; Filippenko, 1998). Typical values of Hubble's constant obtained using this "expanding photospheres method" are in the range $73 \pm 7(\text{statistical}) \pm 6(\text{systematic})$ km s$^{-1}$ Mpc$^{-1}$.

### E. Type-Ib and type-Ic supernovae

If the star has lost its hydrogen envelope before exploding then there is no plateau. Owing to the small radius of the presupernova star, about a solar radius, the breakout transient is brief, faint, and hard. What remains then is a display powered by radioactivity much as in type-Ia supernovae.

For a time, the approximate regularity and especially the narrow width of the observed light curves for type-Ib supernova were puzzling, implying a smaller mass than observed for typical Wolf-Rayet stars (Ensman and Woosley, 1988). The explanation is likely the mass dependence of Wolf-Rayet mass-loss rates (Langer, 1989b), which results in a convergence of the final mass on a value around $3-4M_\odot$. The few Wolf-Rayet stars that die with large masses (because they evolved as single stars and lost their envelopes shortly before dying) could contribute a rare population of type-Ib supernovae with broad faint light curves, or they may be the progenitors of gamma-ray bursts (Sec. VI.B).

Typical Ib supernovae occur in regions where massive stars might be present (i.e., not in elliptical galaxies) and are strong radio sources, as might be expected from their high mass-loss rates. The light curves are consistent with the production of $\sim 0.15M_\odot$ of $^{56}$Ni, which is about what one expects for a $10^{51}$-erg explosion in a helium (or carbon-oxygen) core of $4M_\odot$ (Woosley, Langer, and Weaver, 1995). This is about 1/4 the $^{56}$Ni produced in a normal type-Ia supernova and accounts for a similar decrease in the luminosity at peak. Because of their higher mass and lower average velocities, type-Ib supernovae trap the gamma rays from $^{56}$Co decay more effectively than type-Ia and thus their radioactive tails may in some cases track its half-life (Clocchiatti and Wheeler, 1997). Other Ib's, presumably of lower mass and high velocity, do not.

Type-Ic supernovae are similar in many ways to type Ib but lack a distinctive He I absorption line at 5876 A (Filippenko, 1997). It is debated whether this deficiency implies an actual absence of He in the presupernova star or reflects insufficient mixing of radioactivity in the Ic's to excite energetic transitions in helium (Woosley and Eastman, 1993). Many of the helium stars in Fig. 5 have lost most, but not all, of their helium shell and are essentially balls of carbon and oxygen (plus an iron core) when they explode.

## X. CONCLUSIONS AND FUTURE DIRECTIONS

Qualitatively, the evolution of massive stars and their explosion as supernovae is understood. This understanding allows us to state with some confidence the origin of the elements (Table II), the nature of supernova light curves and spectra (Figs. 30 and 31), the expected masses of neutron stars (Fig. 17), and probably even how the star explodes (Sec. V.C). However, there remain many uncertainties and perhaps it is appropriate to close by enumerating some of them.

- Convection:
  The greatest uncertainty still afflicting our understanding of the presupernova evolution of massive stars—and stars in general—is the rudimentary theory of convection used in their study. Neither the strict Ledoux nor the Schwarzschild criterion is capable of explaining all the observations, and a quantitative theory of semiconvection and convective overshoot mixing is lacking.
- The type-II supernova explosion mechanism:
  Despite 50 years of intensive investigation, we still do not understand exactly how massive stars blow up. Models of increasing complexity and dimensionality exist but still do not adequately predict such fundamentals as the explosion energy and mass cut (including fallback). They are thus unable to predict with necessary precision the mass of neutron stars or the products of explosive silicon burning. Uncertainty in the explosion mechanism as well as the nuclear equation of state makes it difficult to predict which stars will leave neutron stars as remnants and which will leave black holes.
- Rotation and magnetic fields:
  Sufficient calculations have been done to show that both rotation and magnetic fields are quite important in the presupernova star and probably during the explosion. Even if the star rotates rigidly on the main sequence, what is the final distribution of angular momentum? Why do pulsars have the rotation rates that they do? What is their initial magnetic-field distribution and why? Do magnetic fields play a role in the explosion?
- Uncertain nuclear reaction rates:
  We are much better off than when Burbidge *et al.* (1957) wrote their classic paper, but key nuclear quantities still have unacceptably large errors. Chief among these are the reaction rates for $^{12}C(\alpha,\gamma)^{16}O$ and $^{22}Ne(\alpha,n)^{25}Mg$.
- The site for the *r* process and details of the *p* process:
  The neutrino wind (Sec. VIII.B.5) is a promising site for the *r* process, but the simple one-dimensional models lack sufficient entropy or rapid enough expansion to produce the heavy *r* process nuclei. For the *p* process, how are the lighter ones, near $N=50$, made?
- The relation of massive stars to gamma-ray bursts:
  Increasing evidence points to a connection. Are some supernovae powered by jets and not neutrinos? Which stars make gamma-ray bursts and how? What does the stellar counterpart to a gamma-ray burst look like just after the explosion?
- Mass-loss rates:
  The rate at which mass is lost from luminous blue variable stars, red and blue supergiants, and Wolf-Rayet stars greatly influences the presupernova model (Sec. IV.F) and nucleosynthesis (Sec. VIII.D). Particularly uncertain is the mass-loss rate for Wolf-Rayet stars and how all these mass-loss rates scale with metallicity, especially for very metal-deficient compositions.

Given the importance of massive stars and supernovae to so many aspects of modern astrophysics as well as the prowess of modern computers, we are confident that considerable progress will be made on at least several of these questions during the next decade—or at least during the next 40 years.

## ACKNOWLEDGMENTS

We appreciate important contributions to this review by Ron Eastman, Rob Hoffman, Norbert Langer, and Frank Timmes. This research has been supported by the NSF (AST 97-316569), the DOE ASCI Program (B347885), the DOE SciDAC Program (DE-FC02-01ER41176), and the Alexander von Humboldt-Stiftung Program (FLF-1065004).

## REFERENCES

Abel, T., G. L. Bryan, and M. L. Norman, 2000, Astrophys. J. **540**, 39.
Abrikosov, A. A., 1960, Sov. Phys. JETP **12**, 1254.
Acoragi, J.-P., N. Langer, and M. Arnould, 1991, Astron. Astrophys. **249**, 134.
Adelberger, E. G., *et al.*, 1998, Rev. Mod. Phys. **70**, 1265.
Aldering, G., R. M. Humphreys, and M. Richmond, 1994, Astron. J. **107**, 662.
Aloy, M. A., E. Müller, J. M. Ibanez, J. M. Marti, and A. MacFadyen, 2000, Astrophys. J. Lett. **531**, L119.
Anders, E., and N. Grevesse, 1989, Geochim. Cosmochim. Acta **53**, 197.
Angulo, C., *et al.*, 1999, Nucl. Phys. A **656**, 3.
Angulo, C., and P. Descouvemont, 2001, Nucl. Phys. A **690**, 755.
Appenzeller, I., 1970, Astron. Astrophys. **5**, 355.

Arnett, W. D., 1969, Astrophys. J. **157**, 1369.
Arnett, W. D., 1972a, Astrophys. J. **173**, 393.
Arnett, W. D., 1972b, Astrophys. J. **176**, 681.
Arnett, W. D., 1974a, Astrophys. J. **193**, 169.
Arnett, W. D., 1974b, Astrophys. J. **194**, 373.
Arnett, W. D., 1977, Astrophys. J., Suppl. Ser. **35**, 145.
Arnett, W. D., 1987, Astrophys. J. **319**, 136.
Arnett, W. D., 1995, Annu. Rev. Astron. Astrophys. **33**, 115.
Arnett, W. D., 1996, *Supernovae and Nucleosynthesis* (Princeton University, Princeton, NJ).
Arnett, W. D., J. N. Bahcall, R. P. Kirshner, and S. E. Woosley, 1989, Annu. Rev. Astron. Astrophys. **27**, 629.
Arnett, W. D., B. A. Fryxell, and E. Müller, 1989, Astrophys. J. Lett. **341**, L63.
Arnett, W. D., and A. Fu, 1989, Astrophys. J. **340**, 396.
Arnett, W. D., and F.-K. Thielemann, 1985, Astrophys. J. **295**, 589.
Arnett, W. D., and J. W. Truran, 1969, Astrophys. J. **157**, 339.
Arnould, M., 1976, Astron. Astrophys. **46**, 117.
Arras, P., E. E. Flanagan, S. M. Morsink, A. K. Schenk, S. A. Teukolsky, and I. Wasserman, 2002, e-print astro-ph/0202345.
Aubert, O., N. Prantzos, and I. Baraffe, 1996, Astron. Astrophys. **312**, 845.
Aufderheide, M. B., I. Fushiki, G. M. Fuller, and T. A. Weaver, 1994, Astrophys. J. **424**, 257.
Aufderheide, M., I. Fushiki, S. E. Woosley, and D. Hartmann, 1994, Astrophys. J., Suppl. Ser. **91**, 389.
Azuma, R. E., *et al.*, 1994, Phys. Rev. C **50**, 1194.
Bahcall, J. N., M. H. Pinsonneault, and S. Basu, 2001, Astrophys. J. **555**, 990.
Baraffe, I., A. Heger, and S. E. Woosley, 2001, Astrophys. J. **550**, 890.
Barkat, Z., and A. Marom, 1990, in *Supernovae*, Jerusalem Winter School, Vol. 6, edited by J. Wheeler, T. Piran, and S. Weinberg (World Scientific, Singapore/Teaneck, NJ), p. 95.
Barkat, Z., Y. Reiss, and G. Rakavy, 1974, Astrophys. J., Lett., Ed. **193**, L21.
Barnes, C., 1995, Nucl. Phys. A **588**, 295c.
Baron, E., H. A. Bethe, G. E. Brown, J. Cooperstein, and S. Kahana, 1987, Phys. Rev. Lett. **59**, 736.
Baron, E., and J. Cooperstein, 1990, Astrophys. J. **353**, 597.
Baron, E., J. Cooperstein, and S. Kahana, 1985, Phys. Rev. Lett. **55**, 126.
Bartunov, Ol., S. Blinnikov, N. M. Pavlyuk, and T. D. Yu, 1994, Astron. Astrophys. **281**, 53.
Bazan, G., and W. D. Arnett, 1994, Astrophys. J. Lett. **433**, L41.
Bazan, G., and W. D. Arnett, 1998, Astrophys. J. **496**, 316.
Beaudet, G., V. Petrosian, and E. E. Salpeter, 1967, Astrophys. J. **150**, 979.
Bethe, H. A., 1990, Rev. Mod. Phys. **62**, 801.
Bethe, H. A., and G. E. Brown, 1995, Astrophys. J. Lett. **445**, L129.
Bethe, H. A., G. E. Brown, J. Applegate, and J. M. Lattimer, 1979, Nucl. Phys. A **324**, 487.
Bethe, H. A., and J. R. Wilson, 1985, Astrophys. J. **295**, 14.
Biello, J. A., 2001, Ph.D. thesis (Department of Astronomy and Astrophysics, University of Chicago).
Blackmon, J. C., A. E. Champagne, M. A. Hofstee, M. S. Smith, R. G. Downing, and G. P. Lamaze, 1995, Phys. Rev. Lett. **74**, 2642.
Blandford, R. D., and R. L. Znajek, 1977, Mon. Not. R. Astron. Soc. **179**, 433.
Blinnikov, S. I., N. V. Dunina-Barkovskaya, and D. K. Nadyozhin, 1996, Astrophys. J., Suppl. Ser. **106**, 171; **118**, 603(E).
Blinnikov, S., P. Lundquist, O. Bartunov, K. Nomoto, and K. Iwamoto, 2000, Astrophys. J. **532**, 1132.
Blinnikov, S., S. E. Woosley, E. Sorokina, and D. Nadyozhin, 2001, unpublished.
Bodansky, D., D. D. Clayton, and W. A. Fowler, 1968, Astrophys. J., Suppl. Ser. **16**, 299.
Bodenheimer, P., and S. E. Woosley, 1983, Astrophys. J. **269**, 281.
Bond, J. R., W. D. Arnett, and B. J. Carr, 1984, Astrophys. J. **280**, 825.
Braun, H., and N. Langer, 1995, Astron. Astrophys. **297**, 483.
Bressan, A., F. Fagotto, G. Bertelli, and C. Chiosi, 1993, Astron. Astrophys., Suppl. Ser. **100**, 647.
Brocato, E., and V. Castellani, 1993, Astrophys. J. **410**, 99.
Bromm, V., P. S. Coppi, and R. B. Larson, 1999, Astrophys. J. Lett. **527**, L5.
Bruenn, S. W., 1972, Astrophys. J., Suppl. **24**, 283.
Bruenn, S. W., 1989a, Astrophys. J. **340**, 955.
Bruenn, S. W., 1989b, Astrophys. J. **341**, 385.
Bruenn, S. W., and T. Mezzacappa, 1994, Astrophys. J. Lett. **433**, L45.
Brunish, W., and J. W. Truran, 1982, Astrophys. J. **256**, 247.
Buchmann, L., 1996, Astrophys. J. Lett. **468**, L127; **479**, L153(E).
Buchmann, L., R. E. Azuma, C. A. Barnes, J. Humblet, and K. Langanke, 1996, Phys. Rev. C **54**, 393.
Burbidge, E. M., G. R. Burbidge, W. A. Fowler, and F. Hoyle, 1957, Rev. Mod. Phys. **29**, 547.
Burrows, A., and B. A. Fryxell, 1993, Astrophys. J. Lett. **418**, L33.
Burrows, A., J. Hayes, and B. A. Fryxell, 1995, Astrophys. J. **450**, 830.
Burrows, A., and J. Lattimer, 1985, Astrophys. J., Lett. Ed. **299**, L19.
Busso, M., R. Gallino, D. L. Lambert, C. Travaglio, and V. V. Smith, 2001, Astrophys. J. **557**, 802.
Cameron, A. G. W., 1957, Chalk River Report, CRL-41.
Cameron, A. G. W., 1959, Astrophys. J. **130**, 429.
Cameron A. G. W., 2001, Astrophys. J. **562**, 456.
Cardall, C., and G. M. Fuller, 1997, Astrophys. J. **486**, 111.
Caughlan, G. A., and W. A. Fowler, 1988, At. Data Nucl. Data Tables **40**, 283.
Chandrasekhar, S., 1938, *Stellar Structure* (Dover, New York).
Charbonnel, C., G. Meynet, A. Maeder, and D. Schaerer, 1996, Astron. Astrophys., Suppl. Ser. **115**, 339.
Charbonnel, C., G. Meynet, A. Maeder, G. Schaller, and D. Schaerer, 1993, Astron. Astrophys., Suppl. Ser. **101**, 415.
Chevalier, R. A., 1976, Astrophys. J. **207**, 872.
Chevalier, R. A., 1989, Astrophys. J. **346**, 847.
Chevalier, R. A., and R. I. Klein, 1978, Astrophys. J. **219**, 994.
Chevalier, R. A., and N. Soker, 1989, Astrophys. J. **341**, 867.
Chieffi, A., M. Limongi, and O. Straniero, 1998, Astrophys. J. **502**, 737.
Chin, C.-W., and R. Stothers, 1991, Astrophys. J., Suppl. Ser. **77**, 299.
Chiosi, C., G. Bertelli, and A. Bressan, 1992, Annu. Rev. Astron. Astrophys. **30**, 235.
Chiosi, C., and A. Maeder, 1986, Annu. Rev. Astron. Astrophys. **24**, 329.
Clayton, D. D., 1968, *Principles of Stellar Evolution and Nucleosynthesis* (McGraw-Hill, New York).

Clayton, D. D., 1982, in *Essays in Nuclear Astrophysics*, edited by C. A. Barnes, D. D. Clayton, and D. N. Schramm (Cambridge University, Cambridge/New York), p. 401.
Clayton, D. D., S. A. Colgate, and G. J. Fishman, 1969, Astrophys. J. **155**, 75.
Clayton, D. D., W. Liu, and A. Dalgarno, 1999, Science **283**, 1290.
Clocchiatti, A., and J. C. Wheeler, 1997, Astrophys. J. **491**, 375.
Colgate, S. A., and R. H. White, 1966, Astrophys. J. **143**, 626.
Cooperstein, J., and E. Baron, 1990, in *Supernovae*, edited by A. G. Petschek (Springer-Verlag, New York), p. 213.
Costa, V., M. Rayet, R. A. Zappala, and M. Arnould, 2000, Astron. Astrophys. **358**, 67.
Couch, R. G., A. B. Schmiedekamp, and W. D. Arnett, 1974, Astrophys. J. **190**, 95.
Cowan, J. J., F.-K. Thielemann, and J. W. Truran, 1991, Phys. Rep. **208**, 267.
Danziger, I. J., *et al.*, 1988, in *Supernova 1987A in the Large Magellanic Cloud*, edited by M. Kafatos and A. Michalitsianos (Cambridge University, Cambridge/New York), p. 37.
Dayras, R., Z. E. Switkowski, and S. E. Woosley, 1977, Nucl. Phys. A **279**, 70.
De Loore, C., and D. Vanbeveren, 1992, Astron. Astrophys. **260**, 273.
DeJager, C., H. Nieuwenhuijzen, and K. van der Hucht, 1988, Astron. Astrophys., Suppl. Ser. **72**, 259.
Diehl, R., and F. X. Timmes, 1998, Publ. Astron. Soc. Pac. **110**, 637.
Diehl, R., *et al.*, 1995, Astron. Astrophys. **298**, 445.
Domogatskii, G. V., and D. K. Nadyozhin, 1977, Mon. Not. R. Astron. Soc. **178**, 33P.
Domogatskii, G. V., and D. K. Nadyozhin, 1980, Astrophys. Space Sci. **70**, 33.
Duncan, R. C., S. L. Shapiro, and I. Wasserman, 1986, Astrophys. J. **309**, 141.
Eastman, R. G., B. P. Schmidt, and R. Kirshner, 1996, Astrophys. J. **466**, 911.
Eastman, R. G., S. E. Woosley, and T. A. Weaver, 1994, Bull. Am. Astron. Soc. **26** (4), 1362.
Eastman, R. G., S. E. Woosley, T. A. Weaver, and P. A. Pinto, 1993, Bull. Am. Astron. Soc. **25** (2), 836.
Eastman, R. G., S. E. Woosley, T. A. Weaver, and P. A. Pinto, 1994, Astrophys. J. **430**, 300.
El Eid, M. F., and N. Langer, 1986, Astron. Astrophys. **167**, 274.
Ellis, P. J., J. M. Lattimer, and M. Prakash, 1996, Comments Nucl. Part. Phys. **22**, 63.
Endal, A. S., and S. Sofia, 1976, Astrophys. J. **210**, 184.
Endal, A. S., and S. Sofia, 1978, Astrophys. J. **220**, 279.
Ensman, L., and A. Burrows, 1992, Astrophys. J. **393**, 742.
Ensman, L. M., and S. E. Woosley, 1988, Astrophys. J. **333**, 754.
Falk, S. W., 1978, Astrophys. J., Lett. Ed. **225**, L133.
Falk, S. W., and W. D. Arnett, 1973, Astrophys. J. **180**, L65.
Fields, B. D., and K. A. Olive, 1999, Astrophys. J. **516**, 797.
Fields, B. D., K. A. Olive, E. Vangioni-Flam, and M. Casse, 2000, Astrophys. J. **540**, 930.
Filippenko, A. V., 1997, Annu. Rev. Astron. Astrophys. **35**, 309.
Filippenko, A. V., 1998, in *Eighteenth Texas Symposium on Relativistic Astrophysics and Cosmology*, edited by A. V. Olinto, J. A. Frieman, and D. N. Schramm (World Scientific, Singapore/River Edge, NJ), p. 176.
Filippenko, A. V., T. Matheson, and A. J. Barth, 1994, Astron. J. **108**, 2220.
Fliegner, J., N. Langer, and K. A. Venn, 1996, Astron. Astrophys. **308**, L13.
Fontaine, G., H. C. Graboske, and H. M. van Horn, 1977, Astrophys. J., Suppl. **35**, 293.
Fowler, W. A., and F. Hoyle, 1964, Astrophys. J., Suppl. **9**, 201.
Fowler, W. A., S. E. Woosley, and C. A. Engelbrecht, 1978, Astrophys. J. **226**, 984.
Fransson, C., A. Cassatella, R. Gilmozzi, N. Panagia, W. Wamsteker, R. P. Kirshner, and G. Sonneborn, 1989, Astrophys. J. **336**, 429.
Fransson, C., and P. Lundqvist, 1989, Astrophys. J. Lett. **341**, L59.
Freiburghaus, C., S. Rosswog, and F.-K. Thielemann, 1999, Astrophys. J. **525**, 121.
Fryer, C. L., 1999, Astrophys. J. **522**, 413.
Fryer, C. L., and A. Heger, 2000, Astrophys. J. **541**, 1033.
Fryer, C. L., S. E. Woosley, and A. Heger, 2001, Astrophys. J. **550**, 372.
Fukuda, I., 1982, Publ. Astron. Soc. Pac. **94**, 271.
Fuller, G. M., W. A. Fowler, and M. J. Newman, 1980, Astrophys. J., Suppl. **42**, 447.
Fuller, G. M., W. A. Fowler, and M. J. Newman, 1982a, Astrophys. J., Suppl. Ser. **48**, 279.
Fuller, G. M., W. A. Fowler, and M. J. Newman, 1982b, Astrophys. J. **252**, 715.
Fuller, G. M., W. A. Fowler, and M. J. Newman, 1985, Astrophys. J. **293**, 1.
Garcia-Berro, E., and I. Iben, Jr., 1994, Astrophys. J. **434**, 306.
Garcia-Berro, E., C. Ritossa, and I. Iben, Jr., 1997, Astrophys. J. **485**, 765.
Garresberg, E. K., V. S. Imshennik, and D. K. Nadyozhin, 1971, Astrophys. Space Sci. **10**, 28.
Giessen, U., *et al.*, 1993, Nucl. Phys. A **561**, 95.
Glatzel, W., K. J. Fricke, and M. F. El Eid, 1985, Astron. Astrophys. **149**, 413.
Glatzel, W., M. Kiriakidis, and K. J. Fricke, 1993, Mon. Not. R. Astron. Soc. **262**, 7.
Grevesse, N., and A. Noels, 1993, in *Origin and Evolution of the Elements*, edited by N. Prantzos *et al.* (Cambridge University, Cambridge/New York), p. 13.
Grevesse, N., A. Noels, and A. J. Sauval, 1996, in *Cosmic Abundances*, edited by S. Holt & G. Sonneborn, ASP Conference Series No. 99 (Astronomical Society of the Pacific, San Francisco), p. 117.
Habets, G. M. H. J., 1986, Astron. Astrophys. **167**, 61.
Hachisu, I., T. Matsuda, K. Nomoto, and T. Shigeyama, 1994, Astron. Astrophys., Suppl. Ser. **104**, 341.
Hamann, W.-R., and L. Koesterke, 1998, Astron. Astrophys. **335**, 1003.
Hamann, W. R., L. Koesterke, and U. Wessolowski, 1993, Astron. Astrophys. **274**, 397.
Hamann, W. R., L. Koesterke, and U. Wessolowski, 1995, Astron. Astrophys. **299**, 151.
Hamann, W.-R., D. Schoenberner, and U. Heber, 1982, Astron. Astrophys. **116**, 273.
Hansen, C. J., 1968, Astrophys. Space Sci. **1**, 499.
Hashimoto, M., K. Nomoto, T. Tsujimoto, and F. K. Thielemann, 1993, in *Nuclei in the Cosmos II*, edited by F. Käppeler and K. Wisshak (IOP, Bristol), p. 587.
Haxton, W. C., 1988, Phys. Rev. Lett. **60**, 1999.

Heger, A., K. Langanke, G. Martinez-Pinedo, and S. E. Woosley, 2001, Phys. Rev. Lett. **86**, 1678.
Heger, A., and N. Langer, 2000, Astrophys. J. **544**, 1016.
Heger, A., N. Langer, and S. E. Woosley, 2000, Astrophys. J. **528**, 368.
Heger, A., P. A. Pinto, and S. E. Woosley, 2002, unpublished.
Heger, A., and S. E. Woosley, 2002, Astrophys. J. **567**, 532.
Heger, A., S. E. Woosley, G. Martinez-Pinedo, and K.-H. Langanke, 2001, Astrophys. J. **560**, 307.
Heger, A., S. E. Woosley, T. Rauscher, and R. D. Hoffman, 2002, unpublished.
Heger, A., S. E. Woosley, and H. Spruit, 2002, unpublished.
Herant, M., and W. Benz, 1992, Astrophys. J. **387**, 294.
Herant, M., W. Benz, and S. Colgate, 1992, Astrophys. J. **395**, 642.
Herant, M., W. Benz, W. R. Hix, C. L. Fryer, and S. A. Colgate, 1994, Astrophys. J. **435**, 339.
Herant, M., and S. E. Woosley, 1994, Astrophys. J. **425**, 814.
Herant, M., and S. E. Woosley, 1996, unpublished.
Herwig, F., T. Blocker, N. Langer, and T. Driebe, 1999, Astron. Astrophys. **349**, L5.
Hillebrandt, W., 1978, Space Sci. Rev. **21**, 639.
Hillebrandt, W., and P. Höflich, 1989, Rep. Prog. Phys. **52**, 1421.
Hillebrandt, W., P. Höflich, J. W. Truran, and A. Weiss, 1987, Nature (London) **327**, 597.
Hillebrandt, W., and F. Meyer, 1989, Astron. Astrophys. **219**, L3.
Hillebrandt, W., K. Nomoto, and R. Wolff, 1984, Astron. Astrophys. **133**, 175.
Hillebrandt, W., and F.-K. Thielemann, 1978, Mitt. Astron. Ges. **43**, 234.
Hoffman, R. D., S. E. Woosley, G. M. Fuller, and B. S. Meyer, 1996, Astrophys. J. **460**, 478.
Hoffman, R. D., S. E. Woosley, and Y. Z. Qian, 1997, Astrophys. J. **482**, 951.
Hoffman, R. D., S. E. Woosley, and T. A. Weaver, 2001, Astrophys. J. **549**, 1085.
Hoffman, R. D., S. E. Woosley, T. A. Weaver, T. Rauscher, and F.-K. Thielemann, 1999, Astrophys. J. **521**, 735.
Holmes, J. A., S. E. Woosley, W. A. Fowler, and B. A. Zimmerman, 1976, At. Data Nucl. Data Tables **18**, 305.
Howard, W. M., W. D. Arnett, D. D. Clayton, and S. E. Woosley, 1972, Astrophys. J. **175**, 201.
Howard, W. M., B. S. Meyer, and S. E. Woosley, 1991, Astrophys. J. Lett. **373**, L5.
Hoyle, F., and W. A. Fowler, 1960, Astrophys. J. **132**, 565.
Humphreys, R., and K. Davison, 1979, Astrophys. J. **232**, 409.
Iben, I., and A. Renzini, 1983, Annu. Rev. Astron. Astrophys. **21**, 271.
Iben, I. Jr., C. Ritossa, and E. Garcia-Berro, 1997, Astrophys. J. **489**, 772.
Iglesias, C. A., and F. J. Rogers, 1996, Astrophys. J. **464**, 943.
Itoh, M., S. Kumagai, T. Shigeyama, K. Nomoto, and J. Nishimura, 1987, Nature (London) **330**, 233.
Itoh, N., H. Hayashi, A. Nishikawa, and Y. Kohyama, 1996, Astrophys. J., Suppl. Ser. **102**, 411.
Itoh, N., S. Mitake, I. Hiroshi, and S. Ichimaru, 1983, Astrophys. J. **273**, 774.
Itoh, N., M. Nakagawa, and Y. Kohyama, 1985, Astrophys. J. **294**, 17.
Iwamoto, K., F. Brachwitz, K. Nomoto, N. Kishimoto, H. Umeda, W. R. Hix, and F.-K. Thielemann, 1999, Astrophys. J., Suppl. Ser. **125**, 439.
Iwamoto, K., T. R. Young, N. Nakasato, T. Shigeyama, K. Nomoto, I. Hachisu, and H. Saio, 1997, Astrophys. J. **477**, 865.
Iyudin, A. F., *et al.*, 1994, Astron. Astrophys. **284**, L1.
Jaeger, M., R. Kunz, A. Mayer, J. W. Hammer, G. Staudt, K.-L. Kratz, and B. Pfeiffer, 2001, Phys. Rev. Lett. **87**, 202501.
Janka, H.-T., 1995, Astropart. Phys. **3**, 377.
Janka, H.-T., and E. Müller, 1995, Astrophys. J. Lett. **448**, L109.
Janka, H.-T., and E. Müller, 1996, Astron. Astrophys. **306**, 167.
Jaroszyński, M., 1996, Astron. Astrophys. **305**, 839.
Jose, J., and M. Hernanz, 1998, Astrophys. J. **494**, 680.
Käppeler, F., H. Beer, K. Wisshak, D. D. Clayton, R. I. Macklin, and R. A. Ward, 1982, Astrophys. J. **257**, 821.
Käppeler, F., M. Wiescher, U. Giesen, J. Goerres, I. Baraffe, M. El Eid, C. M. Raiteri, M. Busso, R. Gallino, M. Limongi, and A. Chieffi, 1994, Astrophys. J. **437**, 396.
Kato, S., 1966, Publ. Astron. Soc. Jpn. **18**, 374.
Kifonidis, K., T. Plewa, H.-Th. Janka, and E. Müller, 2000, Astrophys. J. Lett. **531**, 123L.
Kippenhahn, R., E. Meyer-Hofmeister, and H. C. Thomas, 1970, Astron. Astrophys. **5**, 155.
Kippenhahn, R., and A. Weigert, 1967, Z. Astrophys. **66**, 58.
Kippenhahn, R., and A. Weigert, 1990, *Stellar Structure and Evolution* (Springer-Verlag, Berlin/New York).
Kirshner, R. P., and J. Kwan, 1974, Astrophys. J. **193**, 27.
Klein, R. I., and R. A. Chevalier, 1978, Astrophys. J., Lett. Ed. **223**, L109.
Knobloch, E., and H. C. Spruit, 1983, Astron. Astrophys. **125**, 59.
Kolbe, E., and K. Langanke, 2001, unpublished.
Kudritzki, R.-P., 2000, in *The First Stars*, edited by A. Weiss, T. G. Abel, and V. Hill (Springer-Verlag, Berlin), p. 127.
Kudritzki, R. P., A. Pauldrach, J. Puls, and D. C. Abbot, 1989, Astron. Astrophys. **219**, 205.
Kudritzki, R.-P., and J. Puls, 2000, Annu. Rev. Astron. Astrophys. **38**, 613.
Kumagai, S., T. Shigeyama, K. Nomoto, M. Itoh, and J. Nishimura, 1988, Astron. Astrophys. **197**, L7.
Kumagai, S., T. Shigeyama, K. Nomoto, M. Itoh, J. Nishimura, and S. Tsuruta, 1989, Astrophys. J. **345**, 412.
Kumar, P., R. Nayayan, and A. Loeb, 1995, Astrophys. J. **453**, 480.
Kunz, R., M. Fey, M. Jaeger, A. Mayer, J. W. Hammer, G. Staudt, S. Harissopulos, and T. Paradellis, 2001, Phys. Rev. Lett. **86**, 3244.
Kunz, R., M. Fey, M. Jaeger, A. Mayer, J. W. Hammer, G. Staudt, S. Harissopulos, and T. Paradellis, 2002, Astrophys. J. **567**, 643.
Lamb, S. A., W. M. Howard, J. W. Truran, and I. Iben, Jr., 1977, Astrophys. J. **217**, 213.
Lamers, H. J. G. L. M., and J. P. Cassinelli, 1999, *Introduction to Stellar Winds* (Cambridge University, Cambridge/New York).
Landré, V., N. Prantzos, P. Auger, G. Bogaert, A. Lefebvre, and J. P. Thibaud, 1990, Astron. Astrophys. **240**, 85.
Langanke, K., and G. Martínez-Pinedo, 1999, Phys. Lett. B **453**, 187.
Langanke, K., and G. Martínez-Pinedo, 2000, Nucl. Phys. A **673**, 481.
Langer, N., 1989a, Astron. Astrophys. **210**, 93.

Langer, N., 1989b, Astron. Astrophys. **220**, 135.
Langer, N., 1991a, in *Wolf-Rayet Stars and Interrelations with Other Massive Stars in Galaxies*, edited by K. van der Hucht and B. Hidayat (Kluwer Academic, Dordrecht/Boston), p. 431.
Langer, N., 1991b, Astron. Astrophys. **252**, 669.
Langer, N., 1991c, Astron. Astrophys. **243**, 155.
Langer, N., 1992, Astron. Astrophys. **265**, L17.
Langer, N., 1998, Astron. Astrophys. **329**, 551.
Langer, N., 2001, private communication.
Langer, N., and M. F. El Eid, 1986, Astron. Astrophys. **167**, 265.
Langer, N., M. F. El Eid, and I. Baraffe, 1989, Astron. Astrophys. Lett. **224**, L17.
Langer, N., M. F. El Eid, and K. J. Fricke, 1985, Astron. Astrophys. **145**, 179.
Langer, N., K. J. Fricke, and D. Sugimoto, 1983, Astron. Astrophys. **126**, 207.
Langer, N., W.-R. Hamann, M. Lennon, F. Najarro, A. W. A. Pauldrach, and J. Puls, 1994, Astron. Astrophys. **290**, 819.
Langer, N., and A. Maeder, 1995, Astron. Astrophys. **295**, 685.
Lattimer, J., and D. N. Schramm, 1974, Astrophys. J., Lett. Ed. **192**, 145.
Lattimer, J., and D. N. Schramm, 1976, Astrophys. J. **210**, 549.
Lauterborn, D., S. Refsdal, and M. L. Roth, 1971, Astron. Astrophys. **13**, 119.
Lauterborn, D., S. Refsdal, and A. Weigert, 1971, Astron. Astrophys. **10**, 97.
LeBlanc, J., and J. R. Wilson, 1970, Astrophys. J. **161**, 54.
Lee, T., D. A. Papanastassiou, and G. J. Wasserburg, 1977, Astrophys. J., Lett. Ed. **211**, 107.
Lee, T., D. N. Schramm, J. P. Wefel, and J. B. Blake, 1979, Astrophys. J. **232**, 854.
Lindblom, L., J. E. Tohline, and M. Vallisneri, 2001, Phys. Rev. Lett. **86**, 1152.
MacFadyen, A., 2001, Bull. Am. Astron. Soc. **33** (2), 834.
MacFadyen, A. I., and S. E. Woosley, 1999, Astrophys. J. **524**, 262.
MacFadyen, A. I., S. E. Woosley, and A. Heger, 2001, Astrophys. J. **550**, 410.
Maeder, A., 1983, Astron. Astrophys. **120**, 113.
Maeder, A., 1990, Astron. Astrophys., Suppl. Ser. **84**, 139.
Maeder, A., and P. Conti, 1994, Annu. Rev. Astron. Astrophys. **32**, 227.
Maeder, A., and G. Meynet, 1989, Astron. Astrophys. **210**, 155.
Maeder, A., and G. Meynet, 2000a, Annu. Rev. Astron. Astrophys. **38**, 143.
Maeder, A., and G. Meynet, 2000b, Astron. Astrophys. **361**, 159.
Maeder, A., and G. Meynet, 2000c, Astron. Astrophys. **361**, 101.
Maeder, A., and G. Meynet, 2001, Astron. Astrophys. **373**, 555.
Maeder, A., and J.-P. Zahn, 1998, Astron. Astrophys. **334**, 1000.
Maheswaran, M., and J. Cassinelli, 1994, Astrophys. J. **421**, 718.
Mathews, G. J., and J. J. Cowan, 1990, Nature (London) **345**, 491.
Mayle, R., 1985, Ph.D. thesis (University of California), UCRL Report 53713.
Mayle, R., 1990, in *Supernovae*, edited by A. G. Petschek (Springer-Verlag, New York), p. 267.
Mayle, R., and J. R. Wilson, 1988, Astrophys. J. **334**, 909.
Mayle, R., and J. R. Wilson, 1991, in *Supernovae*, edited by S. E. Woosley (Springer-Verlag, New York), p. 333.
Mazurek, T., 1973, Ph.D. thesis (Yeshiva University).
Mazurek, T., J. W. Truran, and A. G. W. Cameron, 1974, Astrophys. Space Sci. **27**, 261.
Merryfield, W. J., 1995, Astrophys. J. **444**, 318.
Meyer, B., 1994, Annu. Rev. Astron. Astrophys. **32**, 153.
Meyer, B. S., and D. D. Clayton, 2000, Space Sci. Rev. **92**, 133.
Meyer, B. S., T. D. Krishnan, and D. D. Clayton, 1998, Astrophys. J. **498**, 808.
Meynet, G., and M. Arnould, 1993, in *Nuclei in the Cosmos*, edited by F. Käppler and K. Wishak (IOP, Bristol), p. 503.
Meynet, G., and M. Arnould, 2000, Astron. Astrophys. **355**, 176.
Meynet, G., M. Arnould, N. Prantzos, and G. Paulus, 1997, Astron. Astrophys. **320**, 460.
Meynet, G., and A. Maeder, 2000, Astron. Astrophys., Suppl. Ser. **361**, 101.
Meynet, G., A. Maeder, G. Schaller, D. Schaerer, and C. Charbonnel, 1994, Astron. Astrophys., Suppl. Ser. **103**, 97.
Mezzacappa, A., A. C. Calder, S. W. Bruenn, J. M. Blondin, M. W. Guidry, M. R. Strayer, and A. S. Umar, 1998, Astrophys. J. **495**, 911.
Mitake, S., S. Ichimaru, and N. Itoh, 1984, Astrophys. J. **277**, 375.
Miyaji, S., and K. Nomoto, 1987, Astrophys. J. **318**, 307.
Miyaji, S., K. Nomoto, K. Yokoi, and D. Sugimoto, 1980, Publ. Astron. Soc. Jpn. **32**, 303.
Mowlavi, N., D. Schaerer, G. Meynet, P. A. Bernasconi, C. Charbonnel, and A. Maeder, 1998, Astron. Astrophys., Suppl. Ser. **128**, 471.
Müller, E., B. A. Fryxell, and W. D. Arnett, 1991, Astron. Astrophys. **251**, 505.
Munakata, H., Y. Kohyama, and N. Itoh, 1985, Astrophys. J. **296**, 197; **304**, 580(E).
Myra, E. S., and S. A. Bludman, 1989, Astrophys. J. **340**, 384.
Myra, E. S., and A. Burrows, 1990, Astrophys. J. **364**, 222.
Nagai, Y., M. Igashira, T. Shima, K. Masuda, T. Ohsaki, and H. Kitazawa, 1995, in *Nuclei in the Cosmos III*, edited by M. Busso, R. Gallino, and C. M. Raiten, AIP Conf. Proc. No. 327 (AIP, New York), p. 201.
Nagataki, S., T. M. Shimizu, and K. Sato, 1998, Astrophys. J. **495**, 413.
Nakamura, F., and M. Umemura, 2000, Astrophys. J. **548**, 19.
Nieuwenhuijzen, H., and C. DeJager, 1990, Astron. Astrophys. **231**, 134.
Nomoto, K., 1982, Astrophys. J. **253**, 798.
Nomoto, K., 1984, Astrophys. J. **277**, 791.
Nomoto, K., 1987, Astrophys. J. **322**, 206.
Nomoto, K., and M. Hashimoto, 1988, Phys. Rep. **163**, 13.
Nomoto, K., D. Sugimoto, W. M. Sparks, R. A. Fesen, T. R. Gull, and S. Miyaji, 1984, Nature (London) **229**, 803.
Nomoto, K., T. Suzuki, T. Shigeyama, S. Kumagai, H. Yamaoka, and H. Saio, 1993, Nature (London) **364**, 507.
Nota, A., M. Livio, M. Clampin, and R. Schulte-Ladbeck, 1995, Astrophys. J. **448**, 788.
Nugis, T., and H. J. G. L. M. Lamers, 2000, Astron. Astrophys. **360**, 227.
Olive, K. A., G. Steigman, and T. P. Walker, 2000, Phys. Rep. **333**, 389.
Otsuki, K., H. Tagoshi, T. Kajino, and S. Wanajo, 2000, Astrophys. J. **533**, 424.
Papaloizou, J. C. B., 1973a, Mon. Not. R. Astron. Soc. **162**, 143.

Papaloizou, J. C. B., 1973b, Mon. Not. R. Astron. Soc. **162**, 169.
Patat, F., R. Barbon, E. Cappellaro, and M. Turatto, 1993, Astron. Astrophys., Suppl. Ser. **98**, 443.
Patat, F., R. Barbon, E. Cappellaro, and M. Turatto, 1994, Astron. Astrophys. **282**, 731.
Pauldrach, A. W. A., R. P. Kudritzki, J. Puls, K. Butler, and J. Hunsinger, 1994, Astron. Astrophys. **283**, 525.
Pinto, P. A., and S. E. Woosley, 1988a, Astrophys. J. **329**, 820.
Pinto, P. A., and S. E. Woosley, 1988b, Nature (London) **333**, 534.
Podsiadlowski, Ph., 1992, Publ. Astron. Soc. Pac. **104**, 717.
Podsiadlowski, Ph., 1994, Space Sci. Rev. **66**, 439.
Podsiadlowski, Ph., J. J. L. Hsu, P. Joss, and R. R. Ross, 1993, Nature (London) **364**, 509.
Podsiadlowski, Ph., and P. C. Joss, 1989, Nature (London) **338**, 401.
Podsiadlowski, Ph., P. C. Joss, and J. J. L. Hsu, 1992, Astrophys. J. **391**, 246.
Podsiadlowski, Ph., P. C. Joss, and S. Rappaport, 1990, Astron. Astrophys. Lett. **227**, 9.
Pons, J. A., S. Reddy, M. Prakash, J. M. Lattimer, and J. A. Miralles, 1999, Astrophys. J. **513**, 780.
Popov, D. V., 1993, Astrophys. J. **414**, 712.
Prantzos, N., M. Hashimoto, and K. Nomoto, 1990, Astron. Astrophys. **234**, 211.
Qian, Y. Z., 2000, Astrophys. J. **534**, 67.
Qian, Y. Z., and G. M. Fuller, 1995, Phys. Rev. D **52**, 656.
Qian, Y. Z., G. M. Fuller, G. J. Mathews, R. W. Mayle, J. R. Wilson, and S. E. Woosley, 1993, Phys. Rev. Lett. **71**, 1965.
Qian, Y.-Z., and S. E. Woosley, 1996, Astrophys. J. **471**, 331.
Raiteri, C. M., M. Busso, G. Picchio, and R. Gallino, 1991, Astrophys. J. **371**, 665.
Rakavy, G., G. Shaviv, and Z. Zinamon, 1966, Astrophys. J. **150**, 131.
Ramaty, R., S. T. Scully, R. E. Lingenfelter, and B. Kozlovsky, 2000, Astrophys. J. **534**, 747.
Rauscher, T., A. Heger, S. E. Woosley, and R. D. Hoffman, 2002, Astrophys. J. **576**, 323.
Rauscher, T., and F.-K. Thielemann, 2000, At. Data Nucl. Data Tables **75** (1/2), 1.
Rayet, M., M. Arnould, M. Hashimoto, N. Prantzos, and K. Nomoto, 1995, Astron. Astrophys. **298**, 517.
Renzini, A., and M. Voli, 1981, Astron. Astrophys. **94**, 175.
Ritossa, C., E. Garcia-Berro, and I. Iben, 1996, Astrophys. J. **460**, 489.
Ritossa, C., E. Garcia-Berro, and I. Iben, 1999, Astrophys. J. **515**, 381.
Rogers, F. J., and C. A. Iglesias, 1992, Astrophys. J., Suppl. Ser. **79**, 507.
Rolfs, C. E., and W. S. Rodney, 1988, *Cauldrons in the Cosmos* (University of Chicago, Chicago).
Ryan, S. G., J. E. Norris, and T. C. Beers, 1996, Astrophys. J. **471**, 254.
Sackmann, I.-J., A. I. Boothroyd, and K. E. Kraemer, 1992, Astrophys. J. **418**, 457.
Saio, H., M. Kato, and K. Nomoto, 1988, Astrophys. J. **331**, 388.
Salpeter, E. E., 1961, Astrophys. J. **134**, 669.
Schaerer, D., C. Charbonnel, G. Meynet, A. Maeder, and G. Schaller, 1993, Astron. Astrophys., Suppl. Ser. **102**, 339.
Schaerer, D., and A. Maeder, 1992, Astron. Astrophys., Suppl. Ser. **263**, 129.
Schaerer, D., G. Meynet, A. Maeder, and G. Schaller, 1993, Astron. Astrophys., Suppl. Ser. **98**, 523.
Schaller, G., G. Schaerer, G. Meynet, and A. Maeder, 1992, Astron. Astrophys., Suppl. Ser. **96**, 269.
Schmidt, B. P., R. P. Kirshner, R. G. Eastman, M. Hamuy, *et al.*, 1994, Astron. J. **107**, 1444.
Schmidt, B. P., R. P. Kirshner, R. G. Eastman, M. M. Phillips, N. B. Suntzeff, M. Hamuy, J. Maza, and R. Aviles, 1994, Astrophys. J. **432**, 42.
Schwarzschild, M., and R. Härm, 1959, Astrophys. J. **129**, 637.
Shapiro, S. L., and S. A. Teukolsky, 1983, *Black Holes, White Dwarfs, and Neutron Stars* (Wiley-Interscience, New York).
Shigeyama, T., and K. Nomoto, 1990, Astrophys. J. **360**, 242.
Shigeyama, T., K. Nomoto, and M. Hashimoto, 1988, Astron. Astrophys. **196**, 141.
Shigeyama, T., K. Nomoto, T. Tsujimoto, and M. Hashimoto, 1990, Astrophys. J. Lett. **361**, L23.
Shigeyama, T., T. Suzuki, S. Kumagai, K. Nomoto, H. Saio, and H. Yamaoka, 1994, Astrophys. J. **420**, 341.
Sneden, C., J. J. Cowan, L. B. Debra, and J. W. Truran, 1998, Astrophys. J. **496**, 235.
Sneden, C., J. J. Cowan, I. I. Ivans, G. M. Fuller, S. Burles, T. C. Beers, and J. E. Lawler, 2000, Astrophys. J. Lett. **533**, L139.
Sneden, C., A. McWilliam, G. W. Preston, J. J. Cowan, D. L. Burris, and B. J. Armosky, 1996, Astrophys. J. **467**, 819.
Spruit, H. C., 1992, Astron. Astrophys. **253**, 131.
Spruit, H. C., 1999, Astron. Astrophys. **349**, 189.
Spruit, H. C., 2002, Astron. Astrophys. **381**, 923.
Spruit, H. C., and E. S. Phinney, 1998, Nature (London) **393**, 139.
Stergioulas, N., and J. A. Font, 2001, Phys. Rev. Lett. **86**, 1148.
Stothers, R. B., and C.-W. Chin, 1991, Astrophys. J. Lett. **381**, L67.
Stothers, R. B., and C.-W. Chin, 1992, Astrophys. J. **390**, 136.
Swift, T. P., B. S. Meyer, and L.-S. The, 2000, Bull. Am. Astron. Soc. **197**, 4812.
Symbaisty, E. M. D., D. N. Schramm, and J. R. Wilson, 1985, Astrophys. J., Lett. Ed. **291**, 11.
Takahashi, K., J. Witti, and H.-Th. Janka, 1994, Astron. Astrophys. **286**, 857.
Takahashi, K., M. Yamada, and T. Kondo, 1973, At. Data Nucl. Data Tables **12**, 101.
Talbot, R. J., 1971a, Astrophys. J. **163**, 17.
Talbot, R. J., 1971b, Astrophys. J. **165**, 121.
Talon, S., J.-P. Zahn, A. Maeder, and G. Meynet, 1997, Astron. Astrophys. **322**, 209.
The, L.-S., M. F. El Eid, and B. S. Meyer, 2000, Astrophys. J. **533**, 998.
Thielemann, F.-K., and W. D. Arnett, 1985, Astrophys. J. **295**, 604.
Thielemann, F.-K., M. Arnould, and J. Truran, 1987, in *Advances in Nuclear Astrophysics*, edited by E. Vangioni-Flam (Editions Frontière, Gif-sur-Yvette), p. 525.
Thielemann, F.-K., K. Nomoto, and M.-A. Hashimoto, 1996, Astrophys. J. **460**, 408.
Thielemann, F.-K., K. Nomoto, and K. Yokoi, 1986, Astron. Astrophys. **158**, 17.
Thompson, T. A., A. Burrows, and B. S. Meyer, 2001, Astrophys. J. (in press); e-print astro-ph/0105004.
Thorsett, S. E., and D. Chakrabarty, 1999, Astrophys. J. **512**, 288.
Timmes, F. X., 1996, private communication.

Timmes, F. X., and F. D. Swesty, 2000, Astrophys. J., Suppl. Ser. **126**, 501.
Timmes, F. X., S. E. Woosley, D. H. Hartmann, and R. D. Hoffman, 1996, Astrophys. J. **464**, 332.
Timmes, F. X., S. E. Woosley, D. H. Hartmann, R. D. Hoffman, T. A. Weaver, and F. Matteucc, 1995, Astrophys. J. **449**, 204.
Timmes, F. X., S. E. Woosley, and R. E. Taam, 1994, Astrophys. J. **420**, 348.
Timmes, F. X., S. E. Woosley, and T. A. Weaver, 1995, Astrophys. J., Suppl. Ser. **98**, 617.
Timmes, F. X., S. E. Woosley, and T. A. Weaver, 1996, Astrophys. J. **457**, 834.
Tischauser, P., 2000, Ph.D. thesis (University of Notre Dame).
Travaglio, C., R. Gallino, S. Amari, E. Zinner, S. E. Woosley, and R. S. Lewis, 1999, Astrophys. J. **510**, 325.
Trimble, V., 1975, Rev. Mod. Phys. **47**, 877.
Trimble, V., 1991, Astron. Astrophys. Rev. **3**, 1.
Trimble, V., 1996, in *Cosmic Abundances*, edited by S. Holt and S. Sonneborn, ASP Conference Series No. 99 (Astronomical Society of the Pacific, San Francisco), p. 3.
Truran, J. W., and W. D. Arnett, 1970, Astrophys. J. **160**, 181.
Truran, J. W., and W. D. Arnett, 1971, Astrophys. Space Sci. **11**, 430.
Truran, J. W., J. J. Cowan, and A. G. W. Cameron, 1978, Astrophys. J., Lett. Ed. **222**, L63.
Tuchman, Y., and J. C. Wheeler, 1989, Astrophys. J. **344**, 835.
Tuchman, Y., and J. C. Wheeler, 1990, Astrophys. J. **363**, 255.
Turatto, M., P. A. Mazzali, T. R. Young, K. Nomoto, K. Iwamoto, S. Benetti, E. Cappallaro, I. J. Danziger, D. F. de Mello, M. M. Phillips, N. B. Suntzeff, A. Clocchiatti, A. Piemonte, B. Leibundgut, R. Covarrubias, J. Maza, and J. Sollerman, 1998, Astrophys. J. **498**, 129.
Ulrich, R., 1973, in *Explosive Nucleosynthesis*, edited by D. N. Schramm and W. D. Arnett (University of Texas, Austin), p. 139.
Utrobin, V., 1994, Astron. Astrophys. **281**, L89.
Utrobin, V. P., N. N. Chugai, and A. A. Andronova, 1995, Astron. Astrophys. **295**, 129.
Vanbeveren, D., 2001, in *The Influence of Binaries on Stellar Population Studies*, edited by D. Vanbeveren, Astrophysics and Space Science Library No. 264 (Kluwer, Dordrecht), p. 1.
Vanbeveren, D., C. De Loore, and W. Van Rensbergen, 1998, Astron. Astrophys. Rev. **9**, 63.
van der Hucht, K. A., 1992, Astron. Astrophys. **4**, 123.
Vangioni-Flam, E., R. Ramaty, K. A. Olive, and M. Casse, 1998, Astron. Astrophys. **337**, 714.
Vink, J. S., A. de Koter, and H. J. G. L. M. Lamers, 2001, Astron. Astrophys. **369**, 574.
Walborn, N. R., B. M. Lasker, V. G. Laidler, and Y.-H. Chu, 1987, Astrophys. J., Lett. Ed. **321**, L41.
Walker, T. P., G. Steigman, H.-S. Kang, D. M. Schramm, and K. A. Olive, 1991, Astrophys. J. **376**, 51.
Wallerstein, G., I. Iben, P. Parker, A. M. Boesgaard, G. M. Hale, A. E. Champagne, C. A. Barnes, F. Käppeler, V. V. Smith, R. D. Hoffman, F. X. Timmes, C. Sneden, R. N. Boyd, B. S. Meyer, and D. L. Lambert, 1997, Rev. Mod. Phys. **69**, 995.
Walter, G., H. Beer, F. Käppeler, and R.-D. Penzhorn, 1986, Astron. Astrophys. **155**, 247.
Walter, G., H. Beer, F. Käppeler, G. Reffo, and F. Fabbri, 1986, Astron. Astrophys. **167**, 186.
Wanajo, S., T. Kajino, G. J. Mathews, and K. Otsuki, 2001, Astrophys. J. **554**, 578.
Ward, R. A., and M. J. Newman, 1978, Astrophys. J. **219**, 195.
Weaver, T. A., and S. E. Woosley, 1993, Phys. Rep. **227**, 65.
Weaver, T. A., G. B. Zimmerman, and S. E. Woosley, 1978, Astrophys. J. **225**, 1021.
Wefel, J. P., D. N. Schramm, J. B. Blake, and D. Pridmore-Brown, 1981, Astrophys. J., Suppl. Ser. **45**, 565.
Weiss, A., 1989, Astrophys. J. **339**, 365.
Weiss, A., W. Hillebrandt, and J. W. Truran, 1988, Astron. Astrophys. **197**, L11.
Weiss, A., J. J. Keady, and N. H. Magee, 1990, At. Data Nucl. Data Tables **45**, 209.
Wellstein, S., and N. Langer, 1999, Astron. Astrophys. **350**, 148.
Wheeler, J. C., C. Sneden, and J. W. Truran, 1989, Annu. Rev. Astron. Astrophys. **27**, 279.
Wheeler, J. C., I. Yi, P. Höflich, and L. Wang, 2000, Astrophys. J. **537**, 810.
Williams, R. E., 1987, Astrophys. J. Lett. **320**, L117.
Wilson, J. R., 1985, in *Relativistic Astrophysics*, edited by J. Centrella, J. LeBlanc, and R. Bowers (Jones and Bartlett, Boston), p. 422.
Wilson, J. R., and R. Mayle, 1988, Astrophys. J. **334**, 909.
Wilson, J. R., R. Mayle, S. E. Woosley, and T. A. Weaver, 1986, Ann. (N.Y.) Acad. Sci. **470**, 267.
Witteborn, F. C., J. D. Bregman, D. H. Wooden, P. A. Pinto, D. M. Rank, S. E. Woosley, and M. Cohen, 1989, Astrophys. J. Lett. **338**, L9.
Witti, J., H.-Th. Janka, and K. Takahashi, 1994, Astron. Astrophys. **286**, 841.
Woosley, S. E., 1977, Nature (London) **269**, 42.
Woosley, S. E., 1986, in *Nucleosynthesis and Chemical Evolution*, edited by B. Hauck, A. Maeder, and G. Meynet (Geneva Observatory, Sauverny, Switzerland), p. 1.
Woosley, S. E., 1988, Astrophys. J. **330**, 218.
Woosley, S. E., 1993, Astrophys. J. **405**, 273.
Woosley, S. E., 1997, Astrophys. J. **476**, 801.
Woosley, S. E., W. D. Arnett, and D. D. Clayton, 1972, Astrophys. J. **175**, 731.
Woosley, S. E., W. D. Arnett, and D. D. Clayton, 1973, Astrophys. J., Suppl. **26**, 231.
Woosley, S. E., and R. G. Eastman, 1993, in *Thermonuclear Supernovae*, edited by P. Ruiz-LaPuente, R. Canal, and J. Isern, *NATO Advanced Study Institute, Series C,* No. 486 (Kluwer Dordrecht), p. 821.
Woosley, S. E., R. G. Eastman, T. A. Weaver, and P. A. Pinto, 1994, Astrophys. J. **429**, 300.
Woosley, S. E., W. A. Fowler, J. A. Holmes, and B. A. Zimmerman, 1978, At. Data Nucl. Data Tables **22**, 371.
Woosley, S. E., D. H. Hartmann, R. D. Hoffman, and W. C. Haxton, 1990, Astrophys. J. **356**, 272.
Woosley, S. E., and W. C. Haxton, 1988, Nature (London) **334**, 45.
Woosley, S. E., and R. D. Hoffman, 1992, Astrophys. J. **395**, 202.
Woosley, S. E., and W. M. Howard, 1978, Astrophys. J., Suppl. **36**, 285.
Woosley, S. E., N. Langer, and T. A. Weaver, 1995, Astrophys. J. **448**, 315.
Woosley, S. E., P. A. Pinto, and L. M. Ensman, 1988, Astrophys. J. **324**, 466.
Woosley, S. E., and T. A. Weaver, 1980, Astrophys. J. **238**, 1017.

Woosley, S. E., and T. A. Weaver, 1982, in *Supernovae: A Survey of Current Research*, edited by M. J. Rees and R. J. Stoneham (Reidel, Dordrecht), p. 79.
Woosley, S. E., and T. A. Weaver, 1988, Phys. Rep. **163**, 79.
Woosley, S. E., and T. A. Weaver, 1994, Astrophys. J. **423**, 371.
Woosley, S. E., and T. A. Weaver, 1995, Astrophys. J., Suppl. Ser. **101**, 181.
Woosley, S. E., T. A. Weaver, and R. E. Taam, 1980, in *Type I Supernovae*, edited by J. C. Wheeler (University of Texas, Austin), p. 96.
Woosley, S. E., J. R. Wilson, G. J. Mathews, R. D. Hoffman, and B. S. Meyer, 1994, Astrophys. J. **433**, 229.
Young, T. R., and D. Branch, 1989, Astrophys. J. Lett. **342**, 79.
Zahn, J.-P., 1992, Astron. Astrophys. **265**, 115.
Zhang, W., S. E. Woosley, and A. MacFadyen, 2002, Astrophys. J. (in press).